EFFECT OF GRADING AND GRAIN SIZE ON THE FRICTION CHARACTERISTICS OF A SAND/GEOTEXTILE INTERFACE

Denis Kalumba

Bachelor of Science (Eng.) (Hon.)
Makerere University, Kampala, 1995

A thesis submitted to the University of Cape Town in partial fulfilment of the requirement for the degree of Master of Science in Engineering.

Department of Civil Engineering
University of Cape Town

November 1998

DECLARATION

I, **Denis Kalumba**, hereby declare that this thesis is essentially my own work, except where otherwise indicated, and has not, to the best of my knowledge, been submitted for a degree at any other university.

Signed by candidate

Denis Kalumba,

November 1998

ACKNOWLEDGEMENTS

Sincere gratitude to my supervisor, Dr. F. Scheele for his invaluable contributions, guidance, advise, commitment and constructive criticism in this work.

A special thank you for the assistance received from UCT Civil Engineering staff, particularly Eike von Guerard and Charles Nicholas in the Workshop, and Noor Hassen in the Geotechnical Laboratory.

I acknowledge the steady financial support of NUFU through the NTNU/Makerere University Project for the the last two and half years towards pursuing this Master of Science degree. I wish to particularly identify Prof. T. Haavaldsen, the Coordinator and Assoc. Prof. B. M. Kiggundu, the UOC Coordinator for promoting an enabling environment. My greatest gratitude.

Particular gratitude also goes to my friends; Arthur, Choniso, Harriet, Justin, Michael, Ngoni, Nomalungelo, Patience, Patricia, Phumzile, Rockson, Sylvia, Yeukai and Ziphelele for all their support and encouragement throughout this thesis period.

Mrs Ann Phaswana; her motherly attention, love and care cannot be underestimated.

I register much appreciation to my family for their patience and much understanding while I was away from home. Thank you for having confidence in me for all these years.

I love you all and God bless you.

Nze Denis Kalumba
(KLMDEN001)

DEDICATION

To my **MOTHER** who unreservedly gave all she had in order to take me through school.

SYNOPSIS

Geofabrics are incorporated in geotechnical engineering structures for various reasons and functions. This study addresses the reinforcement function whereby geotextiles are utilised as reinforcing elements in reinforced slopes and fills. It particularly focuses on the soil/geotextile interface behaviour.

Geotextile reinforcements transfer a majority of the shear stress from the soil to the reinforcement and vice versa by friction. This interfacing ability manifested by the soil/geotextile frictional contact is very important in the performance of reinforced soil structures, and depends on the physical characteristics of the backfill as well as the geotextile.

In this investigation, the interaction behaviour of geotextiles with sand is evaluated by conducting extensive laboratory interface tests both in direct shear and pull-out. A comprehensive test program was established to include a needle punched non-woven geotextile interacting with sands of different grading, grain size distributions and grain shapes namely; Cape Flats, Klipheuwel and Munich sands. The respective responses were primarily presented in terms of shear stress/horizontal displacement and pull-out resistance/front displacement relationships; showing the frictional performance of the geotextile in these sands of different physical characteristics. Interface shear strength in both test methods was determined using Mohr-Coulomb's law. The ensuing shear strength values were compared with each other and with the direct shear strengths of the respective sands used in this investigation

Specific emphasis and detailed analyses went into the pull-out experiments in which local displacements of the geotextile specimens were measured as the test progressed. The measurements enabled the study of the stretching characteristics of the geofabric in the different sands. Applying an extrapolation procedure to approximate the constantly changing deformation modulus of the geotextile as it stretched in the respective sands, allowed the *back-prediction* of the pull-out force/displacement relationship, and thus enabled the study of skin friction distribution along the geotextile specimen during pull-out. The effect of the grading and grain size on the development of the interface shear stress, the peak values, and the type of interface failure could be demonstrated.

The analysis of the skin friction along the geotextile specimen led to the development of a generalised shear stress distribution graph which, if validated in further research, may be adopted in practical design situations.

In a design example, it was shown that the assumption of interface shear parameters based on direct shear tests provides too optimistic a factor of safety. This study recommends the use of interface shear parameters derived from pull-out tests. The in-depth analysis of the tests in a variety of sands showed clearly that the shear stress is not uniformly distributed over the embedment length of the reinforcement. This skin friction drops dramatically from a peak value near the loaded end to zero at the free end in all investigated confinements.

TABLE OF CONTENTS

CHAPTER 6

6. PULL-OUT TEST INVESTIGATION

CHAPTER 7

7. RESULTS, ANALYSIS AND DISCUSSIONS

CHAPTER 8

8. PRACTICAL APPLICATIONS

CHAPTER 9

9. CONCLUSIONS

LIST OF ILLUSTRATIONS

Tables **Pages**

NOMENCLATURE

A	m^2	area of contact between soil and geotextile
c	kN/m^2	cohesion of soil
c'	kN/m^2	cohesion of soil in terms of effective stress
c_r'	kN/m^2	residual cohesion in effective stress terms
C_u	-	coefficient of uniformity
C_g	-	coefficient of gradation
C_R	N/div	proving ring calibration (in Newtons per division)
F	kN	pull out force
g	m/s^2	gravitational acceleration
G_s	-	specific gravity of soils
R	divisions	dial reading of proving ring
T_D	kN/m	design strength of the reinforcement
σ_n	kN/m^2	normal or confining pressure
τ	kN/m^2	shear stress
τ_{sg}	kN/m^2	average shear stress along the soil/geotextile interface
ϕ	degrees	angle of internal friction of soil
ϕ'	degrees	angle of internal friction of soil in terms of effective stress
ϕ_r'	degrees	residual angle of internal friction in terms of effective stress
δ	degrees	soil/geotextile friction angle
α	-	friction angle ratio relating soil/geotextile friction angle to internal friction angle of soil
α_c	-	adhesion coefficient relating soil/geotextile interface adhesion to cohesion of soil
α_{cr}	-	adhesion coefficient relating soil/geotextile interface residual adhesion to residual cohesion of soil
α_r	-	friction angle ratio relating soil/geotextile residual friction angle to residual angle of internal friction of soil

CHAPTER 1

INTRODUCTION

1.1 Introduction

Reinforced soil is a general term which refers to the use of placed or insitu soil or other fill material in which tensile reinforcements act through interface friction, bearing or other means to improve stability of the soil. The phenomenon involves inserting the reinforcement into the natural soil, or incorporating it in the fill to either provide steeper slopes than would otherwise be possible or to improve its load bearing capacity. It is a well established geotechnical engineering technique for soil improvement.

Reinforced soil is currently used in a wide range of civil engineering structures including vertical reinforced soil walls and abutments, steep sided embankments and cuttings, slope stabilisation, and basal reinforcement of foundations for low ground bearing structures constructed on soft ground. Two examples of reinforced soil applications are shown in *Fig 1.1*.

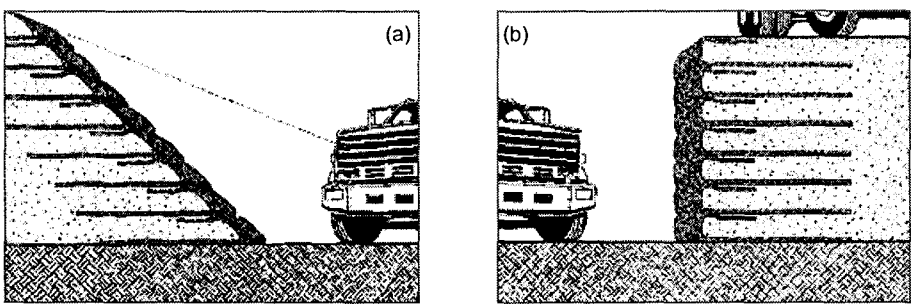

Fig 1.1 Examples of reinforced soil applications; (a) steepened slope, (b) retained wall

The modern form of soil reinforcement was introduced by Henri Vidal in the 1960s. Vidal's concept was for a composite material formed from flat reinforcing strips laid horizontally in a frictional soil, the interaction between soil and the reinforcing members consisted solely of friction generated by gravity of the soil material (Vidal, 1966). This structure he described as '*reinforced earth*', a term that has become generic in many places. The first major retaining walls using the Vidal concept were built near Menton in the southern part of France in 1968, although Vidal had built structures as early as 1964 (Jones, 1996).

Technically, soil has an inherently low tensile strength but a high compressive strength which is only limited by the ability of the soil to resist applied shear stresses (BS 8006:1994). The engineer's objective for using a reinforcement is to make up for this deficiency by absorbing generated tensile

loads, and/or shear stresses, thereby reducing the loads which might otherwise cause the soil to fail in shear or due to excessive deformation.

There is presently a wide selection of materials used to reinforce soil e.g. fabrics, textiles, timber, galvanised steel, plastics, etc. This research, however, concentrates solely on geotextile materials used to specifically reinforce soil.

It is interesting to note that it is only within the last few years that geotextiles have joined the list of traditional alternatives considered in soil improvement situations. In many cases the use of a geotextile (or any other relevant geofabric) can significantly increase the stability of a structure, improve the performance, and reduce costs in comparison with more conventional solutions (Holtz, 1990). For embankments on extremely soft foundations where conventional construction would be either impossible or prohibitively expensive, geotextile reinforcement can often permit the construction to be carried out successfully. The use of geotextiles in earthworks, is therefore now widely accepted as an additional tool for reinforcing unstable soil-structures. However, the surface of a geotextile placed in a soil mass forms a plane of discontinuity causing a movement or even a slippage at the interface when loaded.

One of the critical factors in preventing the fabric from becoming a feature of discontinuity is that of soil/geotextile interface friction (in this context instead of '*friction*', the term '*adhesion*' is sometimes used). In the theoretical analysis and design of a reinforced soil structure, the estimate of the soil/geotextile interface friction is necessary for the soil reinforcement application. Friction parameters such as the interface coefficient of friction must thus first be determined.

In the design of these geotextile reinforced soil structures, the two aspects of greatest importance are:

(i) the frictional behaviour between the soil and geotextile,
(ii) the stiffness of the confined geotextile.

The interface friction influences the stability of the soil structure while the stiffness of the reinforcement affects the serviceability as a whole.

The soil/geotextile interface friction characteristics depend on the geotextile's material composition, thickness and surface texture, as well as the soil's particle shape, structure, fabric, grading and condition. It is this frictional interface interaction, or load transfer behaviour of a particular geotextile in a variety of sandy soils, that was investigated in this study.

1.2 Historical development

The concept of reinforcing soil has been used since the earliest of time. Non soil materials have been used for thousands of years to improve the engineering properties of soils. Examples in nature include the nests of certain insects and birds as well as beaver dams. Tree roots, for example, can be quite effective as slope reinforcement. The fundamentals of the technique are already described in the Bible (Exodus 5, verses 6-9), covering the reinforcement of clay or bricks with reeds or straw for the construction of dwellings. Construction using these techniques is known to have existed in the 5th and 4th millennium BC (Jones, 1996).

Large temples ("Al-Ziggurats") up to 57m high constructed in the ancient city of Ur in Iraq with dried earth blocks and reinforced across the width of the structure with tarred ropes represent one of the earliest reinforced soil structures still in existence (Smith G., 1990). The Great Wall of China, parts of which were completed in 200 BC., contains sections constructed of mixtures of clay and gravel reinforced with tree branches. Reinforcement of earthen revetments and fortifications has been employed in Europe since Roman times, perhaps even earlier (Jones, 1996). Adope bricks common in the Southwest of the USA and Mexico are another example of the same concept (Holtz, 1990).

A notable contribution of reinforcing techniques for military earthworks was made in 1822 when the British Army introduced a form of reinforced soil for military construction (Pasley, 1822). Col. Pasley conducted a comprehensive series of trials and showed that a significant reduction could be made in the lateral pressures acting on retaining walls if the backfill were reinforced by horizontal layers of brushwood, wooden planks or canvas. Similar observations were made with modern reinforced earth backfill over 150 years later (Saran et al., 1979). Arguably, Col. Pasley's work was the first application of geotextile reinforcement to reinforced soil structures, although the resultant structures probably had a relatively short life time (Jones, 1995).

The use of geotextiles for permanent reinforcement could not be contemplated until the development of synthetic polymer based materials. Synthetic fabrics were known prior to 1940 but it was not until the late sixties and early seventies that the advances in synthetic fabric and geotextiles developments produced materials whose longevity could be assured. More about geotextiles, their description, definitions and functions is presented in *Chapter 2.*

1.3 Research objectives and methodology

As highlighted earlier, geotextiles used as reinforcing elements in soil structures transfer the shear stresses from the soil to the reinforcement or vice versa by means of the interface shear friction characteristics. This interfacing ability, manifested by the soil/geotextile frictional contact, is very important in the performance of geotextile reinforced structures.

The British code of practice for strengthened/reinforced soils and other fills, BS 8006:1994, specifies that direct shear tests should be undertaken to determine the soil/geotextile shear parameters for design.

In this study, however, the interaction behaviour of geotextiles with soil is evaluated not only by conducting direct shear tests but also by pull-out tests (of relatively small scale) in the laboratory. It was desirable to compare the frictional parameters obtained from the direct shear tests, with those from pull-out tests in terms of the interface shear parameters and the interface shear stress development as a whole. By comparing the friction parameters obtained from both tests with the individual soil friction parameters, some clarification about the competence of one test method for investigating the soil/geotextile interface behaviour over the other was expected.

Another objective of the study was to investigate how the grading and particle size affects the sand/geotextile interface friction characteristics under varying normal stresses. This was to be attempted by studying the skin friction distribution along the geotextile specimen during testing in each research sand material confined at the same reference pressures.

The results of the two interface shear test configurations were to be compared to determine the most adequate test, suitable for developing '*realistic*' interface properties for the purposes of design. This was to be determined by using the parameters obtained from both test methods in a series of practical design problems employing the same design methodology. With such a comparison and ensuing detailed assessment of results, it was hoped that realistic design values for geotextile - reinforced earth slopes could be established.

A working program was developed to include a needle punched non-woven geotextile interacting with sands of different grain sizes and grading; Cape Flats, Klipheuwel and Munich sands. The research was focussing on a needle punched non-woven geotextile as a reinforcing element. The geofabric is locally manufactured, hence, was easily accessible. To the researcher's knowledge, it is the most widely used geofabric, to this date, for that purpose in South Africa.

1.4 Research Overview

This thesis initially provides a theoretical background of geotextiles and their applications in geotechnical engineering works. A literature review of previous research work with soil/geotextile interfaces is undertaken, in *Chapter 3*, in order to establish a sound basis for achieving the objectives of this work. It was of utmost importance to fully investigate and identify the properties of the soil materials and geotextile used in this study. The mechanical properties of the research materials are discussed in *Chapter 4*. Details of the experimental procedures for the direct shear and pull-out tests have been laid out in *Chapters 5* and *6* respectively. *Chapter 7* contains all the results of the analyses and their discussions. Practical applications consisting of a design problem

utilising the findings of this investigation are presented in *Chapter 8*. Finally, in *Chapter 9*, the results are summarised, conclusions of this research work are drawn, and recommendations for further research given.

CHAPTER 2

GEOTEXTILES IN GEOTECHNICAL APPLICATIONS

2.1 Introduction

Reinforced soil material, as applied in geotechnical engineering, is a material formed by inserting a reinforcement into soil. The term '*soil*' covers all types of mineral material formed by weathering of rocks caused by physical or chemical means, but can also be formed from man-made substances e.g. fragments of concrete, bricks, etc. It includes clay, silt, sand, gravel, stones and rocks of all sizes. In this study, the word '*reinforcement*' is used to refer to all linear materials which are axially stiff and can withstand tensile stresses.

Granular soil alone, according to the definition used in soil mechanics, is made up of non-cohesive particles, but once horizontal layers of flexible, linear reinforcements are introduced, the whole reinforced soil mass exhibits some form of '*cohesion*'; it becomes a structure of reinforced soil. The soil reinforced with geotextiles is called *geotextile reinforced soil.*

Geotextile reinforced soil has many applications in civil engineering which include, its use in the context of retaining walls, reinforced embankments, stabilisation of soil slopes, etc. It is, in fact, becoming a more popular alternative to the traditional gravity wall whenever suitable.

These soil reinforcing elements, the geotextiles, are the focus of this chapter. Starting with the clarification of some definitions, an overview of the various types of geotextiles is given. The manufacturing process of geotextiles is then presented. The basic functions and applications of geotextiles are described. This is followed by a brief on the general construction procedures of a geotextile reinforced structure. The chapter is concluded with the working principles of a geotextile fabric reinforcing soil, which in essence, provides a background for the practical application of the results of this research work presented in the subsequent chapters of the thesis.

2.2 What are geotextiles?

According to the definition by ASTM Committee D-35 on Geotextiles, Geomembranes, and Related Products, geotextiles are, "*permeable textiles used with geotechnical materials as an integral part of a man-made project, structure or system*", (ASTM 04.08). Geotextiles are used in contact with soil, rock, or any other geotechnical engineering related material in civil engineering applications. They are part of a larger family of materials called *geosynthetics*, which are used by civil, geotechnical, environmental and structural engineers in the design of various structural components.

Other materials grouped under geosynthetics include:

- geomembranes,
- geonets,
- geomatresses.

A host of others could be added to the list as new applications are introduced over the years.

Geotextiles can, according to Jones (1996), be divided into two categories ;

- conventional geotextiles, and
- special geotextiles.

Conventional geotextiles are products of the textile industry and include non-woven, woven, knitted and stitch-bonded textiles, as schematically shown in *Fig 2.1.*

Non-woven geotextiles consist of a random arrangement of fibres bonded together by heat (melt bonded) or physically entangled (needle punched). The plan view of a typical structure of non-woven geotextiles is illustrated in *Fig 2.1(a).*

Woven geotextiles consists of fibres arranged essentially at right angles to one another in varying configurations. The general plan and cross-section of a typical woven geotextile structure is shown in *Fig 2.1(b).*

Knitted geotextiles consist of fibres which are inter-looped. This process produces two different structures, i.e. weft knitted and warp knitted geotextiles.

Stitch-bonded geotextiles are formed by stitching fibres (or yarns) together, as shown in *Fig 2.1(c).*

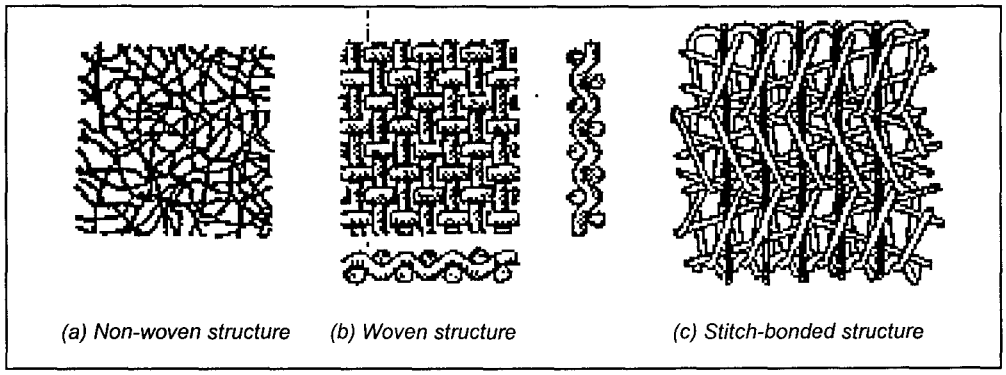

Fig 2.1 Conventional geotextile structures (after Jones, 1996)

Special geotextiles are usually not a product of the textile industry. They are generally divided into two major types; geogrids and geocomposites. Geogrids are formed either by the cross laying of strips which are subsequently bonded together at their cross-over points or by the punching and drawing of polymer sheets. This manufacturing process of geogrids makes them '*open*' structures; where frequently more than 50 per cent of the total material area is open area.

Geocomposites, generally consist of high strength fibres set within a polymer matrix or encased within a polymer skin. In a soil reinforcement context, the fibres provide the tensile properties for the material while the matrix or skin provides the geometrical shape and protects the fibres from damage.

2.3 Manufacturing process of geotextiles

Geotextiles are made from polymer materials, with the most commonly used being polyester, polypropylene and polyamide. The production of geotextiles may be considered in two steps. The first step consists of making linear elements such as filaments, fibres, tapes and yarns from polymer materials. The second consists of combining these linear elements to make a permeable planar material.

Once the linear elements are made, they are woven, in the same manner as cloth in the textile industry, forming a woven fabric called a *woven geotextile*. The weaving process uses any one or in some cases combinations of different types of fibres in the warp and weft directions. The fibres used include split films or tapes, monofilaments or multistrand filaments.

On the other hand, non-woven geotextiles are formed by spinning continuous filaments onto a vibrating bed. The filaments are subsequently either heat bonded to form a *heat bonded non-woven geotextile* or they are tangled using barbed needles to form a *needle punched non-woven geotextile*. The purpose of either of these two processes is to increase the overall tensile strength of the geotextile. In *Fig. 2.2*, the schematic of the manufacturing process of a needle punched non-woven geotextile is shown.

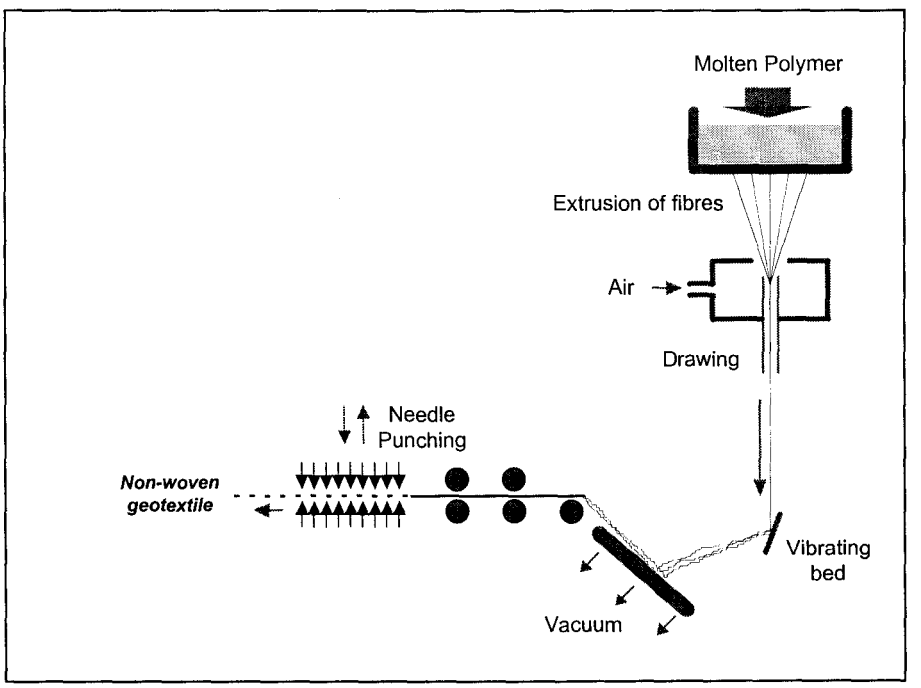

Fig 2.2 Schematic of the manufacturing process of needle punched non-woven geotextiles (after Kaytech Industrial Fabrics, 1995)

2.4 Geotextile functions

There are five main basic end-use functions which are performed by geotextiles when used in design and construction of soil structures supported on or covered by soil/geotextile systems. They are :-

- Reinforcement : The geotextile imparts tensile strength to a soil/geotextile system resulting in increased structural stability.
- Separation : The geotextile forms a boundary between different soils or rock materials, thereby segregating two or more particle sizes.
- Filtration : The geotextile effectively retains particles while allowing water to flow through with little or no increase in pore pressure to the surrounding soil.
- Drainage : The geotextile effectively allows water to flow in the plane of the fabric, thus allowing drainage of water away from a structure or system.
- Moisture Barrier : The geotextile when coated or impregnated with a relatively impermeable material such as asphalt effectively forms a barrier which impedes the flow of moisture through a system.

In any given application, those basic or primary functions stated above may also serve as secondary functions to complement each other. The reinforcement function of geotextiles was of the main interest in this research work.

2.5 Geotextiles as soil reinforcement

The soil reinforcement function of geotextiles lies in the mechanical improvement of soil. The geotextile achieves this mechanical improvement in soil by taking up tensile forces thereby reducing the shear force that has to be carried by the soil, and allowing an increase of the normal stress acting on potential shear surfaces (Jewell, 1996).

Typically, four main applications for geotextiles reinforcement are in use, as shown schematically in *Fig 2.3* :

a) Vertical walls and abutments,
b) Steep slopes,
c) Slip prevention and remedial measures,
d) Embankments on soft soil.

In all these applications, the reinforcement resists the lateral forces which develop upon loading due to the soil self-weight and structural loading.

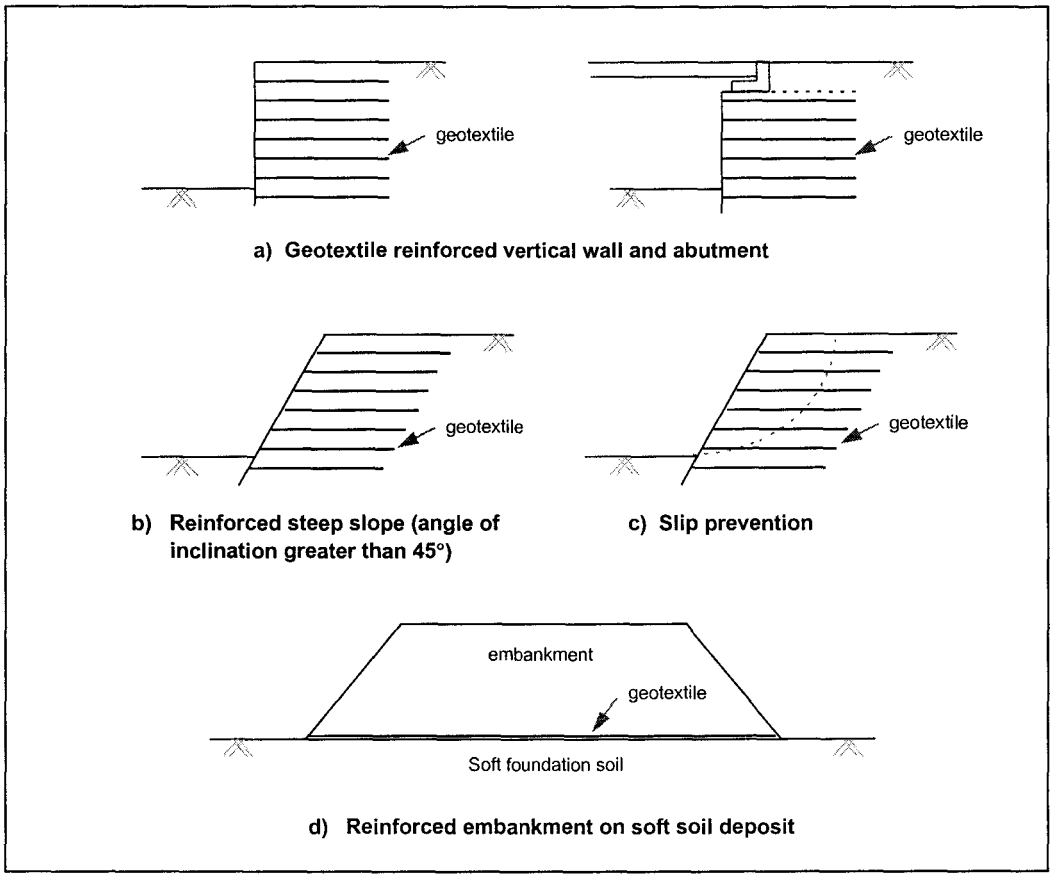

Fig 2.3 Typical applications of geotextile reinforced soil

There is, however, a difference between the lateral support type of applications shown in *Fig 2.3(a)* to *Fig 2.3(c)*, and the use of reinforcement at the base of an embankment on soft soil, shown in *Fig 2.3(d)*. In the first three cases, the reinforcement is required for permanent application; i.e. to maintain stability throughout the life time of the structure (Jewell, 1996). In an embankment on soft soil, the reinforcement is required for short term application (Jones, 1995); i.e. once the foundation soil has increased in its internal strength due to consolidation and settlement, then the reinforcement is no longer required to ensure stability.

2.6 Construction of a geotextile reinforced soil structure

The key aspects of a geotextile reinforced soil structure are its incremental form of construction and the interaction between the reinforcement and the soil forming the structure. To date, the construction method widely used in Europe is the '*wrap around*' technique (Recalcati et al., 1995), in which the structure is constructed using layers of compacted frictional backfill with the geotextile placed horizontally at suitable vertical intervals. The geotextile sheet is then turned up along the face and back into the reinforced mass; wrapping around the face of the wall/slope to protect it from

progressive erosion. Sometimes, vegetation cover has subsequently been added on top of this soft wall/slope surface. This has been known to lessen the impact of erosion in harsh environments (Smith R., 1990). The construction technique may be used with or without formwork but formwork is necessary if a smooth and aesthetic appearance is desired.

Construction of the geotextile wrapped wall/slope structure is done layer by layer, as is shown schematically in *Fig 2.4*. A brief step-by-step construction procedure of a geotextile reinforced structure is listed so as to complete the overview on geotextile applications.

1] If necessary, the ground (or earth) is first levelled as per design instruction. The foundation soil is compacted and formwork subsequently set-up (e.g. against the vertically fixed prefabricated concrete cantilever elements, or otherwise). The formwork supports the geotextile while the soil is being filled in (see *Fig 2.4(a)*).

2] The geotextile sheet of specified length is placed on the just densified underlaying layer with one end of the fabric wrapped around the formwork (see *Fig 2.4(b)*).

3] Soil is laid, levelled and compacted on the fabric (see *Fig 2.4(c)*). Compaction is done carefully and efficiently since it has a major influence on both the design assumptions and final form of the reinforced soil structure (Jones, 1990).

4] Phase 3 is repeated several times till soil reaches the required level in the formwork.

5] The end of the fabric previously wrapped over the formwork is pulled up, tensioned and folded back towards the compacted soil mass. This end of the fabric consequently forms an overlap with the next geotextile sheet placed on top of the layer (see *Fig 2.4(d)*).

6] The present formwork is dismantled and reset, (or adjusted), for the construction of the next layer. The operations 1] to 4] are repeated till the structure reaches the envisaged height.

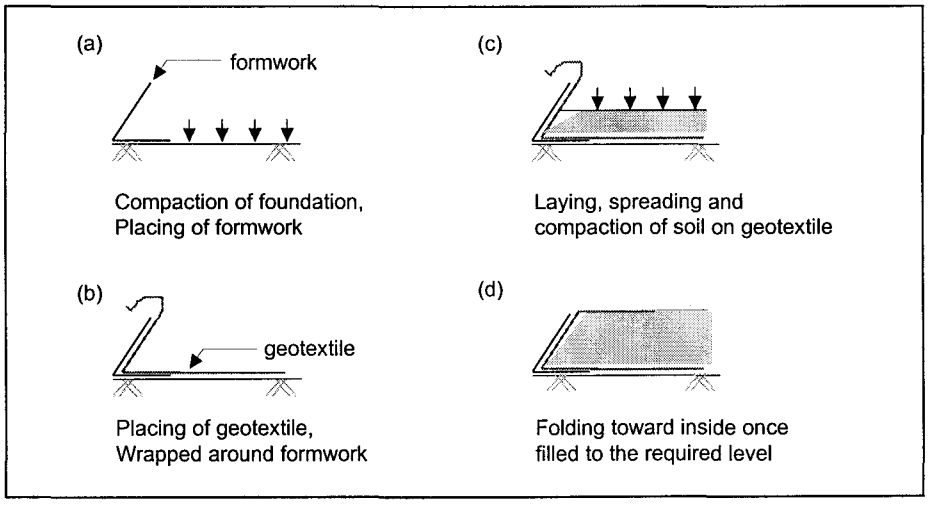

Fig 2.4 Construction procedure of a geotextile reinforced soil layer

2.7 Fundamental mechanisms of geotextile soil reinforcement

Naturally, soil has a low tensile strength but a high compressive strength, which is only limited by the soil's ability to resist shear (*BS 8006:1994*). The concept of how a geotextile fabric, as a soil reinforcing element, makes up for this deficiency can be illustrated by considering a unit of dry cohesionless soil, as shown *Fig 2.5*.

If an external, compressive stress, σ, is applied in a vertical direction on a mass of unreinforced cohesionless soil which is unrestrained horizontally, the soil unit will deform as the soil particles try to realign in order to mobilise shearing resistance. The deformation is observed as an overall strain in the soil, and both vertical, compressive strain, δ_v, and tensile, lateral strain, δ_h, develop as shown schematically in *Fig 2.5(a)*. However, if the same soil mass is reinforced with several horizontal layers of a geofabric which is axially stiff, and the same external compressive stress, σ, is applied, vertical and lateral strains of the magnitudes δ_{vr} and δ_{hr} respectively result, where $\delta_{vr} < \delta_v$ and $\delta_{hr} < \delta_h$ (see *Fig 2.5(b)*).

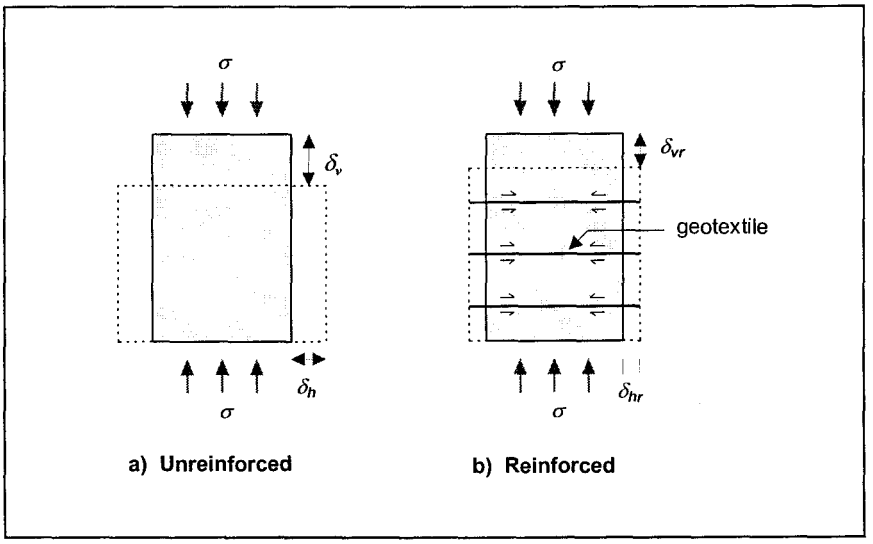

Fig. 2.5 Soil reinforcement mechanism (after BS 8006:1994)

It is important to note that the lateral strain, δ_{hr}, only occurs if the soil can move relative to the reinforcement. The movement of the soil relative to the reinforcement goes hand in hand with the generation of shear stresses at the soil/reinforcement interface. These shear stresses produce tensile loads in the reinforcements which are taken care of by their axial stiffness (refer to *Fig 2.5(b)*).

In an unreinforced soil, general shear failure results when the induced shear stress approaches the shear strength of the soil. But in reinforced soil, the reinforcement interacts with the soil thereby absorbing the stresses and strain which would otherwise cause unreinforced soil to fail. The result is that reinforced soil needs a higher compressive stress to cause failure and the net external effect

of this internal interaction is a reduction of both vertical and lateral deformations compared to unreinforced soil.

The mobilised force in the reinforcement is thus affected by the characteristics of the soil and the reinforcement material, which in turn determine the characteristics of their interaction (Jewell, 1996). The two limiting modes of this interaction are slippage at the soil/reinforcement interface and rupture of the reinforcement. Slippage involves the sliding of a soil mass over a reinforcement layer. Rupture involves the tearing of the reinforcement once the mobilised tensile forces in the geotextile exceed its tensile strength.

Modified direct shear and pull-out tests are generally used to investigate the interaction characteristics of a particular type of geotextile and a specified soil in the laboratory.

As mentioned before, reinforced soil is widely accepted and used in a range of civil engineering structures like slopes and walls. In design, the British Standard BS 8006 (1994) analyses the internal stability of reinforced soil slopes and walls by dividing the soil behind the face into active and resistant zones, as shown in *Fig 2.6*. Without reinforcement the active zone is unstable and prone to failure. The overall design objective of reinforced soil is to transfer securely stresses from the active zone to the resistant zone. (Details of the design procedures of geotextile reinforced slope structures are fully presented in *Chapter 8*).

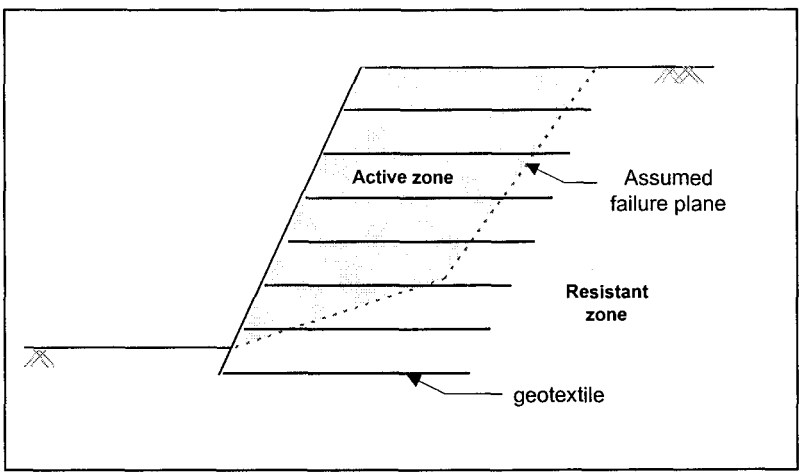

Fig 2.6 Active and passive zones in a reinforced soil slope (after BS 8006)

CHAPTER 3

LITERATURE REVIEW OF PREVIOUS RESEARCH

3.1 Introduction

In general, the examination of the interface frictional characteristics between soils and geotextiles requires that in-soil performance tests such as direct shear and/or pull-out tests be carried out. However, the choice of test used to obtain the relevant interface properties needed in the design process continues to be a matter of debate. Up to date there appears to be some confusion concerning the type of test to be used in the determination of the most '*realistic*' soil/geotextile friction characteristics since the two mentioned ones produce very different loading and displacement mechanisms.

In this chapter, a comprehensive study of experimental work done by various researchers is presented and discussed.

The chapter is divided into two main sections. The first section deals with previously undertaken and published studies of the direct shear tests at the soil/geotextile interface, with all modifications there of. The pull-out tests, again in many variations, at the soil/geotextile interface appear in the second section. Summaries of the relevant findings appear at the end of the respective subsections.

3.2 Direct shear tests at the soil/geotextile interface

The test most widely used to determine maximum and ultimate coefficients of friction of the soil/geotextile interfaces is the direct shear test carried out in a shear apparatus, with the geotextile interface lying in the plane of shear (Bolton, 1990). The test apparatus, whose primary function is to determine the maximum shear stress at the soil/geotextile interface for various normal pressures, is a modification of the conventional standard direct shear apparatus used to determine the angle of internal friction of soils. *Fig 3.1(a)* shows a cross-section of the conventional direct shear apparatus.

The direct shear interface tests have been conducted by various researchers (Myles, 1982; Miyamori et al., 1986; Dembicki et al., 1987; Chen et al., 1990; Wise, 1997) to investigate the soil/geotextile interface behaviour. This section reviews some of their work and presents findings which are relevant to this study.

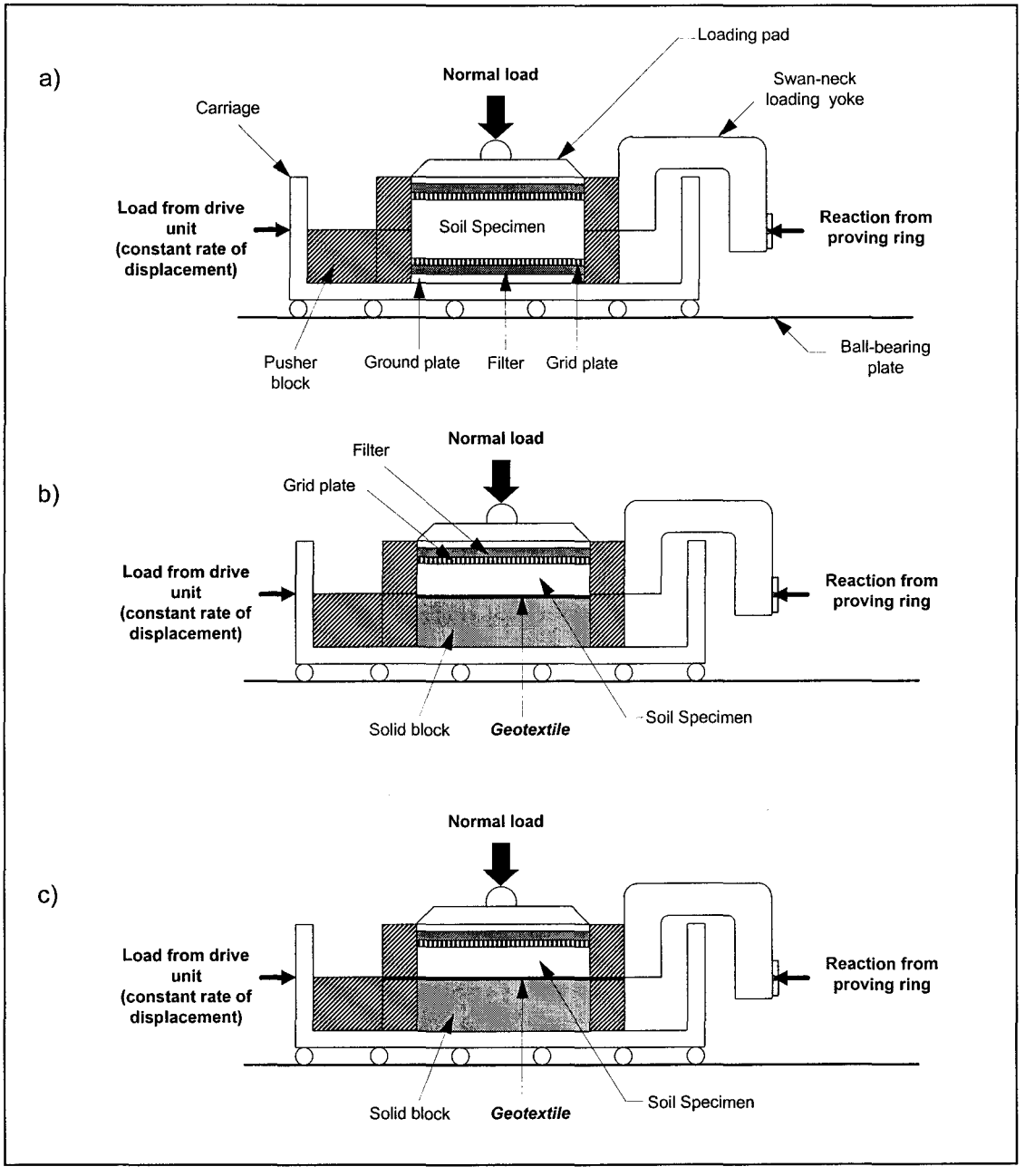

Fig 3.1 Schematic diagrams of a) conventional direct shear apparatus, b) and c) typical soil/geotextile interface test arrangements

3.2.1 Different test arrangements

The test arrangements, shown in the cross-sections in *Fig 3.1(b)* and *Fig 3.1(c)*, are typical of the devices employed in most research studies.

In principle, there have been two different test arrangements adopted by researchers;

a) *varying shear area arrangement* ; that is the soil/geotextile interface shear area changes as the test proceeds, *Fig 3.1(b)*; (used by Garbulewski, 1990; Wise, 1997), and

b) *constant shear area arrangement*; the soil/geotextile interface shear area remains constant throughout the test, *Fig 3.1(c)*; (used by Myles, 1982; Makiuchi et al., 1988; Chen et al., 1990; Wise, 1997). This arrangement has an advantage over the first in that there is no loss of shear area during testing.

In both arrangements, the test device consists of two halves of the standard direct shear apparatus with the geotextile specimen sample usually clamped to the lower frame. There is one exception by Saxena (1985) where the geotextile was attached to the upper frame in some of the tests conducted. The soil is placed and conditioned in the upper frame so that the two materials face each other. A normal pressure (vertical load) is uniformly applied to the loading pad overlying the soil. The upper frame containing the soil, is then sheared at a constant rate over the lower frame and the shear force required is incrementally measured. The test is repeated for at least three different normal pressures. The shear stress - displacement data is recorded and plotted for each of the three normal pressures to produce three curves. By plotting the shear stress at failure against the corresponding normal pressure, a failure envelope (Coulomb envelope) for the interface test series is produced.

In some of the reviewed research works, the lower frame, with the geotextile attached, remained stationary when the top frame was being sheared (e.g. Myles, 1982; Makiuchi et al., 1988), yet in others, the upper frame containing the soil mass remained stationary while the lower one was being displaced during the test (e.g. Saxena et al., 1985, Wise, 1997). Amongst all the reviewed cases, no comparative study has been undertaken on the effects of this difference in shear application on the interface friction characteristics.

It is important to note at this stage, that the dimensions of the direct shear test apparatus, the test arrangements as well as the physical characteristics of the research materials investigated, (e.g. soil mechanical properties, geotextile surface roughness, etc.), varied from researcher to researcher. Therefore, a direct comparison of the results, in many cases, was not possible in view of this variation of soils and geotextiles as well as test apparatus used.

Concerning the size of the test apparatus, BS 8006 : 1994 and ASTM 5321 recommend that the standard interface tests be carried out in a 300 mm square size shear apparatus with the geotextile material fixed at the top of the lower frame and the fill sample occupying the top frame only. The lower frame should, in addition, include a steel block fitting closely inside the lower frame of equal height less the thickness of the geotextile sample material.

The average shear stress developed across the interface is calculated from the measured reaction force exerted on the respective shear frame. By assuming zero friction between the upper and lower frames, and taking the contact shear area to be constant, the average shear stress, τ, is given as:

$$\tau = \frac{F}{A} \qquad (3.1)$$

where,

F shear force acting along the sand/geotextile interface,

A interface contact (shear) area.

The maximum shear stress, τ_{max}, is obtained by substituting the maximum interface shear force experienced, F_{max}, as well as the interface area, *A*, into *Equation 3.1*.

In *Table 3.1*, a summary of the relevant published work for soil/geotextile interface testing using the modified direct shear apparatuses is presented. The table clearly shows a relatively wide range of pressures and test rates which have been covered by researchers.

Author	Shear area Dimension (mm)	Soil / geotextile type	Pressure range (kPa)	$\tau_{max} - \sigma_n$ failure line	Test rate (mm/min)	Displ. at τ_{max} (mm)	Friction angle ratio, α
Myles, 1982	316 x 316	Sand / Woven & Non-woven	50 - 180	Linear	10,25,75	Not reported	0.8 - 1.0 (W) .86 - .91(NW)
Saxena et al., 1985	254 x 254	Sandy clay / Woven & Non-woven	69 - 276	Linear up to 207kPa	0.76	15	1.83 (W) 2.33 (NW)
Miyamori et al., 1986	316 x 316	Sand / Non-woven	Not reported	Linear	Not reported	Not reported	0.72-0.87
Fourie et al., 1987	60 x 60	Clay / Non-woven	50 - 350	Linear up to 150kPa	0.90	3 - 6	0.52-1.65
Dembicki et al., 1987	100 x 100 250 x 400	Sand / Non-woven	Not reported	Non-linear	Not reported	Not reported	Not reported
Makiuchi et al., 1988	316 x 316	Sand & Clay / Woven & Non-woven	50 - 200	Linear	0.50	2 - 6	0.75-0.90
Chandrase-karan , 1988	100 x 100	Sand / Woven	50 - 500	Non-linear	Not reported	Not reported	1.07 (at 40kPa) - 0.77 (at 500kPa)
Chen et al., 1990	150 x 150	Sand / Non-woven	24.5 - 196	Linear	Not reported	Not reported	0.73 -0.96
Garbulewski, 1990	100 x 100	Silty clay / Woven & Non-woven	25 - 100 (W) 5 -100 (NW)	Linear	0.10	5-10 (W) 2 -10 (NW)	0.89 (W) 1.04 (NW)
Venkatappa et al., 1990	60 x 60	Sand / Woven & Non-woven	Not reported	Linear	1.32	Not reported	Not reported
Wise, 1997	60 x 60	Sand / Non-woven	50 - 250	Non-linear	0.61	5 - 6.5	Not applicable
	100 x 100	Sand / Non-woven	50 - 350	Non-linear	0.61	5 - 7	Not applicable

W : woven, NW : non-woven

Table 3.1 Summary of reviewed research work on interface testing in direct shear

3.2.2 Maximum shear stress versus normal pressure relationship

The maximum shear stresses are obtained from the shear stress - displacement curves mentioned in *Section 3.2.1*, and are plotted against the normal pressure to represent a line. This line, linear or non-linear, gives the maximum shear stress (τ_{max}) - normal pressure (σ_n) relationship known as the failure envelope.

Myles (1982) used direct shear tests (316 x 316 mm) to investigate the maximum shear stress (τ_{max}) versus normal pressure (σ_n) relationship. The investigation involved both woven and non-woven geotextiles. The test device was of the type shown in *Fig 3.1(c)*; with the geotextile located in the lower box of the direct shear apparatus while Leighton Buzzard sand (0.60 - 0.85mm) was placed in the upper box. The applied normal pressure ranged from 50kPa to 180kPa. The investigation indicated that the maximum shear stress - normal pressure relationship was linear and varied with the type of geotextile material; woven and non-woven. It was also clearly shown that the rate of testing (10, 25, 75 mm/min) had no significant influence on the τ_{max} - σ_n relationship slope.

Saxena et al. (1985) investigated the soil/geotextile interface friction behaviour using a specially designed direct shear apparatus (254 x 254 mm). The tests were performed over an applied normal pressure range of 69kPa to 276kPa in a '*sandy clay*', consisting of 50% Kaolin clay, 45% Ottawa sand and 5% bentonite. The investigation was conducted at a very slow rate of displacement of 0.76 mm/min compared to those of Myles (1982). The maximum shear stress versus the normal pressure relationship was found to be linear for both woven and non-woven geotextiles, up to a normal pressure of 207kPa. However, at pressures above 207kPa, the relationship for the non-woven geotextiles became non-linear.

Several other researchers using the modified direct shear apparatus of different shear area dimensions, also obtained a linear maximum shear stress - normal applied pressure relationship. They include; Miyamori et al., 1986 (investigating the interface behaviour between sand and a non-woven geotextile); Fourie et al., 1987 (using clay and non-woven geotextile); Makiuchi et al., 1988 (sand & clay and woven & non-woven geotextile); Chen et al., 1990 (sand and non-woven geotextile); Garbulewski, 1990 (silty clay and woven & non-woven geotextiles); Venkatappa et al., 1990 (sand and woven & non-woven geotextiles).

Results obtained by Wise (1997), using a smaller shear apparatus (60 x 60 mm), of type shown in *Fig 3.1(c)*), as well as the 100 x 100 mm shear apparatus analogous to *Fig 3.1(b)*, yielded a non-linear τ_{max} - σ_n relationship shown in *Fig 3.2*. A uniformly graded Cape Flats sand (C_u = 2.26) and a non-woven needle punched geotextile were used at applied normal pressures of 50kPa to 350kPa. Shearing was undertaken at a displacement rate of 0.61mm/min.

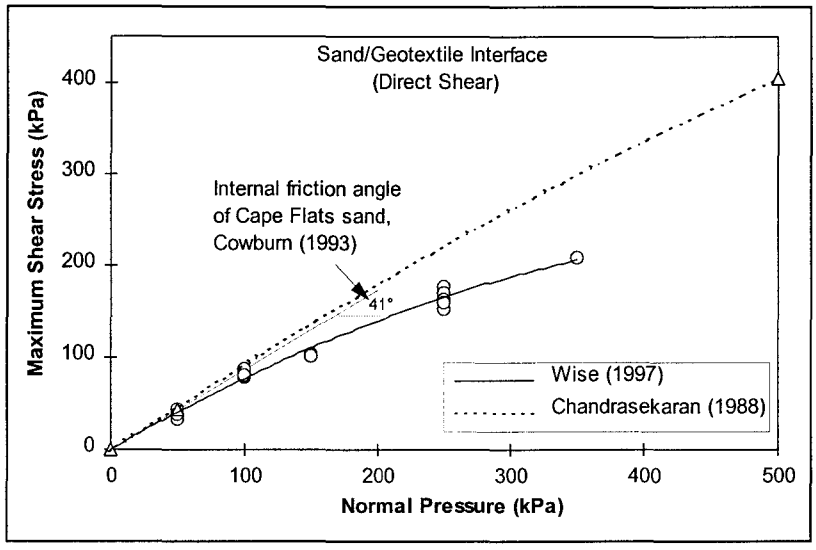

Fig 3.2 Maximum interface shear stress versus normal pressure relationship

It is clear that the trend curve (shown in a solid curve) was non-linear i.e. the friction coefficient was not constant throughout the range of the tested confining pressures. The angle of the slope of a tangent to this trend curve at the origin, was the same as the internal friction angle of the Cape Flats sands. Thus, according to those results, the soil/geotextile interface shear strength is initially equal to the internal shear strength of the soil at very low applied normal pressures, but reduces as the confinement increases. Dembicki et al. (1987) and Chandrasekaran (1988) obtained a non-linear relationship as well. Dembicki et al. (1987) used a non-woven geotextile with sand while Chandrasekaran (1988) used a woven geofabric with sand.

In summary, the results suggest that the maximum shear stress to normal pressure curve varies with the type of geotextile material; woven or non-woven. The relationship is generally linear under low normal pressures, but becomes non-linear at very high pressures (starting at approximately σ_n = 200kPa). It is therefore important to simulate the site specific loading conditions when running the test. In addition, the maximum shear stress to normal pressure relationship has been observed not to be influenced by the rate of testing. In practice, though, soil is very rarely of the type used by Myles (1982) in his experiments, which was mainly a very uniform coarse sand. Although the recommendation for construction of geotextile reinforced soil structures requires selected free draining backfill material, the rates of strain may in fact have some relevance since the applied stress may not be the effective stress. According to Yazdani (1996), the rate of displacement, should be such that no pore water pressure, positive or negative, builds up at the geotextile/soil interface during testing.

3.2.3 Interface friction angle

The *interface friction angle* is defined as the angle the maximum soil/geofabric interface shear stress, τ_{max}, and normal applied pressure, σ_n, line makes with the horizontal axis. The intersection of the τ_{max} - σ_n line with the vertical axis gives the *interface adhesion*. According to Coulomb's law, friction is obtained in terms of a friction angle and an apparent cohesion. Therefore, in a soil/geotextile system, the shearing resistance is of most importance to designers of geotextile reinforced soil structures and is composed of two components, the *interface friction angle* and *interface adhesion*.

The soil/geotextile interface friction angle, denoted by δ, has been evaluated by several researchers (e.g. Myles, 1982; Miyamori et al., 1986; Dembicki et al., 1987; Chen et al., 1990) as indicated in *Table 3.1*.

The investigation by Myles (1982) for the soil/geotextile interface friction, demonstrated that the interface friction angle varied with the type of geotextile material; woven and non-woven used. The same research work showed that there was no significant influence on the interface friction angle for investigated displacements rates of 10, 25, 75 mm/min.

Miyamori et al. (1986) also investigated the soil/geotextile interface friction of non-woven fabric with direct shear tests. The interface friction angle was found to be lower than the angle of internal friction, ϕ', of the investigated soil as determined by direct shear tests. For dense sand, the sand/geotextile interface friction angle was only 0.72 to 0.87 of the peak shear strength of the sand. Those results were confirmed by Venkatappa et al. (1990) who also obtained a lower interface friction from the interface direct shear tests, than the soil internal friction angle.

Unlike Miyamori et al. (1986) and Venkatappa et al. (1990), Garbulewski (1990) obtained a soil/non-woven geotextile interface friction angle which was equal to the internal friction angle of the soil. However, when Garbulewski (1990) used a woven geotextile, the interface friction was lower than the soil internal friction angle. It should be noted that the Garbulewski (1990) investigation dealt with a silty clay soil compared to sandy soils used by the other two researchers.

Dembicki et al. (1987) observed that the obtained interface friction decreased with increasing normal stress. Their interface test data indicated that the size of the shear frame affects values of the interface friction angle. Interface angles obtained for the same sand, non-woven geotextile and normal stresses in the small shear frame were lower than those from the large frame. The difference between the maximum shear stress obtained from tests on the same geotextile and sand in the large and small frames increased as the normal stress increased.

Chandrasekaran's (1988) study also showed that the interface friction angle of the investigated angular sand and woven fabric, decreased with increasing normal pressure from about 41° at low

normal pressure (50kPa) to about 32° when the normal pressure was about 500kPa (refer to *Fig 3.2*). The angle of internal friction angle of the sand as determined by drained triaxial tests was 39°. The reduction of the interface friction angle with increasing confining pressure was thus substantial. His work, unlike that of Dembicki et al. (1987) and Wise (1997), dealt with a woven geofabric.

Generally, past studies have shown that the interface friction angle, δ, is higher under low normal pressures. Research studies reviewed in this subsection have confirmed that values of interface friction angle obtained from the direct shear tests, are lower than the soil internal friction angle, ϕ'. Test data also indicated that the size of the shear frame affects values of the interface friction angle; small samples give lower interface friction angles. It is thus imperative, that the size of the interface direct shear test box be standardised so as to have the same framework of reference for comparison of results from different researchers.

3.2.4 Friction angle ratio

The friction angle ratio, usually denoted by α, is defined as the coefficient relating soil/geofabric interface friction angle, δ, to the angle of internal friction of soil, ϕ'. And is given as;

$$\alpha = \frac{\tan\delta}{\tan\phi'} \qquad (3.2)$$

This ratio has been investigated by some, e.g. Makiuchi et al., 1988; Saxena et al., 1985, in an attempt to determine if it is a constant for a specific geotextile product, irrespective of the soil in which it is confined.

The respective friction angle ratios calculated from different soils/geotextiles combinations, from work done in several studies investigated here, has been presented in *Table 3.1*. Each computed set of values only applies to the particular soil and geotextile product employed by a specific researcher.

There is no common trend regarding the magnitude of the ratio. The friction angle ratio fell within a fairly narrow range in some studies (e.g. Myles 1982), yet in others the range of values was greater (e.g. Chen et al., 1990). However, as earlier mentioned, a direct comparison of the different research results can not provide any meaningful contribution in view of the variation of soils, geotextile materials as well test apparatus used.

The results, therefore, confirm that the friction angle ratio, α, is not a constant of a specific geotextile product but a function of many parameters such as soil physical characteristics (Chen et al., 1990), soil/geotextile combination (Myles, 1982), size of the test apparatus, (Dembicki et al., 1987) and applied normal pressure (Chandrasekaran, 1988; Wise, 1997).

3.2.5 Mobilisation of shear stresses

Maximum shear stress obtained in direct shear tests occurs after a certain amount of horizontal displacement has taken place at the two interfaces. This displacement to the peak shear stress is called *shear stress mobilisation*.

Researchers have been keen to investigate the shear stress development at the soil/geotextile interface during testing in anticipation of predicting the geotextiles' performance in reinforced soils.

Saxena et al. (1985) investigated the shear stress mobilisation at the soil/geotextile interface for the woven and non-woven geotextiles in two modes of shear application; '*disturbed*' and '*undisturbed*'. In the so called '*undisturbed*' state, shearing was applied in the forward direction. While in the '*disturbed*' state shearing was in reversed direction. Three normal pressures were investigated; 69, 138 and 207kPa. Surprisingly, the shear stress development at the soil/geotextile interface, in both cases, reached the peak at a relatively large displacement of 15.2mm. The residual shear stress did not vary significantly from peak shear in both states for both types of geotextile. It was also observed that the shear stress, both at peak and residual, was generally lower in the disturbed state compared to the undisturbed state.

Makiuchi et al. (1988) investigated the shear stress mobilisation by conducting direct shear tests in various clays and sands using both woven and non-woven geotextiles. The results from their work were summarised as friction angle - shear displacement plots for different soil/geotextile combinations and are presented in *Fig 3.3*.

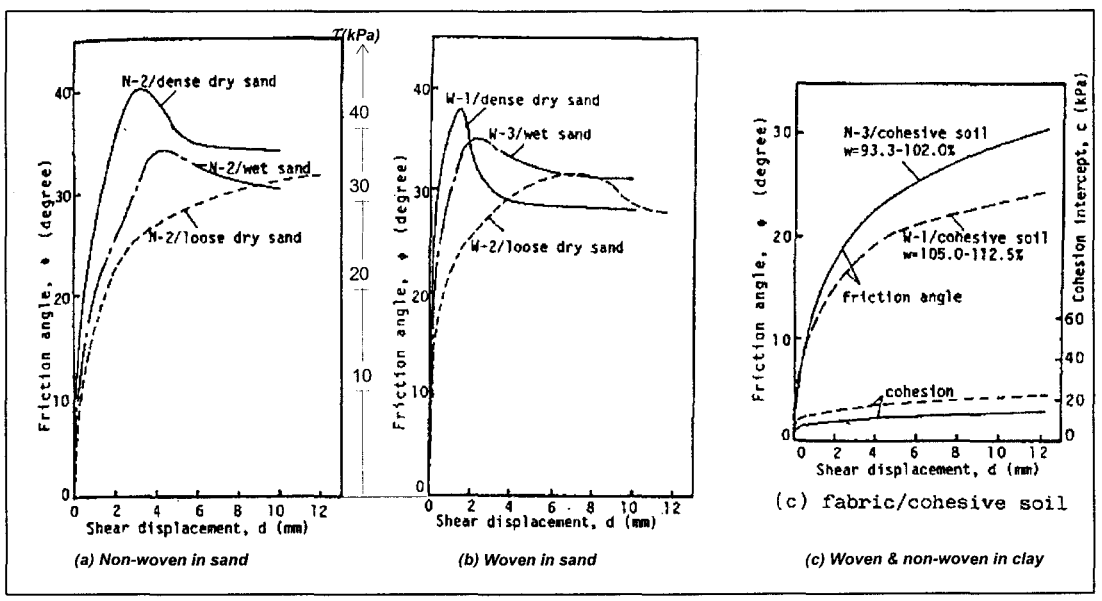

Fig 3.3 Friction angle versus shear displacement relationships for different soil/geotextile combinations (after Makiuchi et al., 1988)

Since at a constant normal pressure the friction angle is proportional to the shear stress, the plots in *Fig 3.3* are a direct reflection of the shear stress development. Tests were specifically conducted at an applied normal pressure of 50kPa.

The mobilisation of the shear stresses occurs over a relatively small shear displacement along both woven and non-woven geotextiles in dense sands; in either wet or dry states. The shear stresses have a sharp peak which decreases to a residual stress level indicated by a constant value after the displacement of about 6 mm. In loose dry sands, however, the plots showed smooth curves with the shear stress increasing gradually over a relatively longer displacement to a not clearly defined residual shear stress. It is also evident from the same plots, that an increase in moisture content of the sand delays (with respect to the displacement required) the appearance of peak shear stress of the interface. In cohesive soils, the shear stresses increase gradually but with no obvious peak during shearing.

In comparison, Saxena et al. (1985) observed a slower shear stress development, for both woven and non-woven geotextiles than Makiuchi et al. (1988). The peak shear stresses occurred at about 15.2 mm shear displacement compared to about 7 mm measured by Makiuchi et al. (1988). It should be noted that the density of the soil is partly responsible for the large displacements to peak shear (Makiuchi et al., 1988). This is because denser soils exhibit higher interface friction than loose soils (Yazdani, 1996). However, as highlighted before, there are many variables influencing the mobilisation of shear stress and the soil density alone can not account for the difference between the two studies.

A study into the effect of the rate of displacement on the shear mobilisation was undertaken by Myles (1982). Three test rates; 10, 25, 75 mm/min, were used. The test results indicated that the peak shear stress was independent of the rate applied. However, the same shear stress mobilisation graphs showed that the residual shear behaviour was highly dependent on the shear rate.

In summary, it is clear from the review of studies, both in woven and non-woven geotextiles, that the shear stress - displacement relationship is a function of the particular soil/geotextile combination, and that the denser the soil, the steeper the shear stress - displacement graph, and the higher the peak. The density used in testing should therefore be related to the degree of compaction required in the field. All the results seem to concur that residual shear stress does not vary significantly from peak shear, however, the strain rate affects this post peak behaviour patterns. There is evidence that an increase in moisture content of the soil delays the appearance of peak shear stress of the interface.

3.2.6 Effect of grain sizes on interface friction characteristics

Information on research into grain size effect is very scarce. The only investigation available, to the best of the writer's knowledge, was undertaken by Chen et al. (1990).

In their investigation of frictional characteristics between sandy soils and non-woven geotextiles, Chen et al., (1990) used a polyester, monofilament non-woven needle punched geotextile, 1 mm thick, and examined it in Fulong sand prepared with various fine contents. Fulong sand is an angular beach sand, mainly composed of quartz. In *Table 3.2* the direct shear test results of the non-woven geotextile with Fulong sand are listed.

Relative density (%)	Fine content (%)	ϕ' (°)	δ (°)	$\alpha = \frac{\tan\delta}{\tan\phi'}$
87	0	47	39	0.76
87	5	41	37	0.87
87	10	37	36	0.96

Table 3.2 Direct shear results from Chen et al. (1990)

At the same relative density of 87%, both the sand/geotextile interface friction angle, δ, and the internal friction angle of sand, ϕ', decreased when the content of fines in sand increased. From the results in the table, it is clear that sand/geotextile interface friction angle is less affected by the fine content of soil than the soil internal friction angle, i.e. the rate of decrease in ϕ' was higher than that in δ. Consequently, the interface friction angle ratio, α, increased with more fine contents.

That study shows that an increase of fines in a soil material results in a reduction of the friction strength at soil/geotextile interface. However, the interface friction angle ratio, α, increases with the increase in fine content since this increase affects the soil internal friction angle, ϕ' more.

3.2.7 Summary

The synthesis of the direct shear tests at the soil/geotextile interfaces has shown that a relatively wide range of soils and geotextiles materials with differing characteristics, have been used amongst the different research studies. It is evident from past research work, that the direct shear interface friction data is typical of a particular soil/geotextile material combination and interface properties.

Experimental studies concerning soil interaction with the geotextile in direct shear showed common tendencies as well as contradiction amongst the diverse research results. Wise (1997), using the same geotextile material as the one available for this study, obtained a non τ_{max} - σ_n linear

relationship which was a contradiction to most research results. This, therefore, prompted the conduction of carefully monitored tests, using a well designed modified direct shear apparatus. The literature review provided a sound basis for doing this.

The scarcity of material on the effect of soil grain sizes (as well as grading of the soil) at the soil/geotextile interface also prompted an investigation into the same. This is necessary especially in the selection of the backfill for reinforced soil structures.

The literature review also exposed the need to assess the feasibility of obtaining realistic and adequate interface friction parameters from direct shear tests, which can be used in design.

3.3 Pull-out tests of geotextiles

In operational circumstances the geotextile used in soil reinforcement is, at least partly, subjected to pull-out forces. In fact reinforcement can only occur if the geotextile can transfer the tensile forces to a stable soil mass in the resistant zone (*Section 2.7*). Consequently, the pull-out resistance phenomenon has been of interest to various researchers.

Pull-out test measurements have been reported from a variety of experimental configurations, ranging from field tests (e.g. Chang et al., 1977) to laboratory models (e.g. Schlosser et al., 1978) and pull-out boxes (e.g. Shen et al., 1979; Delmas, 1997). However, pull-out testing of geotextiles is at best difficult to accomplish and interprete particularly because of the extensibility of the geofabric. Some researchers like Dembicki et al., (1987), still prefer the direct shear test to the pull-out test for that matter.

Nevertheless, tests have been conducted (Bonczkiewicz et al. , 1988; Kharchafi et al., 1993; Forsman et al., 1994; Wise, 1997) to investigate the soil/geotextile interface behaviour as well as the pull-out resistance of geotextiles. This section reviews some of the relevant work in this field, and focuses on findings which are important to this study.

In the first instance, the different test set-up arrangements employed by the various research studies are discussed. This was deemed necessary since the essuing pull-out test results to a large extent are a function of the boundary conditions of the experimental set-up. This is followed by the computational approach used in calculation of the soil/geotextile interface friction. Findings related to the development of shear stress and the maximum shear stress - normal pressure relationship are then presented. Finally, other aspects such as the displacement distribution along the pull-out sample and the effect of grain sizes on the pull-out behaviour are also discussed.

3.3.1 Different test set-up arrangements

At present there are probably as many designs of apparatus used to investigate the pull-out resistance of geotextiles as the number of research projects on pull-out that have been conducted. In principle however, the different test set-up arrangements adopted by researchers can be divided into four main groups. The differences revolve around the transfer of load to the geotextile at the pull-out (sometimes referred to as front) end of the pull-out test device and the way the normal pressure is applied to the soil and the geotextile. The four different set-ups are shown schematically in *Fig 3.4*.

The first type of test set-up arrangement is the most basic of them all and was used by Palmeira (1987). Here, the geotextile sample extends from the inside of pull-out box and gets attached directly to the loading device (*Fig 3.4(a)*). It is assumed that the vertical boundary condition at the pull-out end, has little influence on the pull-out resistance measurement values. However, it is well

established (Abramento et al., 1995) that the front end condition significantly affects the measured pull-out resistance values. An alternative to this option where the geotextile test sample is being pulled-out through an intruded slot, is shown in *Fig 3.4(b)* (used by Juran et al., 1989). It basically involves the construction of a pair of stiff sleeves which extend into the soil mass.

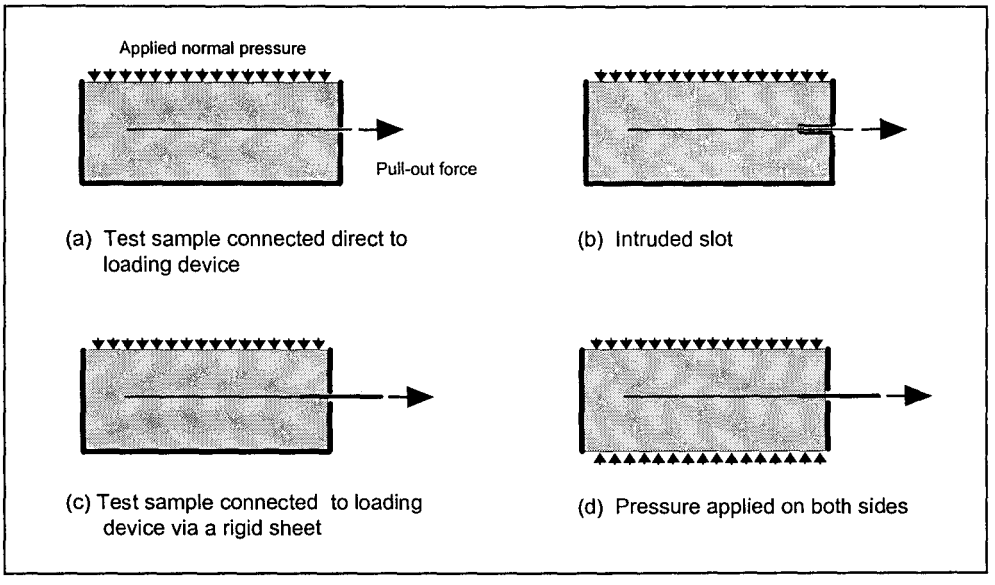

Fig 3.4 Schematics of typical pull-out test set-up arrangements

To ensure that the test specimen is subjected to the load within the soil mass under investigation, Tzong et al. (1987), contended that it was necessary for the whole geotextile specimen to be confined in the soil mass throughout the test. The set-up involves gluing the geotextile sample to a thin-rigid-smooth sheet which, in turn, is attached to the loading device (*Fig 3.4(c)*). The sheet stretches and extends into the soil. This ensures that the entire geotextile sample length remains confined in soil throughout the test.

The test apparatus of the three main groups already discussed had the shape of open containers in which the soil and the geotextile specimen were placed. The confinement was applied at the surface of the soil, thereby compressing the geotextile material and causing it to be more or less constrained laterally.

As a modification to these designs, Wise (1997) argued that in order to make sure that the pressure applied on the soil mass was close enough to that experienced at the soil/geotextile interface, confining pressure should be applied on both the top and bottom ends of the testing device, as shown *Fig 3.4(d)*.

The experimental test procedures in all four test arrangements, involve pulling-out a geotextile sample initially sandwiched between two soil layers. One end of the geotextile is normally free while the other is connected to a loading device. A pressure is applied at the outer boundaries of the soil layers, and is usually done on one side of the box (preferably top) by means of a rigid plate

(e.g. Rowe et al., 1985) or pressure bag (e.g. Juran et al., 1989). This implies that the soil/geotextile interface is loaded via the confined soil. A tensile force is then applied to the geotextile sample at a constant rate, causing it to interact with the soil. The pull-out force is incrementally measured until the test sample fails. The test is repeated for at least three different normal pressures.

In *Table 3.3*, a summary of the reviewed published work for soil/geotextile interface testing using the four pull-out apparatus set-up arrangements is presented.

Author	Test * set-up	Size of pull-out box (Length, Width, Height) (mm)	Size of geotextiles (Length, Width) (mm)	Soil / geotextile type	Confining pressures (kPa)	Studied influences of ...
Fourie et al., 1987	Direct (a)	60, 60, 30	Not reported	Clay / woven & non-woven	15 - 350	Geotextile type, normal pressure, moisture content
Tzong et at., 1987	Plate (c)	1219, 610, 1448	305, 460	Sand / non-woven	30	(only one test performed)
Bonczkiewicz et al. , 1988	Sleeve (b)	1350, 690, 460	1350, 610	Sand, gravel, silt, clay / woven, non-woven, etc.	14 - 103	Geotextile type, normal pressure, soil type
Bourdeau et al., 1990	Plate (c)	2900, 1100, 3000	1500, 850	Sand / non-woven	40	Geotextile type
Palmeira et al., 1990	Direct (a)	1000, 1000, 1000	500, 1000	Sand / non-woven	25 - 100	Geotextile type, normal pressure
Kharchafi et al., 1993	Plate (c)	800, 200, 550	500-800, 200	Sand , silt / non-woven	24 and 34	Geotextile stiffness, soil type, normal pressure
El-Mogahzy et al., 1994	Sleeve (b)	915, 610, 457	915, 102	Sand / non-woven	5 - 16	Geotextile type, normal Pressure
Forsman et al., 1994	Plate (c)	1800, 1000, 800	300-1350, 300	Sand, crushed rock, clay / woven & non-woven	15 - 70	Normal pressure, length, soil type
Abramento et al., 1995	Direct (a)	450,152,520	420, 133	Sand / non-woven	24.5	Pull-out strain rate
Wise, 1997	Plate (d)	288, 300, 50	150, 200	Sand / non-woven	25 - 225	Normal pressure

* Description of the test set-up refers to the various set-up arrangements described in *Fig 3.4*

Table 3.3 Summary of reviewed pull-out tests

3.3.2 Calculation of the soil/geotextile interface friction angle

Pull-out testing generally consists of measuring the force necessary to pull a geotextile test specimen out of a soil mass. This maximum force is commonly referred to as pull-out resistance, *F*.

In the standard interpretation of the pull-out tests, the apparent soil/geotextile friction coefficient, *tan* δ, is reported at the maximum pull-out resistance force, *F*, (Bourdeau et al.,1990). The pull-out interface characteristics are then evaluated by comparing the soil/geotextile interface friction angle, δ, (obtained from a variety of computation methods reviewed below), with the soil internal friction angle, ϕ'.

The soil/geotextile interface friction angle is calculated in a number of ways. Some researchers (e.g. Palmeira et al., 1990; Kharchafi et al., 1993; etc.) have concentrated on developing a method of obtaining the interface friction coefficient, ***tan*** δ, using the shear strength relation;

$$\tau = \sigma_n \cdot \tan\delta \tag{3.3}$$

where,

δ soil/geotextile interface friction angle

τ shear stress resistance acting along the soil/geotextile interface

σ_n applied normal pressure at the interface

And assuming that the pull-out resistance force, *F*, is evenly distributed over the entire surface area of the embedded geotextile, A_s , then the friction coefficient is given as;

$$\tan\delta = \frac{\tau}{\sigma_n} = \frac{F}{A_s \cdot \sigma_n} \tag{3.4}$$

According to various studies (Delmas et al., 1979; Bonczkiewicz et al., 1988), the resistance shear stresses along the geotextile specimen in the direction of pull-out, are not uniformly distributed over the surface area of the geofabric since the tensile strain decreases away from the point of application of the pull-out force. This implies that the assumption that at failure, the maximum pull-out resistance force, *F*, is evenly distributed over the entire surface area of the embedded geotextile is well beyond reality. It is therefore necessary to correct the shear area in order to obtain a more realistic friction angle.

Against that background, other researchers like Leshchinsky et al., (1987); Bonczkiewicz et al. (1988); Forsman et al. (1994) decided to use a modified method for calculating the interface friction coefficient.

$$\tan\delta = \frac{F}{2w(L_o + u)\sigma_n} \qquad (3.5)$$

where,

F maximum pull-out resistance force

w initial width of the geotextile sheet (assumed to remain constant)

L_o initial length of geotextile embedded in the soil

u extension of the geotextile sheet in loading direction

With δ and σ_n defined as before.

The method was referred to as '*modified*' because the calculated area was based on the portion of the sample that was being stressed.

Solomone et al. (1980) presented another methodology for obtaining the pull-out friction coefficient by finding an interaction parameter denoted by K_r. They defined K_r as the slope of the relationship between a pull-out resistance force and the mobilised embedded length of geotextile. It was based on the assumption that at any particular pull-out resistance force, only a certain length of geotextile is mobilised. The following relationship was established :

$$F = K_r \cdot L \qquad (3.6)$$

where,

K_r interaction parameter

L mobilised length

After substituting for F in *Equation 3.4*, the friction resistance coefficient is expressed as:

$$\tan\delta = \frac{K_r}{2 \cdot w \cdot \sigma_n} \qquad (3.7)$$

With w and σ_n as defined before.

On the other hand, in circumstances where the pull-out tests have not been conducted, or the test data being unreliable, the value of the soil/geotextile interface friction angle, δ, has been approximated to be equal to $\frac{2}{3} \cdot \phi'$ (Steward et al., 1977).

Bonczkiewicz et al. (1988) worked out and compared the values of the soil/geotextile interface friction angle, δ, using the above four computation methods. Three of the four methods used pull-out results from tests conducted with a poorly graded Fontainebleu sand of internal friction angle of 35°. And since one type of soil was employed in this comparison, it eliminated soil as a variable. The values of δ obtained by the four methods for a sampling of testing materials are given in *Table 3.4*.

Reinforcement	Elongation at P_{max} (%)	2/3 of ϕ' [a] (°)	Constant Area Method [b] (°)	Corrected Area Method [c] (°)	K_r Method [d] (°)
Coarse woven	20	22	28	29	23 - 27
Smooth woven	26	22	31	34	21 - 29
Needle punched non-woven	94	22	14	27	28
Heat-bonded non-woven	60	22	37	37	25 - 31
Extruded grid	12	22	33	33	11 - 23
Metal strip	0	22	63	N/A	N/A

[a] δ calculated basing on the assumption that its approximately equal to 2/3 of ϕ'
[b] δ calculated from Equation 3.4
[c] δ calculated from Equation 3.5
[d] range of δ calculated using K_r (Equation 3.7)

Table 3.4 Calculation of sand/geotextile friction angle using various equations (after Bonczkiewicz et al., 1988)

For most extensible materials the soil/geotextile interface friction angle, δ, values determined using the corrected area method were found to be greater than those determined using the constant area and K_r methods. The needle punched non-woven geotextile, the most extensible test material of them all (94% at failure), displayed approximately 100% variance between the constant area and corrected area methods. A range of values was reported for each test material when using K_r method demonstrating that this method highly depends on the correct approximations of the corrected and sliding areas. The data in *Table 3.4* therefore clearly indicates that it is possible to obtain a wide range of values for δ depending on the computation method used.

Generally, it has been shown that the method chosen for computation affects the obtained soil/geofabric resulting interface friction angle values. In addition, the more extensible the test material the greater the variance between the interface friction angle values obtained from the different methods.

3.3.3 Maximum shear stress versus normal pressure relationship

The mechanism of interaction in pull-out tests is controlled by shear stress mobilised between the soil and geotextile. Shear stress mobilised at the interface is defined as the ratio of the pull-out resistance force to the geotextile surface area over which it operates. The shear stress mobilised at peak pull-out resistance force, F_{max}, is known as maximum interface shear stress and is defined by the following equation;

$$\tau_{max} = \frac{F_{max}}{A_s} \qquad (3.8)$$

where,

F_{max} maximum pull-out force measured during the pull-out test

A_s shear area determined using one of the three methods described in *Section 3.3.2*

Fourie et al. (1987) investigated the maximum shear stress (τ_{max}) versus normal pressure (σ_n) relationship by conducting pull-test on both woven and non-woven geotextiles in silty clay with plastic index of 13%. The pull-out test speed was 0.9 mm/min for undrained tests and 0.0033 mm/min for the drained tests. Results obtained showed that the shear stress was essentially proportional to the normal pressure for both types of geofabrics at normal pressures below 150kPa. The linearity above 150kPa was however highly dependant on the moisture content. At a moisture content of 17.4%, the relationship remained linear. But at a clay moisture content of 14.8%, the relationship became non-linear above 150kPa. There was no substantial difference between drained clay and sand in pull-out soil/geotextile interaction, as would be expected. For drained tests, the woven geotextile had higher friction angle than the non-woven geotextile.

Palmeira et al (1990), using a pull-out box of the type shown in *Fig 3.4(a),* observed a linear τ_{max} - σ_n relationship for a woven geotextile in sand at confining pressures of up to 100kPa. The shear stress was calculated assuming that the shear area remains constant (*Equation 3.4* in *Section 3.3.2*). However, considering the test set-up arrangement used in the investigation, the geotextile test sample does pull out of sand as the test progresses thereby reducing the magnitude of the contact area between the geotextile and the soil progressively. This reduction in the test area affects the computated results of the maximum shear stress. Thus, little confidence was placed on the results from this study.

Forsman et al. (1994) also investigated the soil/geotextile interface friction behaviour during pull-out by conducting tests on both woven and non-woven geotextiles. The tests were performed in a pull-out box of the type shown in *Fig 3.4(b)* in highly compacted as well as in loose sands. A linear τ_{max} - σ_n relationship was observed for a sand/geotextile pull-out test at normal pressures up to 60kPa. For the loose sand, the gradient of the τ_{max} - σ_n relationship was only half that of the dense sand.

Wise (1997) using a uniformly graded Cape Flats sand (C_u = 2.26) and a non-woven needle punched geotextile, as well as a pull-out test apparatus analogous to *Fig 3.4(d)*, yielded a bi-linear τ_{max} - σ_n relationship. The inflection point of this relationship was at about 50kPa. The highest calculated maximum average interface shear stresses were in the order of 80kPa at confinements of 140kPa and above. This was the level of confinement beyond which that particular investigated geotextile failed in rupture.

Bonczkiewicz et al. (1988) performed pull-out tests in sand at normal pressures up to 103kPa. The τ_{max} - σ_n relationship was found to be non-linear for both woven and non-woven geotextiles. Generally, the maximum shear stress increased with an increase in the normal pressure until a limiting stress value was attained. After this, the increase in shear stress dropped significantly. The results were confirmed by Ingold (1985) who also observed a non-linear τ_{max} - σ_n relationship for

woven and non-woven geotextiles. El Mogahzy et al. (1994) obtained a highly non-linear τ_{max} - σ_n relationship for a non-woven geotextile in sand at normal pressures less than 16kPa.

In *Fig 3.5* a summary of the τ_{max} - σ_n relationships in various sands and types of geotextile, obtained by various researchers, is presented.

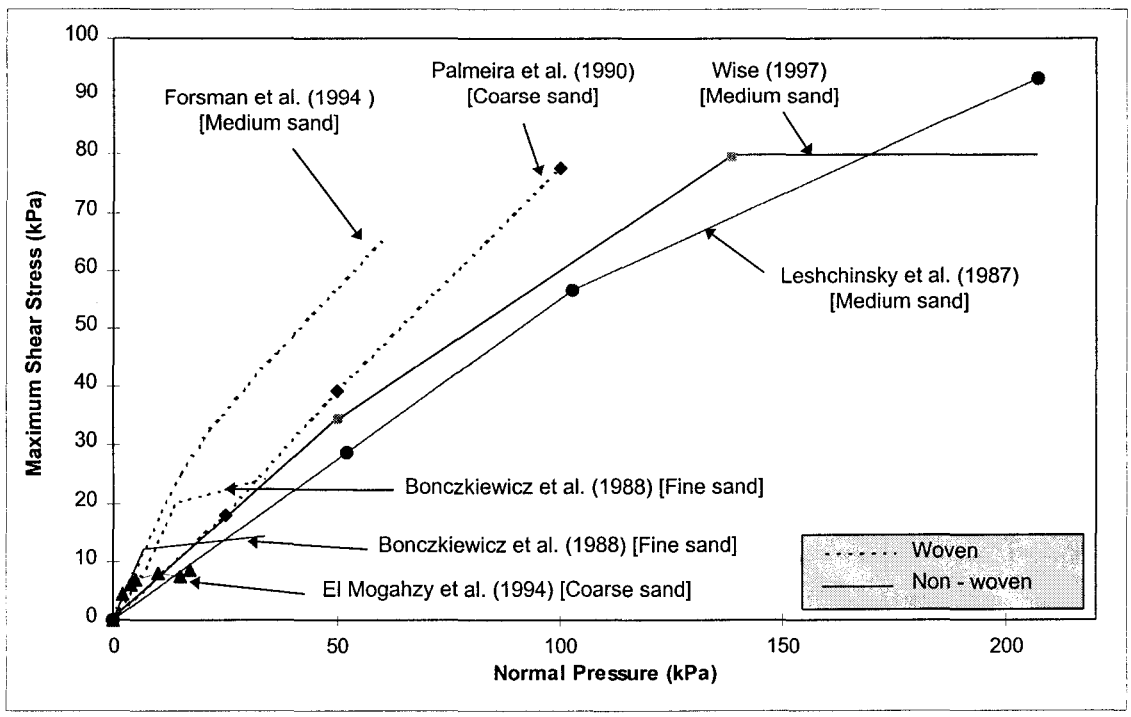

Fig 3.5 τ_{max} - σ_n relationships of geotextiles in sand as observed in pull-out tests conducted by various researchers

It is evident, from *Fig 3.5*, that the sand/geotextile used, has a significant influence on the τ_{max} - σ_n relationship. A direct comparison of the different research results, however, was not possible in view of the variation of soils, geotextile materials as well test apparatus used.

The majority of soil/geotextile combinations, with the exception of the researches by Bonczkiewicz et al. (1988) and El Mogahzy (1994), exhibited a linear τ_{max} - σ_n relationship below 100kPa. It is evident that that the τ_{max} - σ_n relationship is, among others, a function of the soil/geotextile combination. It can therefore be concluded that relationship is generally linear under low normal pressures (below 100kPa), but becomes non-linear at very high pressures.

3.3.4 Development of shear stress

Palmeira and Milligan (1990) produced plots comparing various geosynthetic materials and steel in terms of the friction angle ratio versus displacement. Pull-out friction angle ratio, α, is defined as :

$$\alpha = \frac{\tan\delta}{\tan\phi} = \frac{P}{A \cdot \sigma_n \cdot \tan\phi} = \frac{\tau_{ave}}{\sigma_n \cdot \tan\phi} = \frac{\tau_{ave}}{C} \qquad (3.9)$$

where,

δ soil/geotextile friction angle

ϕ internal friction angle of soil

P pull-out load

A area of contact between soil and geotextile

σ_n confining pressure

τ_{ave} average shear stress along the soil/geotextile interface

C constant when the confining pressure remains the same throughout the test

It is evident from *Equation 3.9*, that at a constant confinement, the friction angle ratio is proportional to the average shear stress. In *Fig 3.6*, the friction angle ratio versus displacement results for a normal pressure of 25kPa are shown. The corresponding average shear stress is shown on the right hand axis.

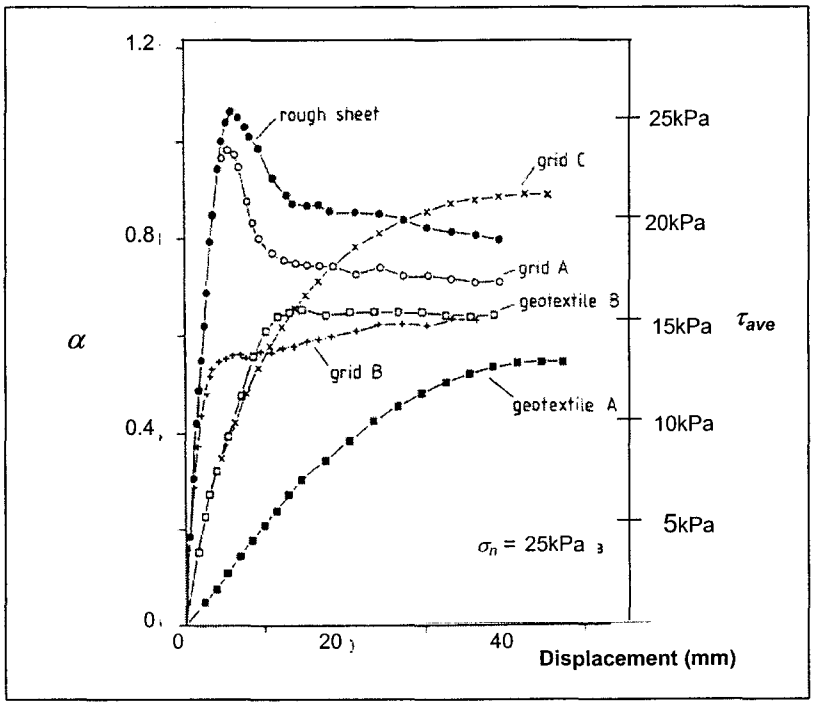

Fig 3.6 Bond coefficient versus displacement results (after Palmeira and Milligan, 1990)

From the plots, it is clear that the shear stress increases as the displacement of the clamped end of the geotextile increases. The metal sheets (described in the figure as *'rough sheet'*) displayed a sharp peak in the bond coefficient (shear stress), followed by a drop-off to a residual value. The geosynthetics, on the other hand, showed a gradual increase and levelling-off to the maximum shear stress. This gradual increase was also observed by other researchers (Tzong et al., 1987; Bonczkiewicz et al., 1988; Juran et al., 1988; Kharchafi et al., 1993 ; El Mogahzy et al., 1994; Forsman et al., 1994; Wise, 1997). A similar difference in pull-out behaviour of steel compared with a geotextile was recorded by Bourdeau et al. (1990). This difference in shear displacement patterns is a clear indication that the soil/geotextile interface behaviour is very different to the soil/steel interface behaviour.

Forsman and Slunga (1994) addressed the post peak interface shear stress behaviour of geotextiles in soil. At low normal pressures, a gradual shear stress drop-off after peak was observed. This drop-off became steeper as the normal pressure increased.

El-Fermaoui et al. (1982) proposed the that the shear stress is distributed along a certain front portion (length) of the geotextile. This portion, they termed it the mobilised length. They explained that as the pull-out force increases, the mobilised length increases until the shear stress is carried over the entire length of the geotextile. At this point the peak shear stress has been reached (the pull-out force is also at a maximum) and the entire sample begins to slip. In the post peak failure state, the shear stress is distributed uniformly over the whole length of the sample because of a re-orientation of the soil particles.

3.3.5 Geotextile displacement behaviour

Extensometers have been used by many researchers to measure the displacement of points along a geotextile sample during pull-out tests. From these measurements, three relationships have been determined (Wise, 1997). These are; the distribution of the displacement along the geotextile sample, the change in elongation (or stretch) of the geotextile as the pull-out load increases, and the displacement of the free end in relation to the pull-out force. The displacement of the free end is termed slippage.

By plotting the displacement measurements of various points along the geotextile, the displacement distribution was determined by Kharchafi et al. (1993) for non-woven geotextiles in a sand. The research showed that the displacement was distributed linearly along the sample at low pull-out forces. As the pull-out force increases, the displacement was found to re-distributed hyperbolically along the sample. A similar pattern was obtained by Juran et al. (1989) in tests performed on an instrumented geotextile reinforced model wall.

The elongation of various points along the geotextile as the pull-out load increased were determined by Tzong et al. (1987) for a non-woven geotextile placed in Ottawa sand. They observed that the

geotextile initially begins to elongate at the front end. As the pull-out load increases, the elongation progresses along the sample to the free end. The observation was confirmed by experimental data from Forsman and Slunga (1994). This behaviour results in the greatest elongation occurring at the clamped end and becoming less towards the free end.

From displacement measurements, researchers were also able to determine the manner in which the free end displaces (slips) during pull-out. Tzong et al. (1987) and Forsman et al. (1994) presented data for low confining pressures, indicating that the free end did not move throughout the duration of the test. Kharchafi et al. (1993), however, found that at a similar pressure, the free end displaced before the peak pull-out force was attained.

Abremento et al. (1995) presented a different approach to interpret the elongation in an extensible reinforcing element, which was termed the shear lag analysis.

Initially, the zone of sliding was said to progress from the clamped end of the geotextile. However, this analysis differs from that of Tzong et al. (1987) in that, prior to slippage of the entire sample, a slippage front propagates from the free end. Failure then takes place when these two slippage fronts meet. After the peak pull-out force has been attained, a snap back is observed. This occurs immediately when the whole length of geotextile is mobilised and the sheet rapidly shortens as the pull-out force decreases. This analysis was confirmed with pull-out tests. It must be noted that the test samples were nylon sheets of relatively narrow width (133 mm) and may not be representative of geotextiles in general.

3.3.6 Influence of the soil type on the pull-out behaviour

In order to determine the influence of the soil type on the pull-out behaviour of a geotextile material, Kharchafi et al. (1992) compared pull-out tests in both sand and silt. The tests indicated that the soil type has a significant influence on the pull-out interface friction angle. The sand/geotextile interface displayed a pull-out friction angle of 42° while the friction angle for the silt/geotextile interface was 18°.

Forsman et al. (1994) performed pull-out tests in a medium dense sand, crushed rock and a light expanded clay aggregate. The medium dense sand produced a friction angle half that of the dense sand. On the other hand, the clay aggregate exhibited a slightly higher friction angle compared with the dense sand. This was in contradiction with Kharchafi et al. (1992) who observed that a finer material produced a lower soil/geotextile friction angle. Also, the friction angle of the rock-geotextile interface was roughly the same as the clay/geotextile interface.

From these two studies, it is not possible to draw clear conclusions regarding the influence the soil type on the friction angle of the soil/geotextile interface.

3.3.7 Summary

The literature review has shown that a relatively wide range of studies involving the pull-out of geotextiles from various soil materials have been conducted. It has also exposed, that not much research has been conducted to investigate the effect of the soil characteristics on soil/geotextile interface behaviour. This review has provided a sound base to conduct tests on the subject.

3.4 Comparison between direct shear and pull-out tests

Comparing the results from the two interface tests, Venkatappa et al. (1990) found that the values of interface friction, δ_d, obtained from the direct shear tests, were lower than the soils' internal friction angle, ϕ, whereas δ_p values from pull-out were greater than δ_d, from direct shear and sometimes even greater than ϕ.

Contrary to Venkatappa et al. (1990) experimental results, the maximum interface shear stresses obtained by Wise (1997) from direct shear tests were greater than those obtained in the pull-out tests. That study showed that the interface friction angle δ_d obtained from pull-out tests was lower than δ_d obtained from the direct shear tests which was also lower than the soils' internal friction angle, ϕ.

Dembicki et al. (1987), based on their direct shear and pull-out interface test investigations, expressed an opinion that the direct shear test would be preferable to the pull-out tests as the standard test method since results of the pull-out test are difficult to interpret.

CHAPTER 4

RESEARCH MATERIALS

4.1 Introduction

This chapter discusses the materials used in the investigation which include the non-woven geotextile and the various sands. Three kinds of sands with different size ranges and grading were specifically selected: Cape Flats sand, Klipheuwel sand and Munich sand. Both Cape Flats and Klipheuwel sands were obtained locally while Munich sand originated from the Munich area in Germany.

The physical properties of the geotextile were obtained from the manufacturer's handbook, (Kaytech Geotechnical & Industrial Fabrics). A summary of those properties is presented in *Section 4.2*. Also included and relevant to this investigation, are test results previously conducted on the same fabric in the structural laboratory.

In order to fully understand the nature of the sand materials, mechanical and chemical tests were undertaken. The results are summarized and listed in various tables in this chapter. The soil mechanical properties of these sands are described and briefly discussed.

Finally, the results of the microscopic analysis undertaken on the research sand materials are presented in *Fig 4.5* and briefly discussed.

4.2 Physical properties of the selected non-woven geotextile

The geotextile used in this study was a light blue, thick non-woven geotextile with filtration properties, conformability and strength. It was a 100% polyester, continuous-filament needle punched fabric manufactured in Atlantis, Western Cape, South Africa, under the brand name '*Kaymat Geotextiles*'.

The manufacturer, Kaytech Geotechnical & Industrial Fabrics, graded the product according to its weight per square metre. In this investigation, a fairly heavy grade of 270g/m^2 (U34), with a specified tensile strength of 18kN/m was used.

By means of a Cambridge S200 microscope stationed at the Electron Microscope Unit of the University of Cape Town, a microscopic image of the non-woven geotextile specimen was obtained (shown in *Fig 4.1*). The filaments of the fabric can be seen entangled multi-directionally in order to afford all round multi directional support (strength). The holes in the geofabric's structure were

created by the needle punching process during manufacturing. The needle punching process was described in *Section 2.3.*

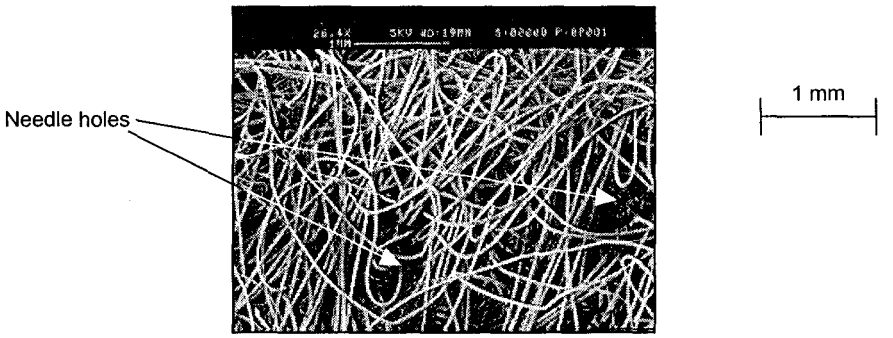

Fig 4.1 Micrograph of grade U34 non-woven geotextile

The specifications (published by the manufacturer) related to the mechanical properties of Grade U34 non-woven geotextile as well as the standards used for determining these specifications, are presented in *Table 4.1* below.

Property	Unit	U34	Standard*
Mass per unit surface	g/m^2	270	SABS 79
Thickness under normal stress of 0.5kPa	mm	2.30	SABS 85
Thickness under normal stress of 200kPa	mm	1.05	EDANA 30074
One-directional tension (50 x 200 mm)	kN/m	14	SABS 93
One-directional tension (100 x 200 mm)	kN/m	18	DIN 53857

*SABC : South African Bureau of Standards
*EDANA : European Disposables and Non-wovens Association
*DIN : Deutsches Institut fur Normung

Table 4.1 Properties of U34 non-woven geotextile (after Kaytech Industrial Fabrics, 1995)

According to the tests conducted by Wise (1997) as recommended in ASTM D1777-64, the thickness of the U34 Kaymat fabric material was found to vary significantly. It ranged from 2.10 mm to 2.35 mm. For a total number of 30 specimens the average thickness was 2.209 mm, with a standard deviation of 0.0659 mm.

Previous research work by Wise (1997) showed that the thickness of the test samples affects both the load - elongation modulus as well as the ultimate tensile strength of the geotextile specimen. Since these characteristics influence the consistency of the responses of pull-out tests (in terms of

pull-out load versus front displacement relationship and ultimate confined tensile strength of the geofabric), it was desirable to use only geotextile samples which fell within a defined thickness range. Thus, in order to eliminate these effects due to thickness, and at the same time maintain continuity with the previous work done using the same geotextile specimen, only geotextile specimens that fell within a thickness tolerance were selected. The thickness tolerance adopted by previous studies (Lai Sang, 1995; Wise, 1997) ranged from 2.18 mm to 2.24 mm.

The relationship between the thickness of the geotextile and the confining pressure, applied normal to the plane of geofabric, is shown in *Fig. 4.2*. The observed thickness at 2kPa was found to be 16% greater than the manufacturer's specification (see also *Table 4.1*). The manufacturer's specified thickness at greater confinements of 20kPa and 200kPa was therefore increased by this difference in the observed thickness in order to obtain a relationship between the fabric's thickness and applied normal pressure. This observed relationship curve was desired in the discussion of pull-out tests presented later in the thesis.

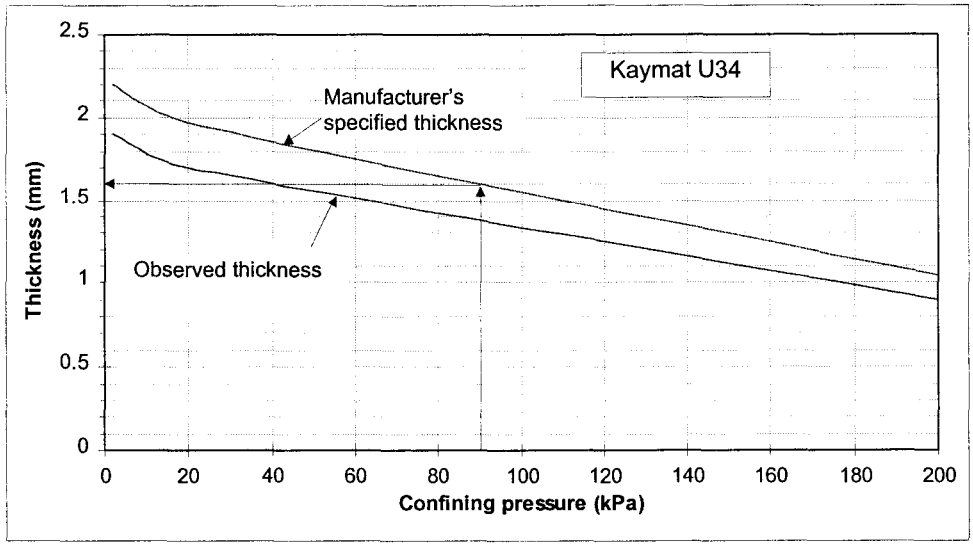

Fig 4.2 Variation of geotextile thickness with normal pressure (after Wise, 1997)

4.3 Mechanical properties of the selected soil materials

Three kinds of sand with different grain sizes and grading were selected for the study, namely: Cape Flats sand, Klipheuwel sand and Munich sand.

Cape Flats sand was subdivided in three particle size groups according to the British Standard subdivisions and were respectively referred to as;

Fine Cape Flats	→	0.063 mm to 0.25 mm,
Medium Cape Flats	→	0.25 mm to 0.6 mm, and
Coarse Cape Flats sands	→	0.6 mm to 2 mm.

Thus, it was hoped that the three extra sands of controlled grain size could be used to help establish the influence of grading and grain size on the interface behaviour of the geotextile used in this research.

The soil mechanical properties of all the sands were determined by conducting standard tests in the Geotechnical Laboratory of the Department of Civil Engineering, University of Cape Town. A summary of the results is presented in *Tables 4.2* to *4.4*. The aim of these tests was to fully investigate a range of each of the sands' properties. The experiments included the determination of specific gravity, dry density/optimum moisture content relationship, particles size distribution and shear strength in terms of angle of internal friction and cohesion. A brief description of the experimental procedures is attached in *Appendix A*.

The grading curves of the research sands are shown in *Fig 4.3*. No attempt was made to define the grain size distribution of the subgroups of Cape Flats sand (i.e. Fine, Medium and Coarse).

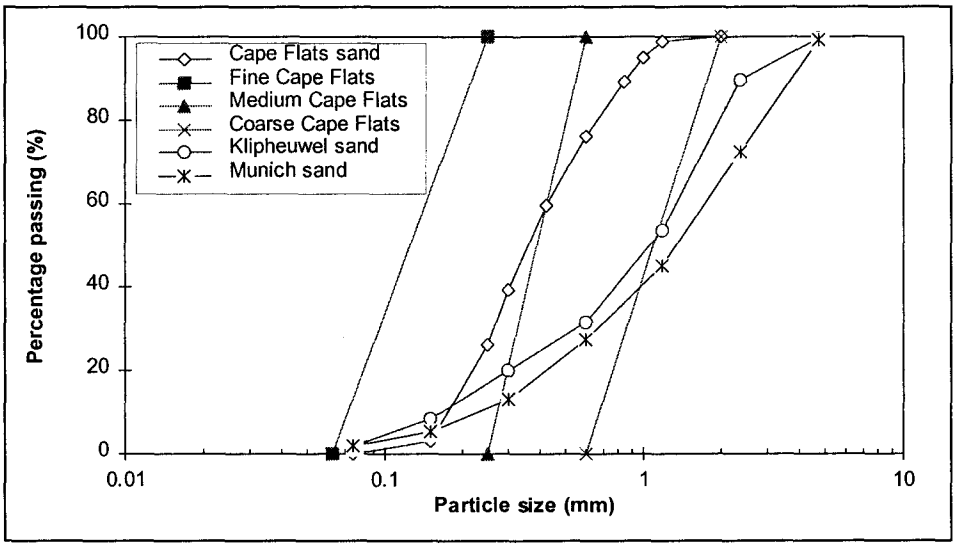

Fig 4.3 Grain size distributions of Cape Flats, Klipheuwel and Munich sands

The grading curves indicate that Cape Flats sand and all its subgroups are uniformly graded, while Klipheuwel and Munich sands are well graded sands containing particles of variety of sizes from fine silt to coarse gravel.

The dry density/optimum moisture content relationships of these research sands obtained in accordance to the standard proctor test procedure, were fitted (dashed lines) on characteristic compaction curves for typical soils (solid lines) published by Head (1980), and is shown in *Fig. 4.4*.

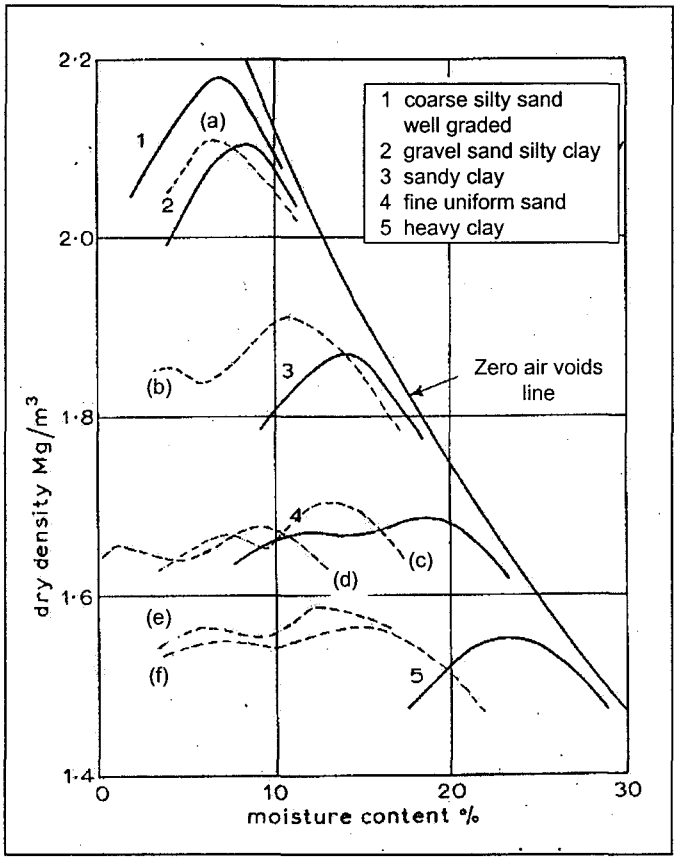

Fig 4.4 Compaction curves (after Head, 1980) and results for a) Munich b) Klipheuwel c) Cape Flats d) Coarse Cape Flats e) Medium Cape Flats f) Fine Cape Flats sands

The results show two distinct density peaks at two optimum moisture contents for each of the investigated sands except the Munich sand. For the purposes of selecting a suitable density for the sands in the direct shear and pull-out tests to be undertaken, it was decided to compact the sand at the optimum moisture content closest to the natural moisture content of the particular sand material under consideration. In addition, throughout the research, preparation of the test sand samples was aimed at achieving the approximate maximum dry density compaction conducted at the respective selected optimum moisture contents. The respective maximum dry densities and optimum moisture contents were obtained from these curves.

4.3.1 Cape Flats sand

The sand is a medium dense, light grey, clean quartz, subround-grained (see also *Fig. 4.5*) silty aeolian sand that originated from the Cape Flats, near Cape Town. Based on the sieve analysis, the uniformly graded sand has grain sizes varying between 0.063 mm and 0.2 mm with a coefficient of uniformity of 2.3.

Chemical tests conducted by applying drops of hydrochloric acid to the sand, revealed that it contains traces of calcite which cements the sand particles together.

Direct shear tests performed on the sand to obtain the shear properties yielded an angle of internal friction, ϕ', of 41° with an apparent cohesion, c', of 2.8 kN/m^2 at an average dry density of 1650 kg/m^3 and a moisture content of 7%.

Physical tests were also conducted for the different Cape Flats sand subgroups. The results showed that Fine Cape Flats sand had the least shear strength of 36.5° with an apparent cohesion, c', of 6.5 kN/m^2 at an average dry density of 1520 kg/m^3 and a moisture content of 8%. It was followed by Medium Cape Flats sand with an angle of internal friction, ϕ', of 38° with an apparent cohesion, c', of 5.3 kN/m^2 at an average dry density of 1550 kg/m^3 and a moisture content of 6%. Coarse Cape Flats sand with the angle of internal friction, ϕ', of 40.5° and an apparent cohesion, c', of 2.1 kN/m^2 having an average dry density of 1650 kg/m^3 and a moisture content of 8.8% had the highest shear strength. The higher shear strength in Coarse Cape Flat sand is a reflection of its texture.

The cohesion is due to capillary forces acting between the grains. The higher cohesion value in Fine Cape Flats sand can be attributed to higher capillary forces acting between the fine grains.

The results showed almost the same value of residual shear strength, ϕ_r', for Cape Flats sand and all its subgroups despite the difference in grain size distributions.

A summary of the soil mechanical properties of Cape Flats sand and the respective subgroups is provided in *Table 4.2*.

Property	Unit	Cape Flats	Coarse Cape Flats	Medium Cape Flats	Fine Cape Flats
Specific Gravity, G_s	-	2.67	2.67	2.67	2.67
Natural moisture content	%	3.1	3.1	3.1	3.1
Optimum moisture content, (Proctor)	%	7.0	8.8	6.0	8.0
Maximum dry density, (Proctor)	kg/m^3	1660	1670	1572	1542
Average dry densest state	kg/m^3	1765	1758	1679	1632
Average dry loosest state	kg/m^3	1487	1547	1477	1428
Particle range	mm	0.063 - 2	0.6 - 2	0.25 - 0.6	0.063 - 0.25
Mean grain size, D_{50}	mm	0.365	1.300	0.425	0.157
Coefficient of uniformity, C_u	-	2.26	1.93	1.56	2.08
Coefficient of gradation, C_g	-	0.62	0.82	0.86	0.78
Angle of friction, ϕ'	degrees	41	40.5	38	36.5
Residual shear strength, ϕ_r'	degrees	30	30	29	29
Cohesion, c'	kN/m^2	2.8	2.1	5.3	6.5

Table 4.2 Soil mechanical properties of Cape Flats sand and the respective subgroups

4.3.2 Klipheuwel sand

Klipheuwel sand is a medium dense brown, slightly silty, fine to coarse gravelly sand. It is a well graded sand, as shown previously in the grading curves diagram in *Fig 4.3*, with the coefficient of uniformity of 8.2. Its grain sizes vary between 0.075 mm and 4.75 mm. The specific gravity of this sand is 2.70.

The standard proctor test provided a maximum dry unit weight of 1915 kg/m^3 at an optimum water content of 10.8%. The angle of internal friction obtained from direct shear tests was 54° with an apparent cohesion of 5.3 kg/m^2 at an average dry density of 1890 kg/m^3 and a moisture content of 10.8%. The residual friction angle, obtained at the same test conditions, was 35°.

Chemical tests conducted using drops of hydrochloric acid on the sand (as in Cape Flat sands) revealed no traces of $CaCO_3$.

The mechanical properties determined in the laboratory tests are presented in *Table 4.3*.

Property	Unit	
Specific Gravity, G_s	-	2.70
Natural moisture content	%	4.0
Optimum moisture content, (Proctor)	%	10.8
Maximum dry density, (Proctor)	kg/m^3	1915
Particle range	mm	0.075 - 4.75
Mean grain size, D_{50}	mm	1.15
Coefficient of uniformity, C_u	-	8.24
Coefficient of gradation, C_g	-	1.27
Angle of friction, ϕ'	degrees	54
Residual shear strength, ϕ_r'	degrees	35
Cohesion, c'	kN/m^2	5.3

Table 4.3 Soil mechanical properties of Klipheuwel sand

4.3.3 Munich sand

Munich sand is a medium dense light grey, silty, slightly gravelly, well graded, subround-grained quartz sand that originated from the Munich area, Germany. Its coefficient of uniformity is 7.8.

Chemical tests revealed traces of calcite in the sand. Soil mechanical tests also showed that it had the highest specific gravity of 2.76. The standard proctor test provided the optimum water content of 8.7% with the maximum dry unit weight of 2040 kg/m^3.

The angle of internal friction obtained from direct shear tests was 48.5° with an apparent cohesion of 8.2 kN/m^2, at an average dry density of 2010 kg/m^3 and moisture content of 8.7%. The residual

friction angle was the same as the one for Klipheuwel sand despite the differences in soil mechanical properties.

A summary of the soil mechanical properties of Munich sand as obtained from the laboratory experiments is presented in *Table 4.4*.

Property	Unit	
Specific Gravity, G_s	-	2.76
Natural moisture content	%	4.12
Optimum moisture content, (Proctor)	%	8.7
Maximum dry density, (Proctor)	kg/m^3	2040
Average densest state of sand	kg/m^3	2070
Average loosest state of sand	kg/m^3	1690
Particle range	mm	0.075 - 4.75
Mean grain size, D_{50}	mm	1.4
Coefficient of uniformity, C_u	-	7.8
Coefficient of gradation, C_g	-	1.12
Angle of friction, ϕ'	degrees	48.5
Residual shear strength, ϕ_r'	degrees	35
Cohesion, c'	kN/m^2	8.2

Table 4.4 Soil mechanical properties of Munich sand

4.4 Micrographs of the various research sand materials

A thorough study of the physical structure of the research sands was considered a priority before any of these materials could be used in this research. Photomicrographs of representative samples of each sand material were taken. The magnification used was both low enough to include as many grains as possible in each photomicrograph and high enough to make the finest sand fractions visible. *Fig 4.5* shows a representative set of photomicrographs of the various sand materials using a Cambridge S200 microscope. The magnification is not the same in the different figures. A brief description of the observations follows:

- **Cape Flats sand** (*Fig 4.5(a)*)

consists of uniformly sized grains of clean quartz, with the larger grains fairly rounded and elongated, while the medium sized particles are sub-angular.

- **Coarse Cape Flats sand** (*Fig 4.5(b)*)

is a clean, very uniformly sized quartz sand. The grains are elongated with smooth radially orientated edges.

♦ **Medium Cape Flats sand** (*Fig 4.5(c)*)

is also a very uniformly sized quartz sand, with sharp edged, shell (plate) like, sub-angular grains. It appears that the grains are crushed coarse particles.

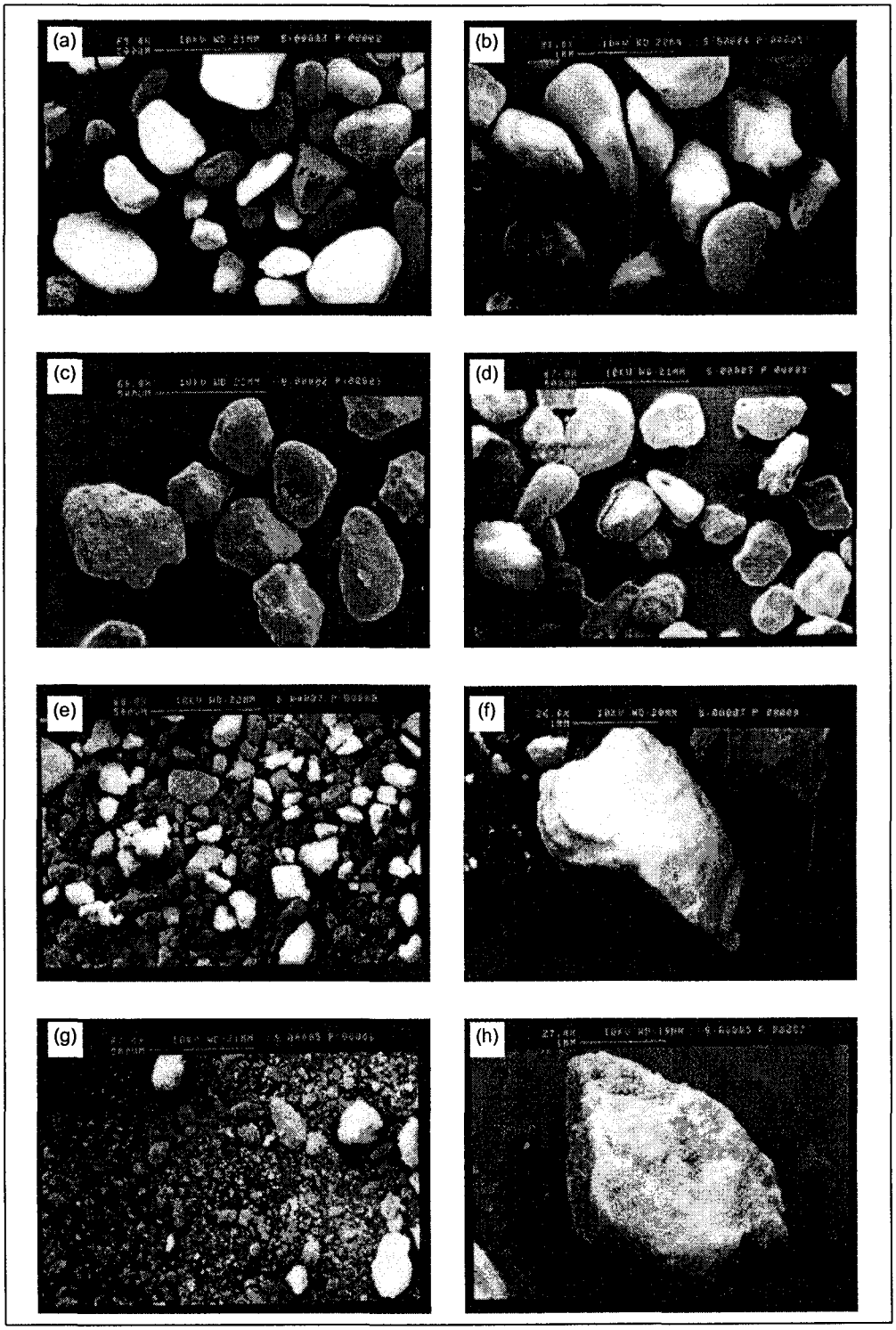

Fig 4.5 Photomicrographs of sand particles a) Cape Flats sand b) Coarse Cape Flats sand c) Medium Cape Flats sand d) Fine Cape Flats sand e) and f) Klipheuwel sand g) and h) Munich sand

- **Fine Cape Flats sand** (*Fig 4.5(d)*)

is a quartz sand which consists of very fine, very uniformly sized, plate-like, sub-angular grains.

- **Klipheuwel sand** (*Fig 4.5(e)*)

is a very coarse-grained, well graded quartz sand, with an abundance of big diameter fragments (see *Fig 4.5(f)*). A moderate amount of fine material is present. Visual observation of the photomicrographs clearly reveals that the sand is generally composed of '*broken*', sharp edged, angular grains with fractured surfaces.

- **Munich sand** (*Fig 4.5(g)*)

is fairly well graded with traces of coarse angular big diameter fragments (see *Fig 4.5(h)*). Traces of fine material sticking onto the fairly edged angular coarse grain can also be seen. The presence of these fine particles gives the sand its *gritty-sticky* texture.

CHAPTER 5

DIRECT SHEAR INVESTIGATION

5.1 Introduction

This chapter deals with the measurement of the shear strength at the sand/sand, sand/geotextile and geotextile/geotextile interfaces in the laboratory.

The direct shear investigation involved the sliding of sand on sand, and sand on geotextile. The sliding of the geotextile on geotextile was also included, in order to assess how the geotextile/geotextile interface shear strength behaviour compares with the other two interface combinations. This was necessary since in a geotextile reinforced soil structure, there are short structural sections where the two geotextile surfaces overlap.

The sand on sand tests were conducted using a 100 mm square *Wykeham Farrance SB1* constant rate of strain shear apparatus as shown in *Fig 5.1*, and were done according to BS 1377: Part 7: 1990. A brief description of the test procedure appears in *Appendix A*. In this chapter, only the direct shear test procedures for the sand/geotextile and geotextile/geotextile interfaces are presented.

The six different types of sands, used in the investigation were; Cape Flats, Coarse Cape Flats, Medium Cape Flats, Fine Cape Flats, Klipheuwel and Munich sands.

Full details of the test results and their discussions are presented in *Chapter 7*.

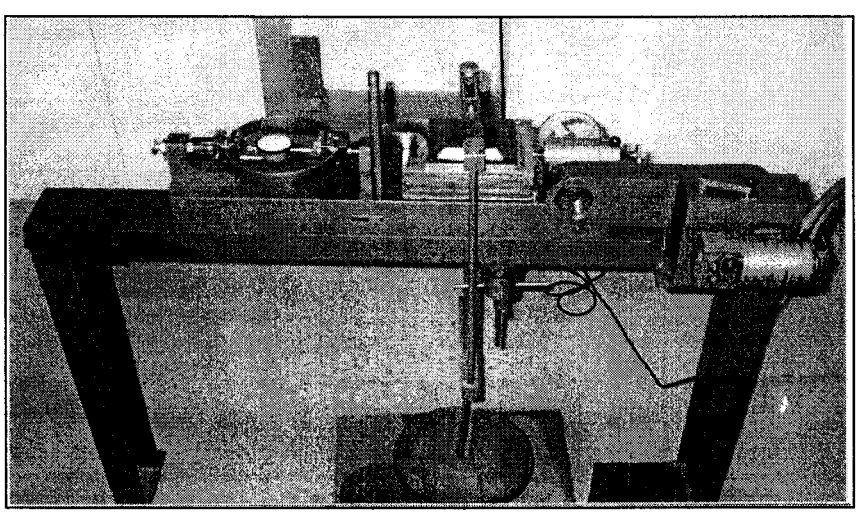

Fig 5.1 Wykeham Farrance SB1 constant rate of strain shear apparatus

5.2 Direct shear test program

In total, forty direct shear tests were conducted at three normal pressures, namely 25, 50, and 100kPa. Eighteen of those involved sand only (*SS*) while another eighteen were interface tests, sand and geotextile (*SG*). Three tests were undertaken investigating the shear of geotextile on geotextile (*GG*). One '*zero*' test, in which an '*empty*' top frame of the shearbox was sheared on a geotextile sheet, was also performed. The complete test program is listed in *Table 5.1*.

The following subsections describe the test procedures of the interface studies in detail.

Test	Research material	Test number	Normal pressure (kPa)	Dry density (kg/m^3)
Sand-sand	Cape Flats sand (C)	SS/C25 SS/C50 SS/C100	25 50 100	1648 1653 1649
	Coarse Cape Flats sand (Z)	SS/Z25 SS/Z50 SS/Z100	25 50 100	1650 1654 1647
	Medium Cape Flats sand (M)	SS/M25 SS/M50 SS/M100	25 50 100	1547 1552 1553
	Fine Cape Flats sand (F)	SS/F25 SS/F50 SS/F100	25 50 100	1522 1515 1519
	Klipheuwel sand (K)	SS/K25 SS/K50 SS/K100	25 50 100	1891 1887 1893
	Munich sand (X)	SS/X25 SS/X50 SS/X100	25 50 100	2011 2013 2009
Sand-geotextile	Cape Flats sand and geotextile	SG/C25 SG/C50 SG/C100	25 50 100	1648 1647 1645
	Coarse Cape Flats sand and geotextile	SG/Z25 SG/Z50 SG/Z100	25 50 100	1651 1650 1649
	Medium Cape Flats sand and geotextile	SG/M25 SG/M50 SG/M100	25 50 100	1551 1544 1543
	Fine Cape Flats sand and geotextile	SG/F25 SG/F50 SG/F100	25 50 100	1520 1515 1517
	Klipheuwel sand and geotextile	SG/K25 SG/K50 SG/K100	25 50 100	1891 1886 1894
	Munich sand and geotextile	SG/X25 SG/X50 SG/X100	25 50 100	2003 2007 2009
Geotextile-geotextile	Geotextile (A)	GG/A25 GG/A50 GG/A100	25 50 100	Not applicable
Steel frame - geotextile	Top frame of the shearbox on geotextile	BG/01	0	Not applicable

Table 5.1 Direct shear test program

5.3 Direct shear test of sand/geotextile interface

The sand/geotextile investigation utilised a 100 mm by 100 mm *Wykeham Farrance* SB1 constant rate of strain shear apparatus modified to allow the inclusion of a non-woven geotextile, as shown in *Fig 5.2.* The modification was in such a way as to facilitate a constant contact area between the soil and geotextile throughout the test. Although BS 8006:1994 recommends that the standard tests be carried out in a 300 mm square size shearbox, this research was limited to a 100 mm by 100 mm sand shear area due to a lack of adequate facilities.

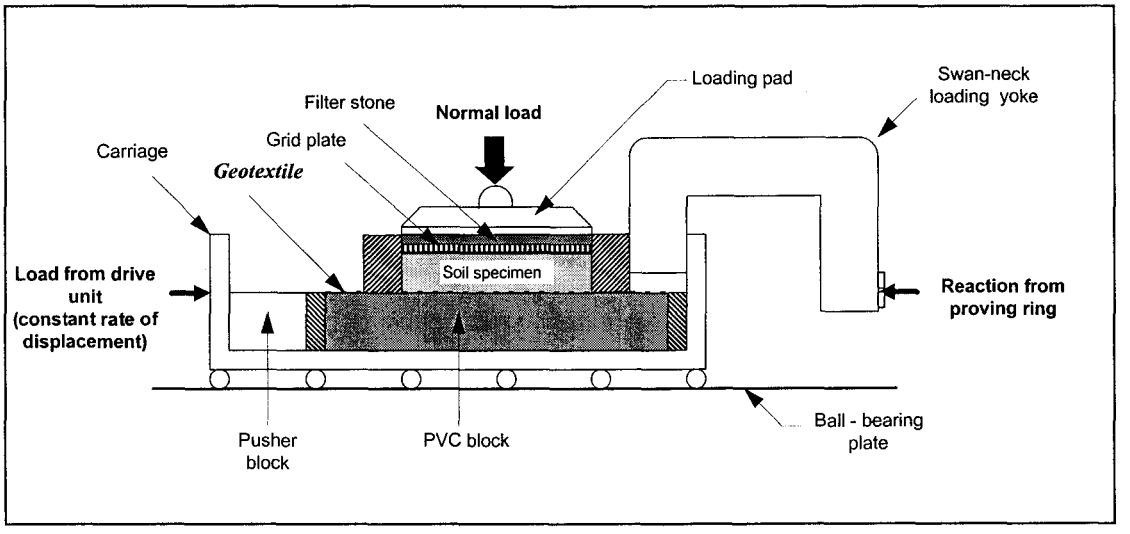

Fig 5.2 Arrangement of modified direct shear test apparatus

A 100 mm by 100 mm sand specimen, occupying the top half of the shearbox (a rigid top metal frame), was prepared to slide along the non-woven geotextile surface by the action of a constant rate controlled horizontal shearing force, while a constant normal load was applied (via a yoke and hanger) to the plane of relative movement, as shown in *Fig 5.2.*

Test conditions were achieved by first compacting the sand to approximately its maximum dry density, in the rigid top metal frame, square in plane, '*sitting*' on the geotextile which had been carefully stretched and fixed onto a PVC block. The various test components are shown in *Fig 5.3.*

During the shearing process, the relative displacement of the top metal frame and geotextile, and the applied shearing force were monitored, thus enabling a plot of the respective load/displacement relationship.

In each sand category, investigations were conducted at three normal pressures; 25, 50 and 100kPa, at a displacement rate of 1.2 mm/min.

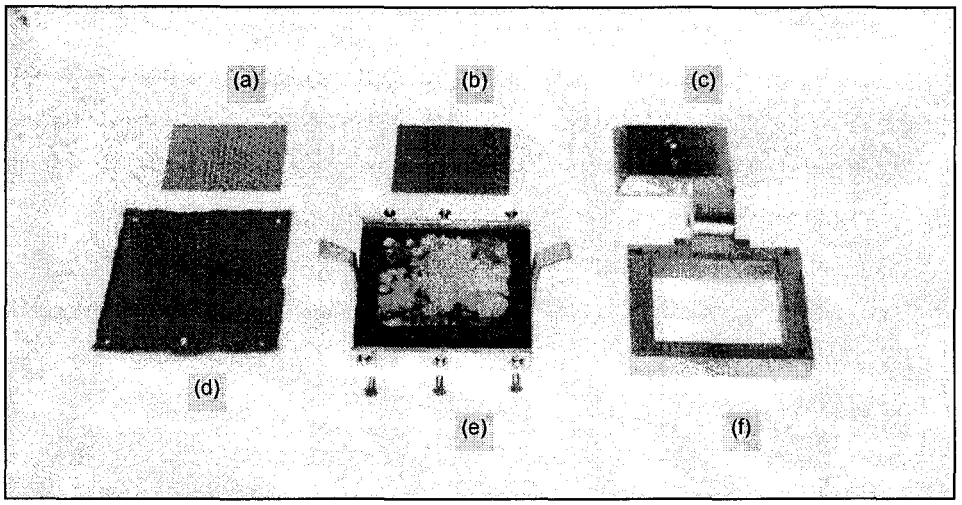

Fig 5.3 Component parts of the sand/geotextile shear test; (a) perforated grid plate (b) filter stone (c) loading pad (d) geotextile (e) bottom half (f) top metal frame of a shearbox

5.3.1 Preparation of geotextile test specimen

Test samples were cut from an industrial geotextile roll and were each trimmed to a length of 188 mm and a width of 138 mm in order to fit onto the PVC block whose dimensions were 142 mm by 138 mm and 23 mm in height. In a slightly but carefully stretched mode, the geotextile specimen was fixed on both ends of the block with the help of screws (three at each end) and aluminium plates, as shown in *Fig 5.4*. Prior to this, a grade *P80* sand paper had been glued onto this PVC block using a double sided tape. This was to simulate in-situ friction characteristics between the geotextile and the soil underneath. The geotextile test direction was in accordance with the industrial machine production direction.

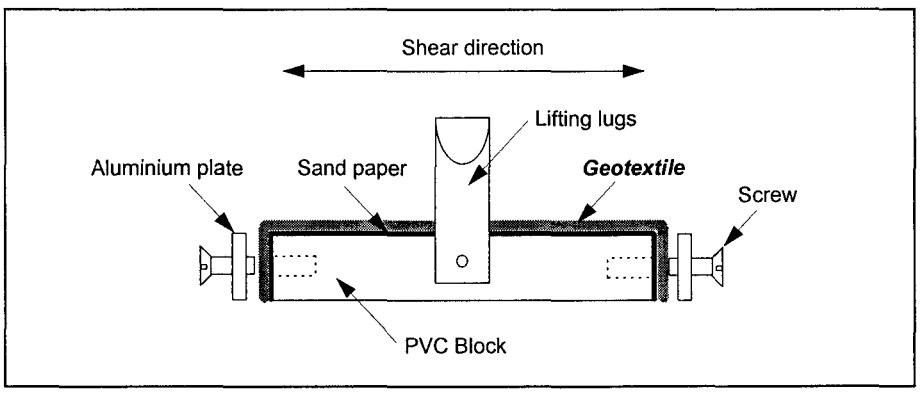

Fig 5.4 Cross-section of bottom half of modified direct shear test apparatus

The PVC block, with the attached geotextile specimen, was placed inside the carriage. Wedges were used to ensure that it was properly fixed in position and to prevent any movement during compaction and testing. The upper half of the shearbox (top metal frame), fitted with a 'swan-neck yoke', was then gently placed on the geotextile surface. Another set of wedges was used to keep this rigid top metal frame in place in order to avoid movement during handling and compaction.

For each sand category under investigation, test samples were mixed with the predetermined mass of water to obtain the optimum moisture content (refer to *Tables 4.2* to *4.4*). As a check, three small wet samples were obtained, weighed and dried in the oven for at least 24 hours. By weighing the dry samples, the average moisture content of each test sand batch was determined in accordance with BS 1377: Part 2: 1990 (see *Appendix A.3* for the procedure). A known mass of soil was then placed in the rigid metal frame in two equal layers. A 4 mm thick solid plate covering the entire soil area was placed gently on top of each layer before being subjected to ten tampings with a hand tamper, as schematically shown in *Fig 5.5*. The hand tamper consisted of a metal rod attached to a solid rectangular plate with a drop weight of 2.325 kg. Each layer received 10 drop weight blows from a height of 100 mm. The exact amount of compaction had previously been determined by trial.

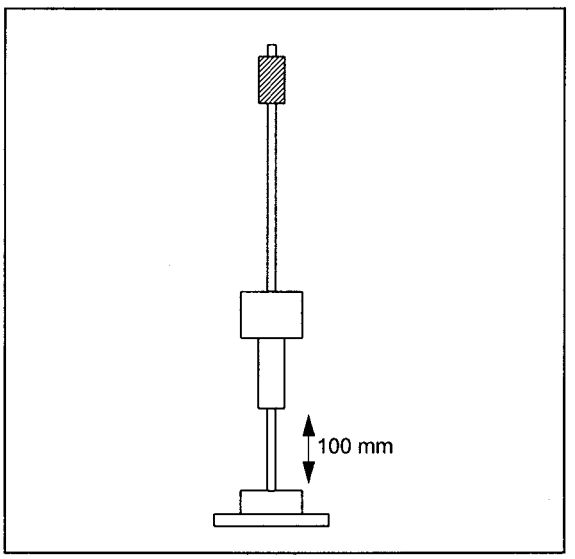

Fig 5.5 Hand tamper (or drop weight) compactor

After compacting the second layer, the solid plate was carefully removed using a magnet. A perforated grid plate was placed on the already levelled sand surface, with the ribs direction perpendicular to the direction of shear. The plate was pressed down evenly so that the ribs bedded into the sand with the top surface level. The distance from the top of the box to the back of the grid plate at the mid-point of each side was measured. The height of the specimen was, thus, determined and consequently, its volume and bulk density obtained from calculations.

5.3.2 Assembly of apparatus

The whole assemblage was placed onto the low-friction ball-bearings in the testing machine bed taking care not to bump the carriage. The top grid plate was checked to make sure it was correctly positioned and that there was a small clearance all around the edge. The filter stone was placed on top of the grid plate. The loading pad was then placed on top, again ensuring that there was a small all round clearance.

The worm drive unit and the tail stock were adjusted by hand, so that contact was just made at all the necessary contact points. The worm drive was positioned so that it could give at least 12 mm of forward movement.

The ball-bearing was placed in the spherical seating on the loading pad. The load hanger was then lifted and placed gently until the recess under the yoke registered the ball-bearing. The load ring was then adjusted to the zero load position and the dial gauge set to zero.

The weight required on the hanger was calculated to give the desired normal stress on the specimen.

a) *Loading yoke only* : was used for the normal stress of 25kPa since it was within the carrying capacity of the loading yoke. The equation used was as follows :

$$W_1 = \frac{\sigma_n \cdot L^2}{9.81 \times 1000} - W_h \qquad (5.1)$$

where

W_1 mass to be put on the loading yoke, (kg)

σ_n pressure exerted onto the soil specimen, (kPa)

L length of the side of the square top half of the shear box frame, (mm)

W_h mass of the loading yoke with hanger, loading pad, porous plate and perforated grid plate, (kg)

b) *Lever arm loading* : The use of the lever arm was necessary for the normal stresses of 50 and 100kPa . These stresses were greater than those which could be sustained with the hanger alone. The equation used in the calculation of the total load, *W*, in kilograms, applied to the soil specimen was :

$$W = W_h + W_1 + W_b \frac{b}{a} + (W_j + W_2)\frac{c}{a} \qquad (5.2)$$

where

W_h mass of the loading yoke with hanger, loading pad, porous plate and perforated grid plate, (kg)

W_1 mass placed on yoke hanger, (kg)

W_2 mass placed on beam hanger, (kg)

W_j mass of beam hanger suspended from lever arm beam, (kg)

W_b mass of lever-arm beam, (kg)

a distance from fixed fulcrum to pivot point of beam, (mm)

b distance from fulcrum to centre of gravity of beam, (mm)

c distance from fulcrum to hanger suspended from beam, (mm)

5.3.3 Testing

Before proceeding to the shearing stage, the following items were checked :

- Contact made at all contact points,
- Dial gauges set correctly,
- Load pad not tilted or jammed,
- Machine rate correctly set,
- Dial gauge reading recorded in the initial '*zero*' position, and
- Timer set to zero.

Finally, the wedges holding the rigid box in position were carefully removed taking care not to cause any displacement. The motor was switched on and the timer started simultaneously. At regular time intervals, the proving ring readings were recorded. Shearing continued until it was well past the maximum stress or peak point so as to obtain residual values as well. The shearing rate was 1.2 mm/min.

The procedure was repeated on two additional identical specimens by applying different normal pressures to obtain a set of three points in the τ - σ diagram, which identify the Mohr-Coulomb failure envelope.

5.3.4 Data processing

Normal stress : The calculation of the normal stress, σ_n, follows the *Equation 5.1* in *Section 5.3.2.*

Shear stress : Shear stresses act parallel to the plane being considered, and develop when applied forces tend to activate resisting forces in the sand and geotextile. The shear stress, τ, acting along the interface, was computed using the equation :

$$\tau = \frac{F}{A} \qquad (5.3)$$

where

F shearing force applied to one half of the sample in a horizontal direction while the other is restrained by the load measuring device, proving ring, (kN)

A shear contact area which is constant throughout testing, (m^2)

with

$$F = C_R \cdot R \qquad (5.4)$$

C_R constant of proving ring, in Newtons per division, (N/div)

R proving ring reading, in divisions.

$$A = L \cdot L \tag{5.5}$$

L length of side the square top half of the shear box frame (m)

and

Therefore, the shear stress (in kN/m^2) is defined as,

$$\tau = \frac{C_R \cdot R}{L^2} \times 1000 \tag{5.6}$$

5.4 Direct shear test of geotextile/geotextile interface

In this investigation, the apparatus was the same as the one used in *Section 5.3*, except that sand in the top rigid metal frame was replaced by a PVC block with a geotextile specimen attached to it, as shown in *Fig 5.6*.

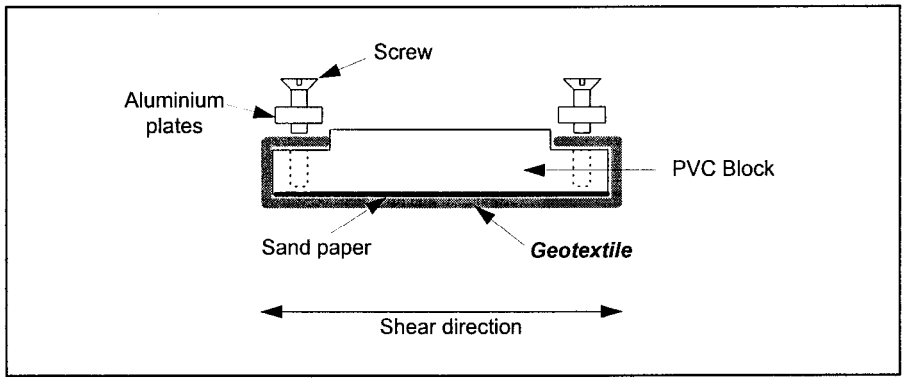

Fig 5.6 Cross-section of the top half of the geotextile/geotextile shear test set-up

The geotextile sample was cut to dimensions of 160 mm by 100 mm and wrapped, in a slightly but carefully stretched mode, onto a 100 mm by 100 mm square PVC block. Prior to this, a grade *P80* sand paper had been glued onto this PVC block using a double sided tape. Once again, this was to simulate in-situ friction characteristics between the geotextile and the soil on top. The geotextile test direction was in accordance with the industrial machine production direction. The loading pad was then placed on top, ensuring it was level and that there was a small clearance all round the inside edge of the top metal frame.

The procedure for carrying out the test and for calculating, plotting and reporting results was in principle similar to that described in *Sections 5.3.2* to *5.3.4*. All the test results and their discussions are presented in *Chapter 7*.

The components of the geotextile/geotextile interface tests are shown in *Fig 5.7*.

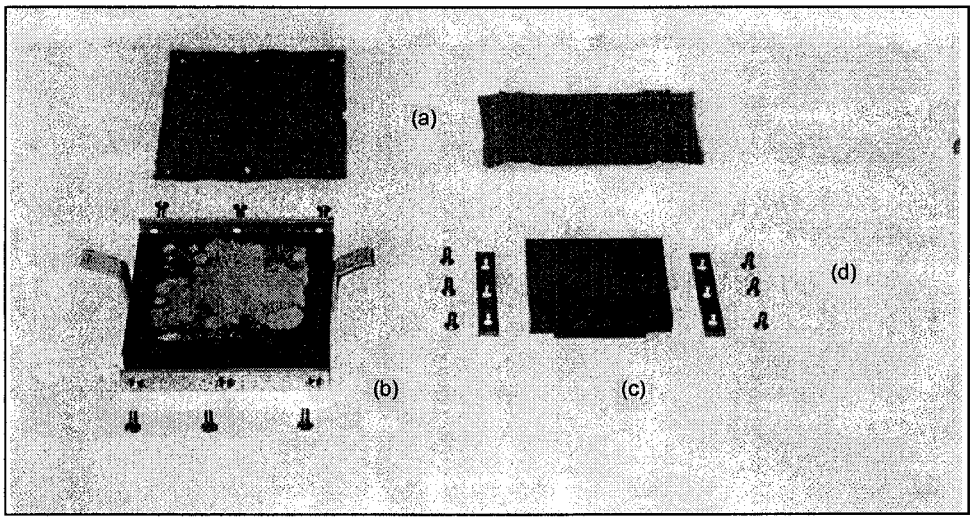

Fig 5.7 Component parts of the geotextile/geotextile shear test; (a) geotextile specimens (b) bottom half (c) top half (d) clamping screws and aluminium plates

CHAPTER 6

PULL-OUT TEST INVESTIGATION

6.1 Introduction

Subsequent to the direct shear tests, pull-out tests were conducted in order to compare the frictional parameters obtained from the two shear investigations with opposing '*role players*': in the direct shear test, the geotextile remains stationary during testing while in the pull-out test, the geotextile moves relative to the soil.

The tests were performed in the Geotechnical Laboratory at the University of Cape Town using a specially manufactured test apparatus fabricated for this kind of study. The apparatus consisted of an aluminium frame with inner dimensions; 288 mm x 300 mm x and 50 mm (length x width x depth), into which the sand was placed, with the geotextile specimen sandwiched in between. Pressure pads were fitted, with one on either side of the frame, and were kept in position by means of a rigid clamping device. The pressure pads consisted of parallel, flexible tubes which could be pressurised for the purpose of applying a uniformly distributed pressure to the sand. A schematic of the pull-out box is shown in *Fig 6.1*.

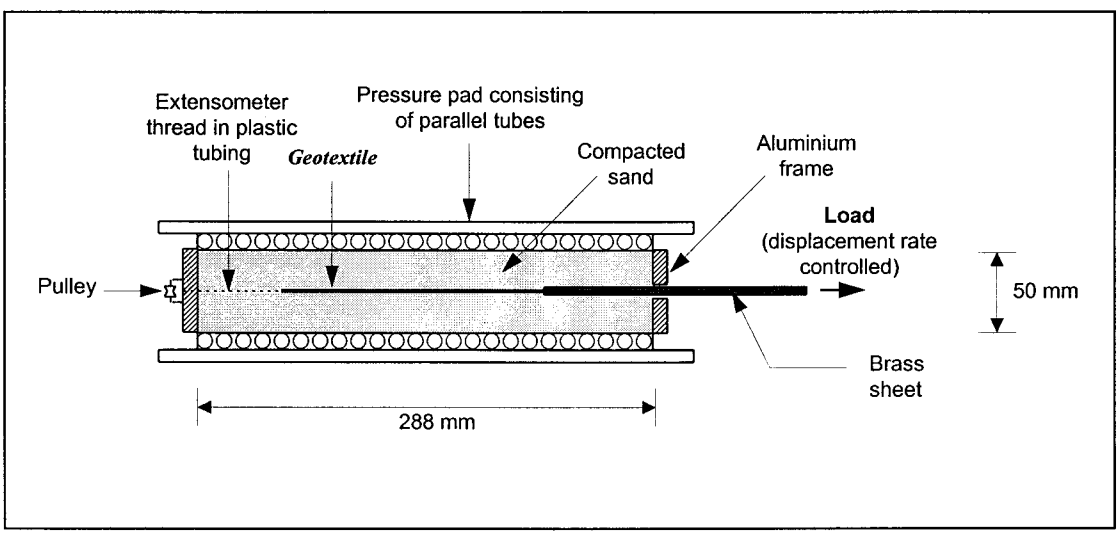

Fig 6.1 Schematic of the pull-out box

The apparatus was mounted onto the lower cross head of the loading frame of a computer controlled Zwick universal material testing machine, shown in *Fig 6.2*. A pull-out load was applied to the geotextile specimens confined in sand, in a displacement controlled manner. The attached

personal computer carried out the machine controls and displayed the measured values: tensile load versus front displacement, in graphical format.

The tests involved pulling a non-woven geotextile sandwiched in sands of different grading and sizes. The research soil materials used in this investigation were the same as those described in the previous chapter namely; Cape Flats, Coarse Cape Flats, Medium Cape Flats, Fine Cape Flats, Klipheuwel and Munich sands.

The comprehensive test program of this investigation is firstly laid out. The test equipment used in the study together with the detailed testing procedure are then described. Special emphasis was placed on the local measurements of the geotextile specimen during load application. Full details of the test results and their discussions are presented in *Chapter 7.*

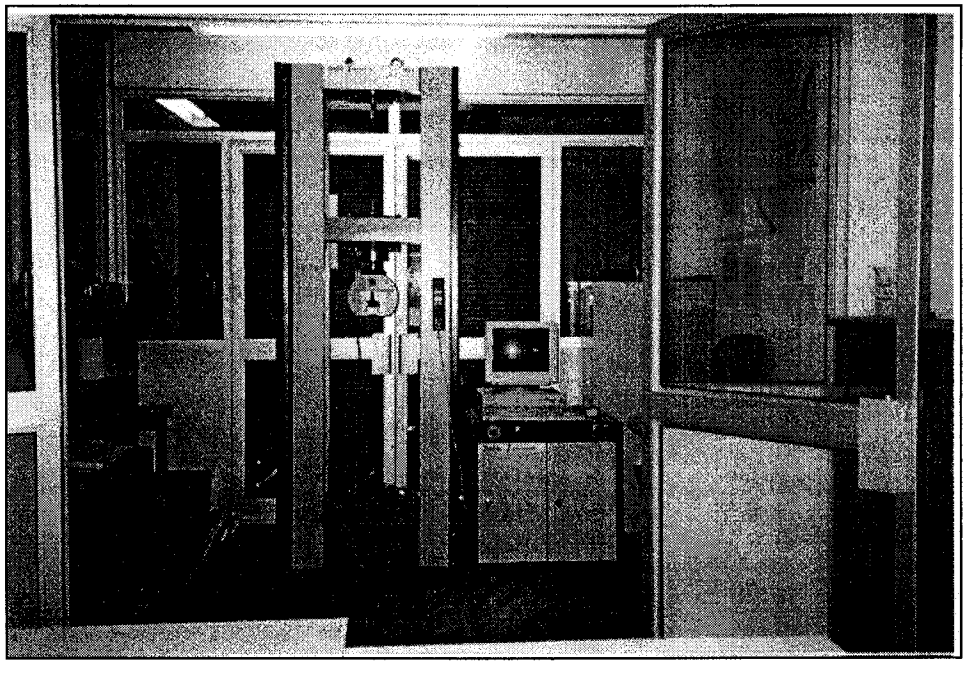

Fig 6.2 Universal material testing machine

6.2 Pull-out test program

For each sand category, one '*standard*' and one '*control*' test were performed at any specified normal pressure. The '*standard*' test involved pulling the geotextile specimen, connected to a brass sheet at the front end, out of the soil, while the '*control*' test involved pulling the same brass sheet, this time without the geotextile specimen, out of the soil. The later was done in order to determine the pull-out resistance offered by the brass sheet only. By subtracting the pull-out resistance force from the one measured in the *standard* test, the pull-out resistance offered by the geotextile specimen only could be determined. The *control* tests were also utilised to determine the adjustment required for the extensometer thread readings to account for the elongation of the threads due to friction forces between the threads and the thin flexible plastic tubes as well as the

pulleys. By connecting threads to the brass sheet in the *control* test, it was possible to compare the displacements of the brass measured via the displacement transducers with the measurements which were obtained independently by the universal material testing machine. In these tests, it was assumed that the brass sheet was rigid and did not deform during load application.

In total, 38 pull-out tests were undertaken, half of which were *control* tests. The experiments were conducted for applied normal pressures between 0 and 140kPa, all at a displacement rate of 10 mm per minute. For each particular sand material under investigation, pull-out tests were conducted at the same bulk density and moisture content as previously conducted with direct shear tests. Necessary steps and check-measurements were undertaken to ensure consistency in the test bed preparations. *Table 6.1* presents the complete pull-out test program.

Sand material	Nature of Test	Test Number	Applied Pressure (kPa)	Dry density (kg/m^3)
Cape Flats sand	Standard	CS/40	40	1653
		CS/70	70	1649
		CS/100	100	1647
	Control	CC/40	40	1655
		CC/70	70	1652
		CC/100	100	1653
Coarse Cape Flats sand	Standard	ZS/40	40	1656
		ZS/70	70	1651
		ZS/100	100	1649
	Control	ZC/40	40	1653
		ZC/70	70	1654
		ZC/100	100	1651
Medium Cape Flats sand	Standard	MS/40	40	1551
		MS/70	70	1550
		MS/100	100	1553
	Control	MC/40	40	1546
		MC/70	70	1549
		MC/100	100	1552
Fine Cape Flats sand	Standard	FS/40	40	1516
		FS/70	70	1519
		FS/140	140	1519
	Control	FC/40	40	1525
		FC/70	70	1522
		FC/140	140	1523
Klipheuwel sand	Standard	KS/0	0	1890
		KS/20	20	1892
		KS/40	40	1893
		KS/70	70	1888
	Control	KC/0	0	1895
		KC/20	20	1889
		KC/40	40	1891
		KC/70	70	1890
Munich sand	Standard	XS/40	40	2011
		XS/70	70	2010
		XS/100	100	2013
	Control	XC/40	40	2016
		XC/70	70	2015
		XC/100	100	2011

Table 6.1 Pull-out test program

6.3 Geotextile specimen preparation

Pull-out geotextile test samples were cut from the same non-woven geotextile industrial roll as that used in the direct shear tests. They were trimmed to a length of 300 mm and a width of 200 mm with an accuracy of ±0.5 mm. Half of the 300 mm of the geotextile specimen length was allocated for clamping purposes.

Samples were cut at random sections from a standard roll of Kaymat geotextile, grade U34. The thickness of each sample was measured according to the ASTM D1777-64 standard at a confinement of 2kPa. The test length (i.e. 300mm) was in the direction of manufacturing of the fabric.

In order to eliminate the effects of thickness in the consistency of pull-out tests responses, only geotextile specimens that fell within a given thickness tolerance were tested, (refer also to *Section 4.2*). As before, the geotextile thickness tolerance used ranged from 2.18 mm to 2.24 mm.

One half of each geotextile specimen was initially soaked in polyester resin and wrapped in a brass sheet as is shown schematically in *Fig 6.3*. During the hardening process, weights were placed on the brass sheets. Excess resin penetrated through and hardened in the twenty four holes of 4 mm diameter previously drilled through one end of each machined brass sheet to achieve a perfect bond between the geotextile and brass sheeting. Thus, a geotextile test specimen of the dimensions, 200 mm by 150 mm was left exposed.

The objectives of using the brass sheet were two fold;

- to facilitate a solid clamping connection of the geotextile specimen with the testing machine, and
- to ensure that the geotextile specimen shear area remained in sand throughout the experiment.

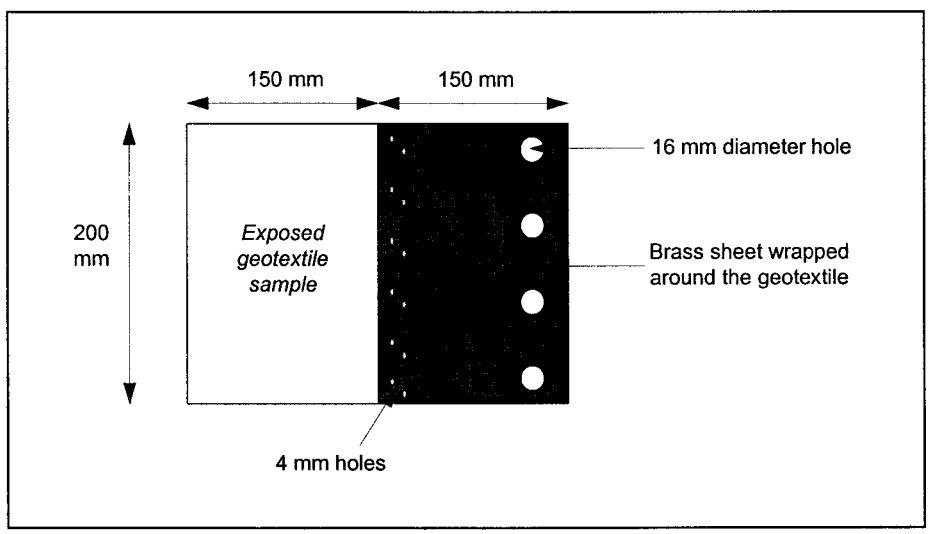

Fig 6.3 Plan view of the geotextile specimen

Once the resin had hardened, four 16 mm diameter holes were drilled through the brass sheet and the geotextile. These holes were used to secure the test specimen in the universal material testing machine using 4 steel pins of 16 mm diameter.

For the purposes of monitoring the displacement and stretching of the geotextile specimen during testing, three extensometers threads were carefully attached at three different points on one side of the exposed geotextile surface (using super glue). Each of the extensometer threads, a strong thin cotton string, was connected to a Linear Variable Displacement Transducer (LVDT). The measuring points were located at distances of 25, 75 and 150 mm from the front (pull-out) end of the test specimen (in the loading direction), and the other end of the threads fed through a thin flexible plastic tube so as to minimise frictional forces between sand and the thread.

6.4 Pull-out test procedure

The various phases of preparation of a pull-out test are described in this section. They involved the compaction of the six sand specimen to a specified density into the aluminium frame, placing the geotextile specimen and pressure transducers within the compacted sand, and assembling and mounting of the test apparatus into the universal material testing machine. A brief description of the basic data processing has been also included.

6.4.1 Mixing and compaction of the sand bed

Each sand type was mixed with the respective mass of water to obtain the optimum moisture content (refer to *Tables 4.2* to *4.4*). Per test, two batches of approximately 4 kg each were prepared. As a check, three small wet samples were obtained, weighed and dried in the oven for atleast 24 hours. By weighing the dry samples, the average moisture content of each sand batch was determined in accordance with BS 1377: Part 2: 1990 (see also *Appendix A.3*).

A rigid PVC board was bolted below the frame of the pull-out box to act as a base onto which the moist sand was placed and compacted. The sand required per layer was carefully weighed before placement to ensure that the correct mass of moist material was compacted into the frame to obtain the desired average density. The sand was then compacted in four equal layers, of approximately 12.5 mm in thickness, using a specially manufactured hand-operated impact tamper (similar to one shown in *Fig 5.5*). It consisted of a metal rod attached to a solid rectangular plate with a drop weight of 4.53 kg. The dimensions of the plate were calculated in order to cover the whole area of the compacted soil in six placements of the compactor, with a 10 mm overlap along each edge. Each layer was subjected to 10 drop weight blows from a height of 100 mm. The exact amount of compaction had previously been determined in a trial test.

6.4.2 Placement of the geotextile sample and measuring equipment

After compaction of the second layer of sand, with the surface of the compacted sand at level with the centre of the pull-out slot, the geotextile specimen was placed in position. Its level and alignment were checked to ensure that it was well positioned in the centre with 100 mm of the brass sheeting protruding through the slot. The remaining 50 mm of the brass sheet embedded in the sand ensured that the geotextile remained in the sand mass throughout the pull-out test.

The three threads attached to the geotextile specimen, each in a plastic tubing, were fed through the frame around the pulleys at the end of the frame box. Each thread was slightly tensioned and fixed in position. The brass sheet was also firmly fixed in position with a tape to prevent any movement of the specimen during compaction of the upper sand layers. Two 20 mm diameter pressure transducers (10 mm in thickness), consisting of two active faces each, were placed just behind the free end of the geotextile. Prior to their placement, the sand below the transducers was gently compacted and levelled to obtain a perfectly flat contact between the soil and transducers membranes. The pressure transducers were installed in-order to measure the pressure at the level of the sand/geotextile interface in the pull-out test apparatus.

Once the geotextile and the two pressure transducers were in position, the upper sand coverage (25 mm in depth) was placed, again in two layers. After compaction, the sand surface was skimmed with a straight edge to the level of the frame. The average density of the sand was calculated based on the total weight of the pull-out box and all its contents. That is, knowing the weight of the frame, base, geotextile, and instrumentation, the mass of the sand was calculated by subtracting these weights from total weight of the whole box assemblage. The sand mass was divided by the volume of the pull-out box, reduced by the volume of the geotextile and pressure transducers, to obtain the bulk density.

6.4.3 Assembly and mounting of pull-out apparatus

At this stage, one of the pressure pads was placed on top of the frame. The rigid PVC base, frame and pressure pad were all carefully turned upside down as a unit, bringing the base to the top. The PVC base was removed from the frame and the second pressure pad fitted. The whole pull-out test apparatus unit was finally placed in the clamping device and securely fixed. This assemblage was then mounted in a vertical position into the load frame of the universal material testing machine, as shown schematically in *Fig 6.4*. The geotextile specimen, with the brass sheet at one end, and confined by sand in the pull-out test apparatus, was then attached to the upper wide width clamp of the universal material testing machine with the help of four 16 mm steel rods. This connection completely eliminated slip between the brass and clamp.

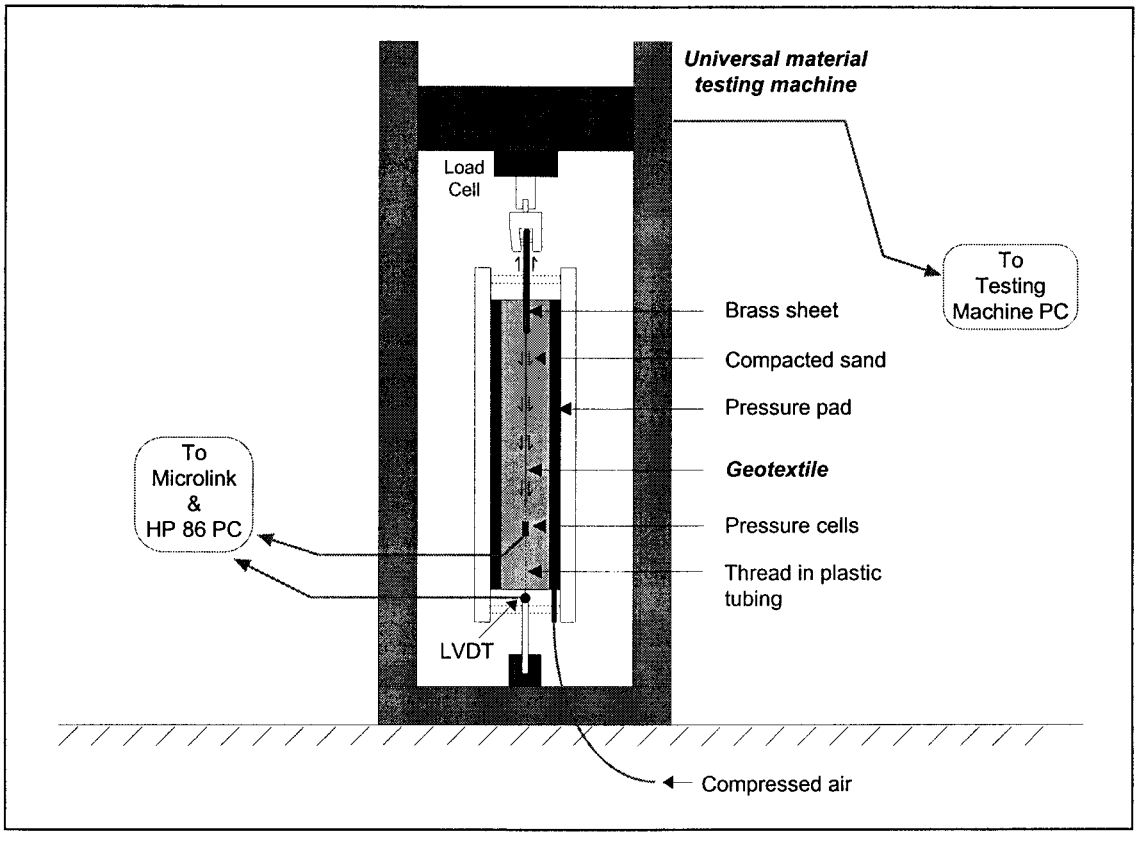

Fig 6.4 Pull-out apparatus mounted in the universal material testing machine

Each thread was connected to a Linear Variable Displacement Transducer (LVDT) by means of adjustable brass connectors. The three LVDTs had a measurement range between -25 mm and +25 mm, allowing a total displacement of 50 mm to be measured. The LVDTs and pressure transducers were connected to a data logger controlled by an HP 86 series Personal Computer in the data acquisition unit.

The data acquisition unit had been set up in order to read the signal voltages from the two pressure cells and the three LVDTs. Control and output information was transferred between the Microlink and PC through an Interface Bus (HP-IB). A photograph of the data acquisition equipment is shown in *Fig 6.5.* A simple BASIC computer program instructed the Microlink to collect the voltage reading of a specific channel, store the data on a disk and address the next channel.

Finally, compressed air was supplied to the pressure pads. The pressure pads comprised of rows of silicon tubing, encased in a silicon bed (see *Fig 6.1*). Each tube was connected to an air supply manifold, which in turn was coupled to one of the four input valves. The pressure pads induced a uniformly distributed confining pressure at the interface between the sand and pads. The required pressure was obtained by adjusting the pressure release valve. The pull-out load was then applied in a displacement controlled manner and testing commenced.

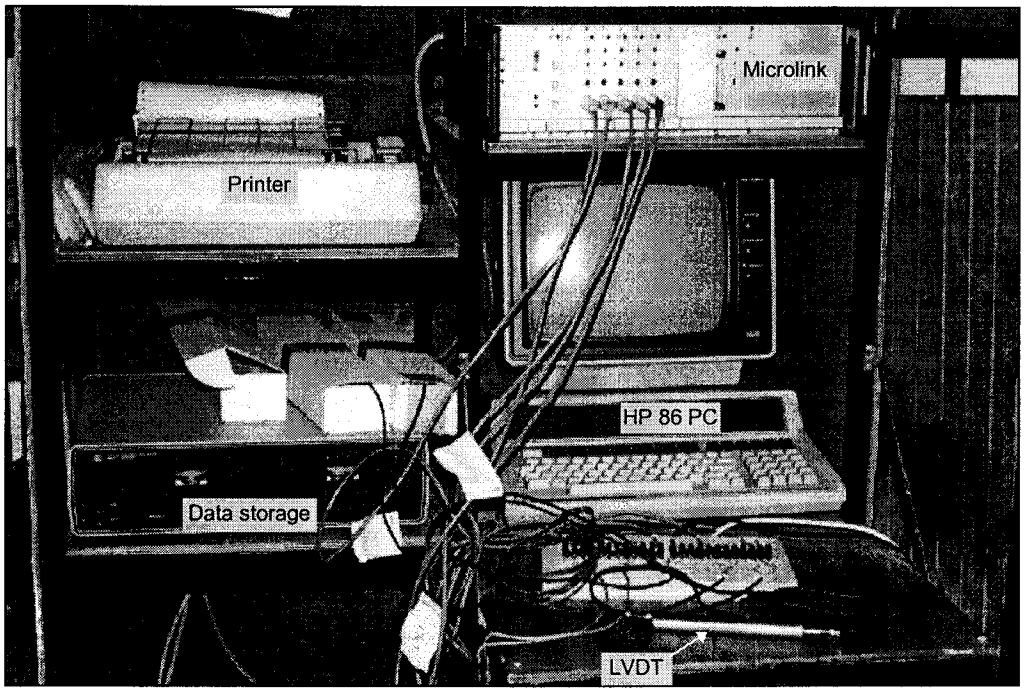

Fig 6.5 Data acquisition unit for LVDTs and pressure transducers signals

All the test results and the respective discussions are presented in *Chapter 7*.

Fig 6.6, shows a typical geotextile test specimen with the brass sheeting before and after pull-out testing.

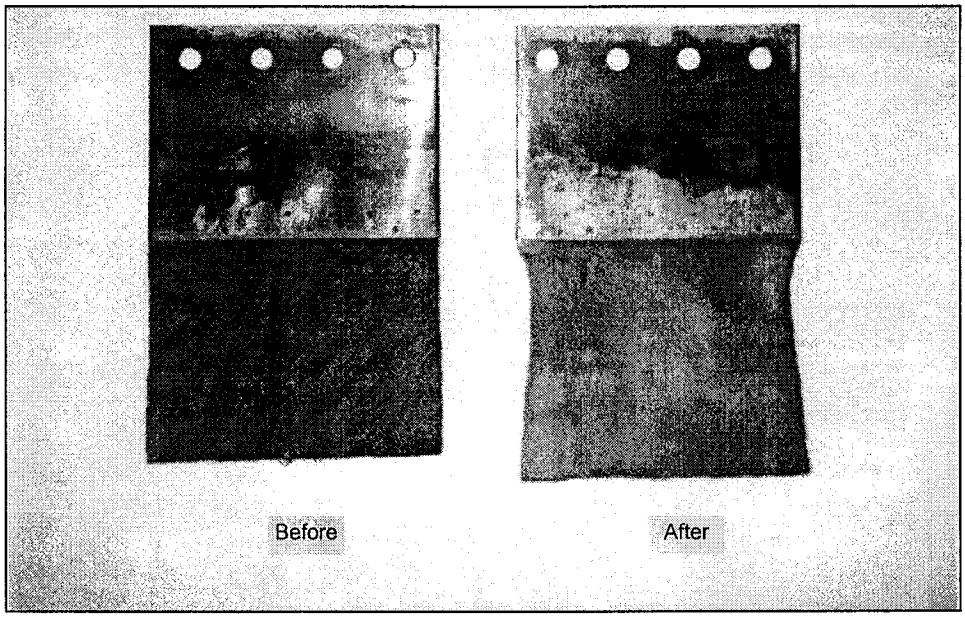

Fig 6.6 Plan view of a geotextile test specimen before and after pull-out testing

6.5 Data processing

6.5.1 Effect of confining pressure on the maximum average interface shear stress

The maximum average interface shear stress, τ, is defined as the average shear stress acting across the sand/geotextile interface at failure. It was assumed to be constant over the entire surface of the interface and was calculated by dividing the geotextile pull-out resistance load at failure by the area of contact between sand and geotextile, i.e.;

$$\tau = \frac{P}{A} \tag{6.1}$$

where

P pull-out resistance load of the geotextile at failure

A area of contact between the sand and geotextile

During the test, the change in the area of contact between the sand and geotextile due to the elongation of the geotextile sample was considered by using the modified method (refer to *Section 3.3.2*). Although lateral contraction (necking) of the geotextile test sample did occur, it was experimentally not possible to determine the magnitude of this deformation and the associated change in area. Thus, when calculating the contact area, the reduction in area due to necking effects was ignored. The contact area, A, was therefore calculated using Equation 6.2.

$$A = W \cdot (L_o + \Delta l) = W \cdot (L_o + u_c - u_{fe}) \tag{6.2}$$

where

W original width of the sample (assumed to be constant)

L_o original length of the sample

Δl elongation

with $\Delta l = (u_c - u_{fe})$

where, u_c clamp displacement (displacement of the front end of the sample)

u_{fe} displacement of the free end (or slippage).

One limitation to this method is that it assumes that the interface shear stress is distributed uniformly over the entire contact area of the geotextile specimen. Following Solomone et al. (1980) who suggested that the interface shear stress at failure is acting across the entire sand/geotextile interface and assuming that the maximum average interface shear stress occurs at failure, the above mentioned approach can then be used to determine the maximum shear stress value. However, in this thesis an attempt is made to step beyond this conventional approach and evaluate a more '*realistic*' shear stress distribution acting in the interface zone or contact surface of the geotextile (see also *Section 7.3*).

6.5.2 Computation of skin friction

By definition, Young's Modulus, ***E***, of the geotexile is defined as the ratio of applied stress to the strain experienced by the geotextile. That is :

$$\boxed{E = \frac{\sigma}{\varepsilon}} \qquad \textbf{(6.3)}$$

where,

σ stress in geotextile

ε strain experienced

$$\boxed{\sigma = \frac{F}{A}} \qquad \textbf{(6.4)}$$

F pull-out resistance load (termed as skin friction)

A cross section area of the geotextile computed as :

$$\boxed{A = t \cdot w} \qquad \textbf{(6.5)}$$

where,

t thickness of geotextile (assumed constant throughout the test, was taken to be equal to 2.2 mm)

w width of geotextile (also assumed constant throughout the test, change due to stretching and necking ignored)

But

$$\boxed{\varepsilon = \frac{\Delta l}{l}} \qquad \textbf{(6.6)}$$

where

Δl elongation of geotextile (u_c - u_{fe}) determined from the extensometer readings

l original section length

Substituting into equation 6.6, yields

$$\boxed{F = \frac{\Delta l}{l} \cdot t \cdot w \cdot E} \qquad \textbf{(6.7)}$$

The skin friction, ***F***, could therefore be determined at any particular geotextile elongation, Δl, and modulus, ***E***.

CHAPTER 7

RESULTS, ANALYSIS AND DISCUSSIONS

7.1 Introduction

All test results of the direct shear and pull-out tests conducted in Cape Flats sands, Klipheuwel sand and Munich sand are presented in this chapter.

The chapter is divided into three main sections. The first section presents and discusses the direct shear tests results. The pull-out tests results and discussions appear in the second, while the last section briefly discusses the comparisons and research findings of the two test methods.

7.2 Investigation of direct shear test results

The direct shear results are initially presented in form of interface shear stress development versus horizontal displacement diagrams. This is followed by a discussion of interface shear stress - horizontal displacement relationship. Also included are the development of the interface shear stress with shear displacement, and the relationship between the maximum interface shear stress (as well as the residual interface shear stress) and the applied normal pressure.

7.2.1 Shear stress - horizontal displacement relationship

The shear stress versus horizontal displacement relationships of all materials tested according to the direct shear test program (*Table 5.1*), are shown in *Fig 7.1*. For each sand material, a separate graph was produced (*Fig 7.1(a)* to *Fig 7.1(f)*). In each diagram, i.e. *(a)* to *(f)*, there are three sets of responses representing sand/sand, sand/geotextile and geotextile/geotextile interface tests, as indicated in the legend at the bottom of the figures. Again, each of the interface tests was conducted at three different normal pressures namely at 25, 50 and 100 kN/m^2. Hence, there are three curves of the same type of line.

- ***Sand/ Sand***

Relating the individual sand/sand direct shear responses in *Fig 7.1(a)* to *Fig 7.1(f)* (presented as solid lines), the relationships show that the rate of development of shear stress with horizontal displacement increased as the normal pressure increased. This was expected since the higher the applied normal pressure, the higher the induced contact stresses between the sand particles. This causes the particles to adhere and interlock more tightly thereby developing an increase in resisting interface shear stresses. Comparing the magnitudes of peak shear stresses, it is noted that at any

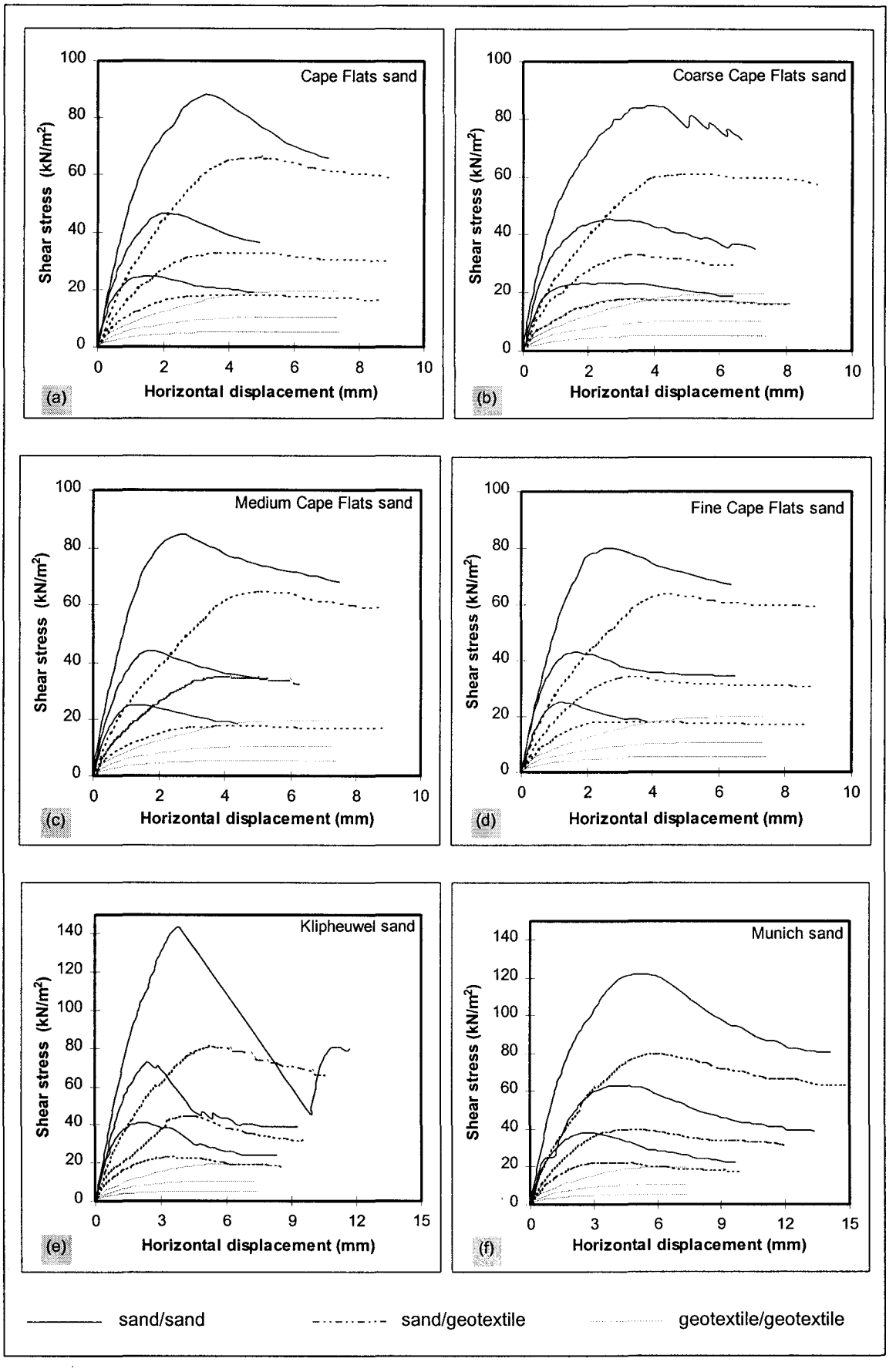

Fig 7.1 Direct shear stress versus horizontal displacement of research materials

particular normal pressure, Klipheuwel sand had the highest shear stress development, followed by Munich sand; while Fine Cape Flats sand had the least. Klipheuwel sand was a well graded fairly coarse sand material, while Fine Cape Flats sand was a uniformly graded, fine sand.

The shear stress - horizontal displacement relationship exhibited smooth curves in four of the six sand cases namely; Cape Flats sand (*Fig 7.1(a)*), Medium Cape Flats sand (*Fig 7.1(c)*), Fine Cape Flats sand (*Fig 7.1(d)*) and Munich sand (*Fig 7.1(f)*). However, Coarse Cape Flats sand (*Fig 7.1(b)*) and Klipheuwel sand (*Fig 7.1(e)*) developed a dramatic softening behaviour after the peak shear stress was reached. It is considered that this '*saw-toothed*' behaviour was caused by an interlock - slip phenomenon arising from a repeated process of build-up and subsequent collapse of resistance forces between the coarse and angular shaped sand particles. Coarse Cape Flats sand and Klipheuwel sand had the largest percentage of sand particles greater than 0.6 mm (refer to *Fig 4.3*).

In all six sand categories, the maximum shear stress occurred after a certain amount of horizontal displacement. For any particular sand material, it can be seen that the higher the normal pressure, the higher is the required horizontal displacement to fully mobilise the peak shear stress. An increase in normal pressure exerted on soil particles results in a proportional increase of the matrix compression, thereby enhancing the degree of granular interlock. As a consequence, displacing the grain particles in shear direction, would require an increased shear force mobilisation. The measure of this displacement will be of interest in comparison to those experienced in the interface shear tests.

In *Fig. 7.2*, the shear displacements required to mobilise the maximum shear stress were measured from respective sand responses (refer to *Fig 7.1*) and were plotted against the applied normal pressures.

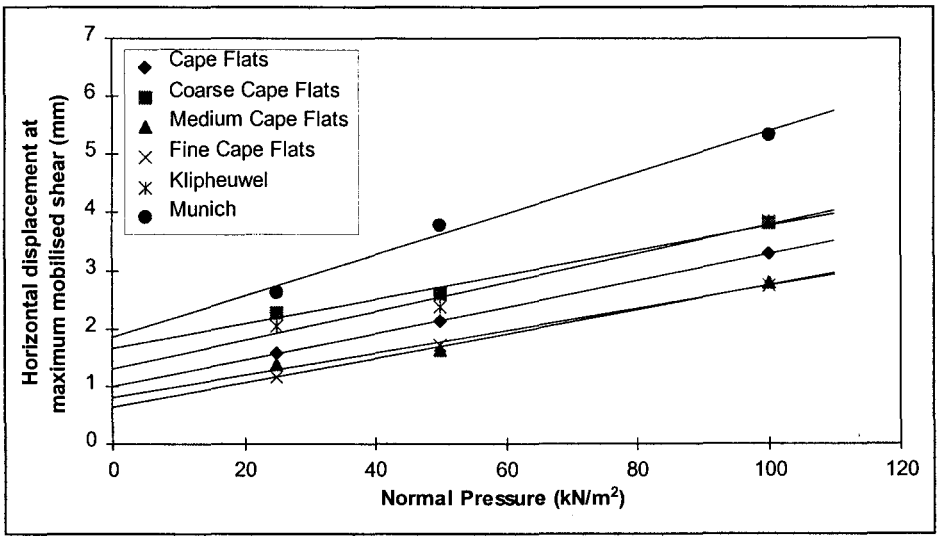

Fig 7.2 Horizontal displacement required to mobilise shear stresses to maximum at various confining pressures in the test sands

The plots demonstrate that the displacement required to fully mobilise the shear stress increases linearly with confining pressure. At any particular applied normal pressure, Munich sand exhibits the highest displacement, followed by Coarse Cape Flats sand and Klipheuwel sand.

Amongst the Cape Flats sand and its subgroups, Coarse Cape Flats sand showed the highest horizontal displacement to mobilise maximum shear stress at any particular confining pressure, followed by Cape Flats, Medium Cape Flats and Fine Cape Flats sands. This demonstrates quantitatively, the effect of the respective texture and grain size on the interface shear mobilisation. *Fig 7.2* also shows that the Cape Flats sands peak points, in terms of displacement at peak shear stress, were on a straight line and that the gradients of these lines were about the same. The line for the fine graded sand was the lowest and the one for coarse grading the highest.

- ***Sand/Geotextile***

All shear stress - displacement results of the sand/geotextile interface tests were extracted from *Fig 7.1*, and are shown superimposed upon each other in *Fig 7.3*.

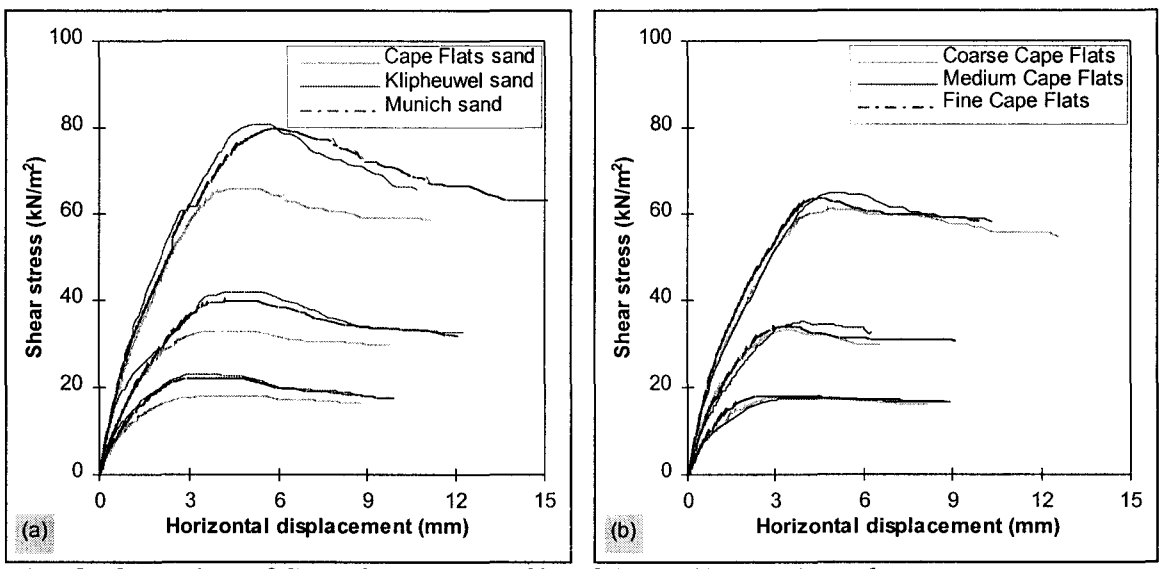

Fig 7.3 Comparison of direct shear stress profiles of the sand/geotextile results

It was observed that, in general the sand/geotextile responses as compared to those of sand/sand, were less '*dramatic*', the individual curve steepness was lower as well as the ultimate shear stress at each confinement.

The sand/geotextile shear stress - displacement relationship can be described as bilinear up to the peak, after which a gentle drop-off (softening) is experienced. The bend in the bilinear relationship is at a shear stress of about 20 kN/m^2 and a displacement of about 1 mm. It is believed that, this sort of shear displacement is required to activate the entire geotextile area. Thereafter, deformation and reorientation of the fibres in the direction of shear combined with the shear deformation of the respective sand, comes into play. The characteristics of the sand material do not appear to be of

importance since the gradient of the shear - displacement relationship is very much the same. The type of sand, however, has a significant bearing on the peak shear stress with Cape Flats sand being the lowest when compared with the responses of Klipheuwel and Munich sands.

The Klipheuwel sand/geotextile interface produced the highest limiting value followed by Munich sand/geotextile interface. The difference between the two interfaces increased with increasing normal pressure. It is evident from the results that Klipheuwel sand, consisting of broken, angular coarse grains and having the highest coefficient of uniformity (C_u = 8.24), interlocked better into the fabric than Munich sand (C_u = 7.8). Also, at higher applied normal pressure, higher interlocking and '*punching*' effect of the grains into the fabric resulted in an increased resistance to shear at the interface.

The failure shear stress level at the sand/geotextile was a fraction of the maximum sand/sand interface shear stress. It occurred between 88 and 95% in Cape Flats sands, 78 - 83% in Klipheuwel and Munich sands. After the failure (peak) point, the interface shear stress decreased to a residual value which was about the same in both configurations.

Similar interface shear stress - horizontal displacement responses were obtained for all investigated Cape Flats subgroup sand/geotextile test combinations, as shown in *Fig 7.3(b)*, despite the different particle size ranges of the three sands. They all had about the same coefficient of grading but different grain sizes and maximum dry densities. This suggests that in the direct shear tests, the geotextile material dominates the sand/geotextile interface shear stress behaviour.

The results in *Fig 7.3* show that the peak shear stress occurred after a certain amount of horizontal displacement had taken place. In *Fig 7.4*, the horizontal displacements required to fully mobilise the interface shear stresses at various confining pressures, for the different sand/geotextile interface tests, are plotted.

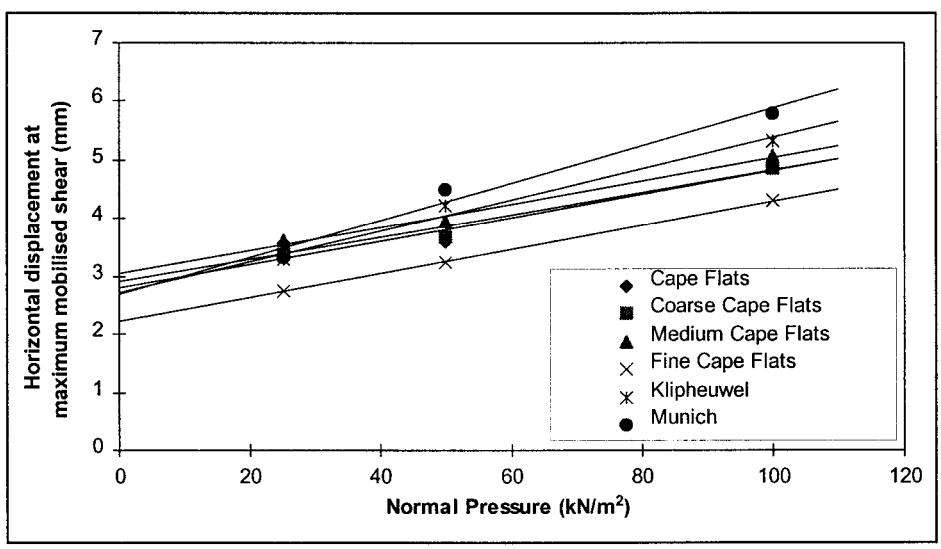

Fig 7.4 Displacement required to mobilise shear stresses to maximum at various confining pressures for different sand/geotextile interfaces

As in Fig 7.2, the plots in *Fig 7.4*, show a linear relationship between the displacement at failure and the applied normal pressure.

At the normal pressure of about 20 kN/m^2, all interfaces except the Fine Cape Flats sand/geotextile one, responded with almost the same shear mobilisation distance. As the confining pressure increased, there was a linear diversion with Munich sand/geotextile test arrangement showing the highest increase, followed by Klipheuwel/geotextile interface. This revealed once again, that the coarser and more well graded the sand is, the greater the horizontal displacement required to mobilise the shear stress to the maximum value. The same results show that Cape Flats, Coarse Cape Flats and Medium Cape Flats sands/geotextile interfaces had almost the same horizontal displacement at failure at the applied confining pressures. There is a clear indication of a lower sensitivity of the shear stress mobilisation displacements with confining pressure within a certain grain size range confirming the fact that in the direct shear test, the geotextile dominates the behaviour of shear stress development at the soil/geotextile interface.

It is interesting to note that the horizontal displacement at any particular confining pressure required to achieve maximum shear at the Fine Cape Flats sand/geotextile interface was well below those of other sand/geotextile interfaces. This may imply that very fine sand grains only fill the geotextile surface structure but do not '*punch through*', reducing the interface mobilisation interaction to a minimum.

Comparing the sand/sand with sand/geotextile interface results (see *Fig 7.1*), a reduction in shear at failure of between 25 and 40 percent in respective sand materials was observed. The difference becomes more significant with increasing confining pressure. The shear resistance between the soil particles and the geotextile fabric is lower because an intimate contact can not be established. It seems apparent that the geotextile lining forms a '*real*' discontinuous plane of weakness with respect to shear stress.

It was also observed in *Fig 7.1*, that prior to failure, for a given horizontal displacement, the rate of increase in shear stress at any sand/geotextile interface test arrangement, was lower than that at the respective sand/sand interface. However, there was no clear relationship between the results of this shear stress mobilisation at the different sand/geotextile interface test arrangements and those obtained at the sand/sand interface.

According to the data obtained from the direct shear tests, it seems apparent that the inclusion of the non-woven geotextile in a non-cohesive soil reduces both maximum shear stress achieved at failure as well as the rate of shear stress mobilisation. However, it increases the peak shear mobilisation displacement.

- ***Geotextile/Geotextile***

In order to show the lower extreme of direct shear interface behaviour, the geotextile/geotextile interface test results were included in *Fig 7.1*. It is evident that at any particular confining pressure, the maximum shear stress obtained at the geotextile/geotextile interface was much lower than that at the sand/geotextile interface, and only about a third of the corresponding sand/sand interface responses.

The reduction was in the order of,

- 77 to 79% at the sand/sand interface, and 68 to 70 % at the sand/geotextile interface in all Cape Flats sand and subgroups,
- 86 to 88% at the sand/sand interface, and 75.5 to 78% at the sand/geotextile interface in Klipheuwel sand,
- 83.5 to 87% at the sand/sand interface, and 75 to 77.5% at the sand/geotextile interface in Munich sand.

In terms of the horizontal displacement to shear failure, the geotextile/geotextile responses were much higher at any given normal pressure, than those experienced in the other two direct shear interface tests.

These observations confirm that the geofabric specimen is responsible for ; the lower peak shear stresses at the sand/geotextile interface as compared to the respective sand/sand interface; and the higher peak shear stress mobilisation displacements at the sand/geotextile interface as compared to those of the respective the sand/sand interface. However, it can be stated that the coarser and better graded the soil material, the more significant is the soil's effect on the geotextile material and thus on this interface shear stress behaviour.

7.2.2 Shear stress - normal stress relationship

This section is a discussion of the relationship between maximum shear stress and the applied normal pressure. For further comparison, the residual shear stress - normal pressure relationship is also included in the study. *Fig 7.5* to *Fig 7.8*, show the typical Coulomb envelopes obtained from the data generated from the graphs in *Section 7.2.1*. In each direct shear test, both maximum shear stresses as well as corresponding residual shear stresses were read-off from the graphs in *Fig 7.1* and plotted against their respective normal pressures. The summary of results obtained from *Fig 7.5* to *Fig 7.8*, is quantitatively given in *Table 7.1(a)* and *Table 7.1(b)*. The indices 's' and 'g', of the cohesion terms, stand for sand and geotextile respectively while 'r' and 'd' stand for residual and direct shear respectively.

Sand	Particle Range	Average		Cohesion		Friction Angle		Ratio	
	(mm)	Dry Density (kg/m^3)	Moisture Content (%)	c_s' (kN/m^2)	c_g (kN/m^2)	ϕ' (degrees)	δ_d (degrees)	$\alpha_d = \frac{\tan\delta_d}{\tan\phi'}$	$\alpha_c = \frac{c_g}{c_s'}$
Cape Flats	0.2 - 2.0	1650	7.0	2.8	1.6	41.0	32.5	0.73	0.57
Coarse C. Flats	0.6 - 2.0	1650	8.8	2.1	3.5	40.5	30.0	0.68	1.67
Medium C. Flats	0.25 - 0.6	1550	6.0	5.3	2.7	38.0	32.0	0.80	0.51
Fine C. Flats	0.063-0.25	1520	8.0	6.5	3.5	36.5	31.0	0.81	0.54
Klipheuwel	0.075-4.75	1890	10.8	5.3	3.6	54.0	37.5	0.56	0.68
Munich	0.075-4.75	2010	8.7	8.2	2.5	48.5	37.5	0.68	0.30

Table 7.1a Summary of direct shear test results

Sand	Cohesion		Friction Angle		Ratio	
	c_{sr}' (kN/m^2)	c_{gr} (kN/m^2)	ϕ_r' (degrees)	δ_{dr} (degrees)	$\alpha_r = \frac{\tan\delta_{dr}}{\tan\phi_r'}$	$\alpha_{cr} = \frac{c_{gr}}{c_{sr}'}$
Cape Flats	2.5	2.1	30.0	29.6	0.98	0.84
Coarse C. Flats	1.4	3.3	30.2	27.8	0.91	2.36
Medium C. Flats	3.4	3.6	29.2	28.9	0.99	1.06
Fine C. Flats	3.2	3.1	29.1	28.9	0.99	0.97
Klipheuwel	5.4	1.6	35.0	32.4	0.91	0.30
Munich	3.5	1.7	35.0	31.7	0.88	0.49

Table 7.1b Summary of residual shear parameters

- ***Sand/Sand***

In *Fig 7.5* the values of shear stress at failure are plotted against the normal stress, and the best straight lines fitted through the respective test results. Their inclination to the horizontal axis corresponds to the internal angle of shearing resistance of the sand, ϕ'. The intercept on the vertical (shear stress) axis gives the cohesion, denoted by c'.

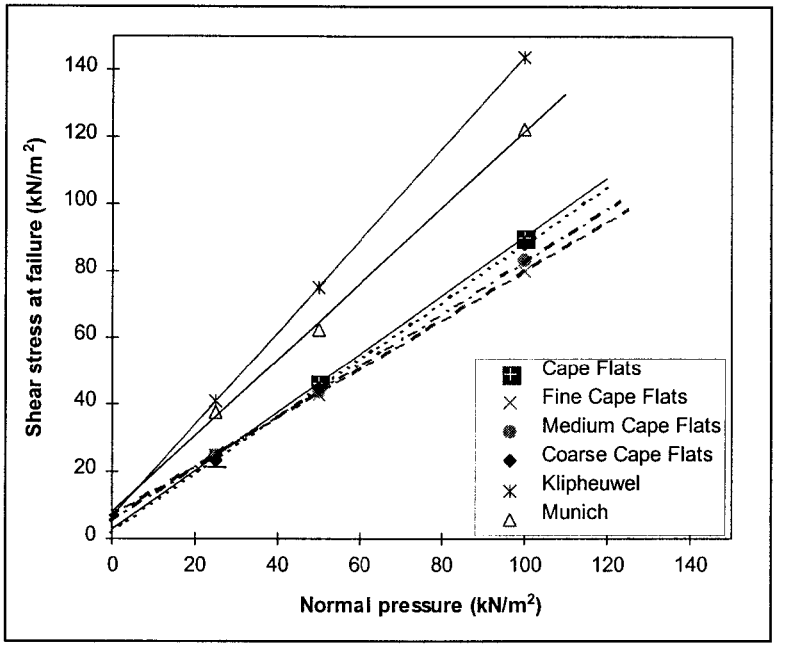

Fig 7.5 Shear strength diagram of the test sands

The shear strength and residual strength parameters were obtained for the various test sands and are summarised in *Table 7.1(a)* and *Table 7.1(b)*.

Klipheuwel sand had the highest internal friction angle, followed by Munich and Cape Flats sands, while Fine Cape Flats sand had the least. From the micrograph images in *Fig. 4.5*, Klipheuwel sand grains were the most angular and had the roughest texture. This characteristic combined with good grading (C_u = 8.24) accounted for the high internal shearing resistance angle. It is apparent that a more balanced distribution of particle sizes results in a higher degree of interlocking. Munich sand was well graded (C_u = 7.8) while Cape Flats sand was uniformly graded (C_u = 2.26) which explains why Munich sand had a higher shearing resistance than Cape Flats sand.

The internal friction angles of Cape Flats, Coarse Cape Flats, Medium Cape Flats and Fine Cape Flats sands were; 41°, 40.5°, 38° and 36.5°, respectively. In this category of sands, Cape Flats had the highest internal friction, followed by Coarse and Medium Cape Flats sands. The coefficient of uniformity, C_u , was almost the same in the Cape Flats sands category. It is believed that the sand grain size affected the observed difference in shearing resistance behaviour.

At a normal pressure of 34 kN/m^2, all three sand subgroups of Cape Flats sand had the same maximum mobilised shear stress of 32 kN/m^2.

It was interesting to see that the intercepts of the failure envelopes were approximately the same throughout.

After overcoming the high inter-particle frictional forces at failure, the shear strength decreased towards the residual values reflected in terms of residual strength parameters ϕ'_r and c'_r.

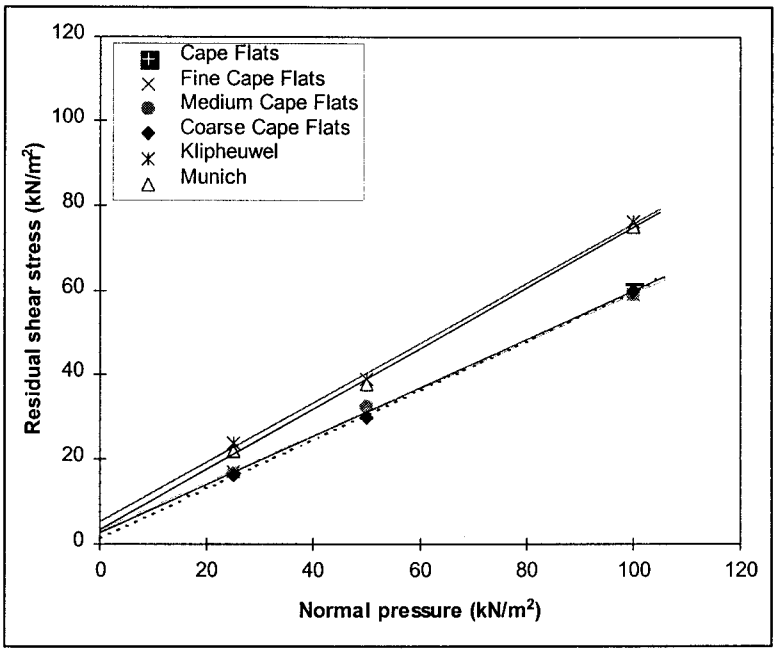

Fig 7.6 Residual shear strength diagram of the test sands

Klipheuwel sand, like Munich sand, had the same residual internal friction of 35°. Cape Flats sand and its three subdivisions showed a residual friction angle of about 30° in the residual condition of the respective materials.

The little difference in the values of residual friction angles within the different size categories of Cape Flats sands, suggests that a narrow shear zone developed in which the translation of particles took place, the thickness of which was in the order of the grain sizes. In the case of Klipheuwel and Munich sand residual friction conditions, a similar scenario can be envisaged.

- ***Sand/Geotextile***

In *Fig 7.7* and *Fig 7.8* the failure envelopes of sand/geotextile interface in terms of interface strength parameters and residual strength parameters are shown.

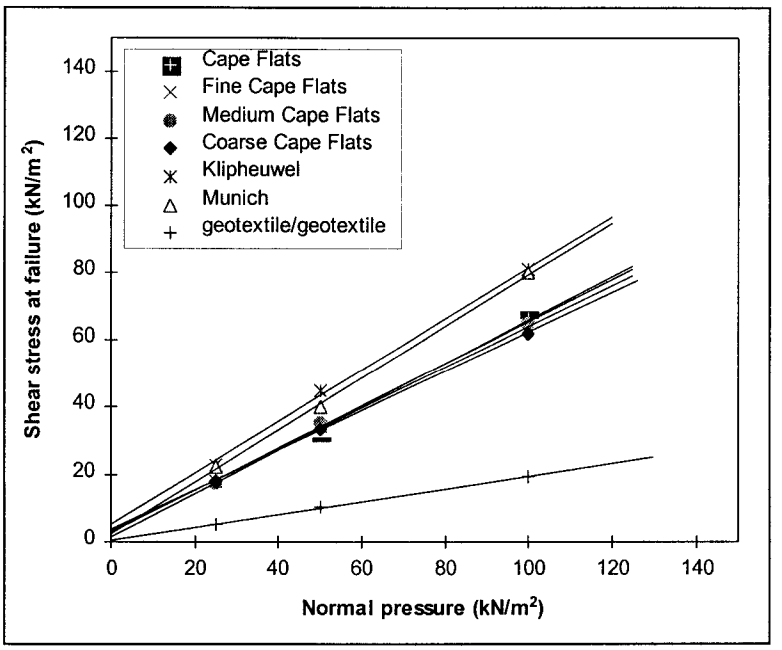

Fig 7.7 Shear strength diagram of the sand/geotextile and geotextile/geotextile interface tests

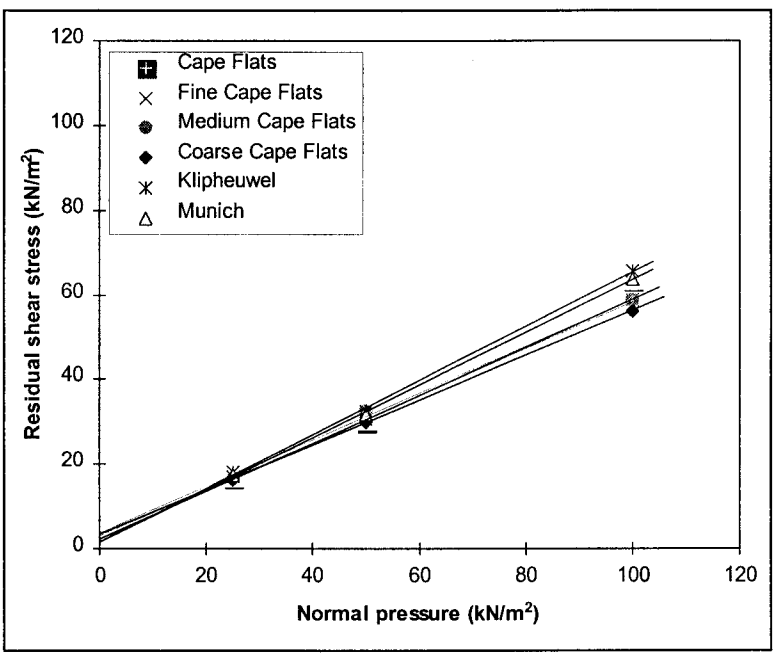

Fig 7.8 Residual shear strength diagram of the sand/geotextile interface test

The results again show a linear τ_{max} - σ_n relationship. The summary of the respective test strength values is presented in *Table 7.1(a)* and *Table 7.1(b)*.

Klipheuwel sand/geotextile interface showed the same peak interface friction, δ_d, of 37.5° as Munich sand/geotextile interface tests. Both test configurations had a significantly higher interface friction angle than those at the Cape Flats sands/geotextile interfaces.

The sand/geotextile interface friction angles of Cape Flats, Coarse Cape Flats, Medium Cape Flats and Fine Cape Flats sand were 32.5°, 30°, 32° and 31°, respectively. It is evident that the sand/geotextile interface friction angles for the different Cape Flats sand categories were almost the same. This suggests that the sand grain size may have negligible effect on the friction characteristics at the sand/geotextile interface.

Further observation reveals that for any sand/geotextile test arrangement, the interface friction angle, (δ_d), was lower than that of the sand/sand internal friction angle (ϕ'), when considering the same sand. The slip surface at the point of failure during shearing, was curved into the depth of the specimen in the sand/sand direct shear test set-up while that of the sand/geotextile interface was identical with the surface of the geotextile and thus plane. The yielding and failure process is an '*in-depth*' process involving a relatively big shear volume in the sand/sand direct shear test and, therefore, a higher shear strength mobilisation is developed in comparison to the shear activities in the very thin shear zone along the sand/geotextile interface.

The adhesion values obtained in the conducted interface tests, were equally negligible as the sands' cohesion values from the direct shear tests. They were essentially below 5kN/m^2. Respective peak adhesion and residual adhesion coefficients α_c and α_{cr} computed and given in *Table 7.1(a)* and *Table 7.1(b)*, revealed no specific trend, associated with sand grading and grain size.

Table 7.2 shows a comparison between the sand/geotextile interface friction angle (δ_d) of each test material and the corresponding residual sand internal friction angle (ϕ'_r).

Sand	δ_d sand/geotextile (°)	ϕ_r' sand/sand (°)	Difference ($\delta - \phi_r'$) (°)
Cape Flats	32.5	30.0	2.5
Coarse Cape Flats	30.0	30.2	≈ 0
Medium Cape Flats	32.0	29.2	2.8
Fine Cape Flats	31.0	29.1	1.9
Klipheuwel	37.5	35.0	2.5
Munich	37.5	35.0	2.5

Table 7.2 Comparison of δ_d and ϕ_r'

The results obtained show an average deviation of two degrees of the interface friction angle. Basing on this research work, it can be concluded that the sand/geotextile interface angle obtained from the direct shear tests is about the same as the residual friction angle of the sand.

- ***Geotextile-Geotextile***

In *Fig 7.7* the geotextile/geotextile interface shear results are also shown. The line of best fit goes through the origin of the graph. The friction angle was about 10.5°.

Comparison of the investigation results shows that the geotextile/geotextile friction (interface) angle was much lower than any of the researched sand/geotextile interface angles. These interface results reiterate the emphasis required in design especially at the joints where geotextile materials overlap.

7.3 Investigation of pull-out test results

The pull-out test responses of the geotextiles are in the first instance, presented as pull-out resistance versus front displacement graphs. In the same diagrams, a detailed record of the stretching behaviour of the test specimens, in the various sand embedments, in relation to the front displacement of the geotextile at a selected confinement, is also shown.

The term '*front*' is used in this section to refer to the loaded pull-out end (or clamped end) of the geotextile test specimen. '*Front displacement*' refers to the movement of the geotextile at this clamped point, relative to its initial position at the start of the test. The '*pull-out resistance*' is the force required to pull-out the geofabric from sand that has been subjected to a particular confinement. The term '*confinement*' is used interchangeably with '*normal pressure*', and refers to the compressive stress applied to the sand material by means of the pressure pads on either side of the pull-out box (refer to *Fig 6.1*).

A discussion of the pull-out resistance-front displacement relationship follows the presentation of all pull-out tests results. Thereafter the stretching behaviour of the geotextile specimen in the sands of different physical characteristics is analysed.

An attempt is made into the investigation of the distribution of pull-out resistance forces including the transmission of these forces, in terms of skin friction, along the geotextile test specimen during loading. In concluding this subsection, a study of the influence of the confining normal pressure on the maximum average sand/geotextile interface shear stress is also presented.

7.3.1 Pull-out resistance versus front displacement

Pull-out resistance versus front displacement responses of the various sand/geotextile test configurations investigated in this study, are presented in *Fig 7.9* to *Fig 7.14*. The pull-out resistance-front displacement relationships, which appear as *solid* lines, were obtained by first subtracting the '*control*' test responses (pull-out of brass sheets only) from the '*standard*' pull-out test responses (pull-out of geotextile specimens and brass sheets). As described in *Section 6.2*, both were conducted in the same sand of the same density at the same confinement.

Each sand/geotextile pull-out test configuration was tested at three different normal pressures; hence the three *solid* curves shown in each graph.

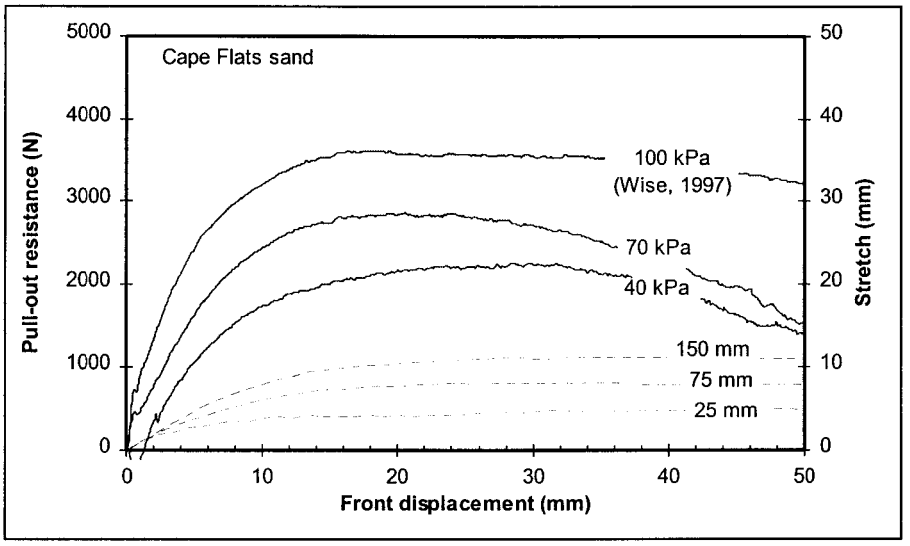

Fig 7.9 Pull-out resistance and stretch of geotextile (at σ = 70kPa) versus clamp displacement in Cape Flats sand

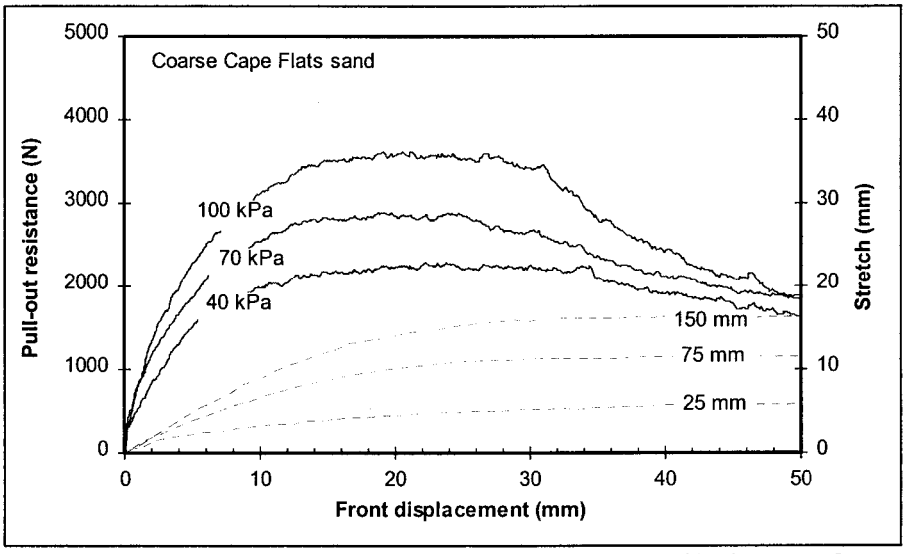

Fig 7.10 Pull-out resistance and stretch of geotextile (at σ = 70kPa) versus clamp displacement in Coarse Cape Flats sand

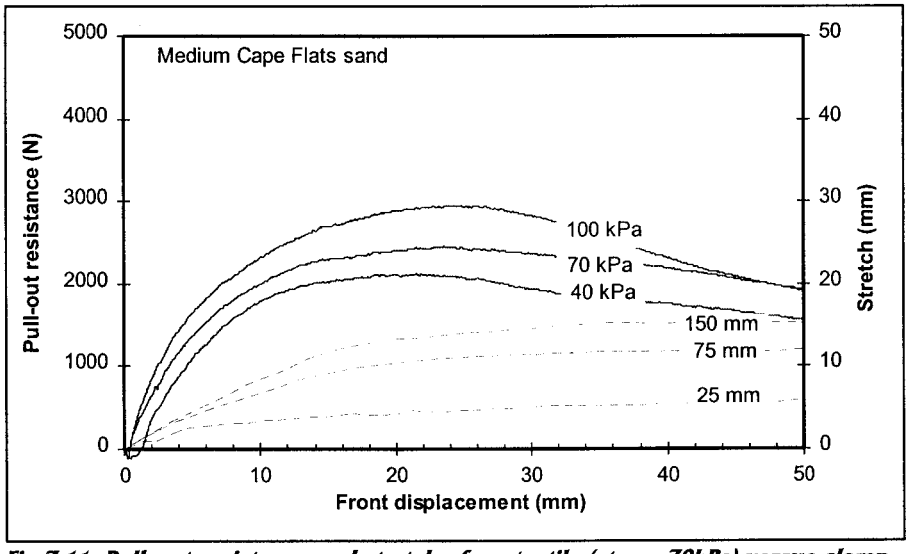

Fig 7.11 Pull-out resistance and stretch of geotextile (at σ = 70kPa) versus clamp displacement in Medium Cape Flats sand

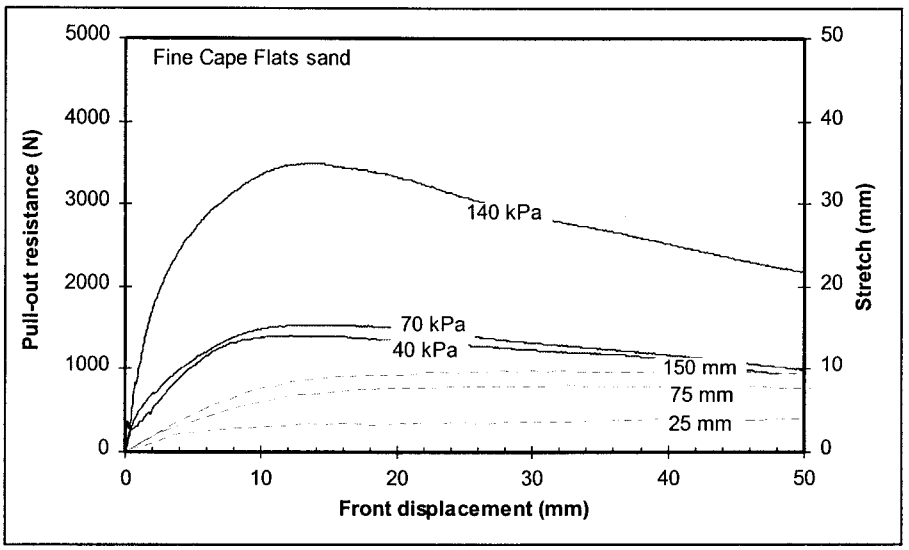

Fig 7.12 Pull-out resistance and stretch of geotextile (at σ = 70kPa) versus clamp displacement in Fine Cape Flats sand

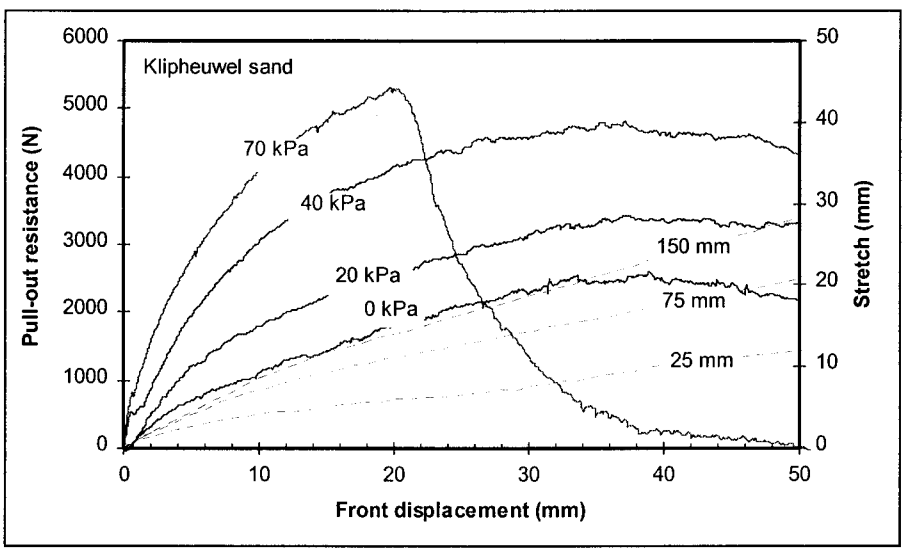

Fig 7.13 Pull-out resistance and stretch of geotextile (at σ = 40kPa) versus clamp displacement in Klipheuwel sand

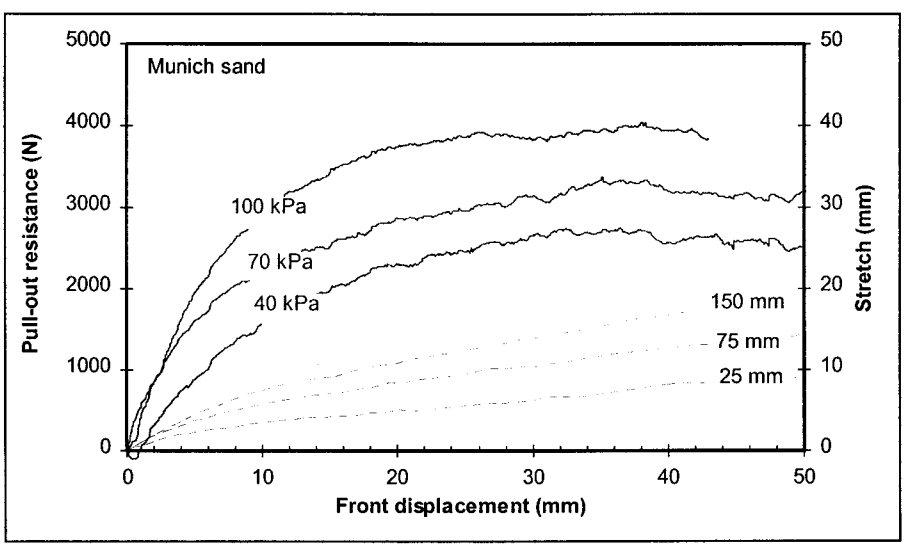

Fig 7.14 Pull-out resistance and stretch of geotextile (at σ = 70kPa) versus clamp displacement in Munich sand

In general, the pull-out resistance-front displacement responses for all tests showed that at any particular confinement, there was an increase of the pull-out resistance with increasing displacement until a maximum (peak) point was reached (*Fig 7.9* to *Fig 7.14*). This maximum point is defined as the *failure* point. Beyond this failure point, the pull-out resistance either decreased to, or remained constant at the residual values. It should be pointed out at this stage, that the observed front displacements beyond 30 mm should be treated with caution since it appears the 4 mm holes in the brass sheet (see *Section 6.3*) interfered with the frame of the pull-out box while the sheet was passing through the slot during testing. In Cape Flats sand and Coarse Cape Flats sand, the residual pull-out resistance at different confinements converged to about the same value, while Medium Cape Flats and Fine Cape Flats sands showed less residual pull-out resistance.

Two types of failure modes can be identified from the graphs. In the first, pull-out resistance increased to peak and then gradually decreased with increasing front displacement. The second failure mode, observed only in Klipheuwel sand at a confinement of 70kPa, the residual pull-out resistance decreased rapidly to zero with increasing front displacement. The former was due to *slippage* failure while the later failure mode was a result of the *rupture* of the geotextile. Both failure modes could also be confirmed by the shape of the distorted geofabric specimen after dismantling the pull-out box.

For any given confinement, the rate of change of pull-out resistance with front displacement, known as *pull-out resistance modulus*, was highest at the beginning but decreased progressively with increasing front displacement. After overcoming the initial interlock of the sand particles due to high compaction, the density of the sand in the interface shear zone deteriorated, which meant that a lower pull-out force was required to displace the geofabric specimen. Consequently, the resisting stresses decreased progressively. At the failure (peak) point, no increase in pull-out resistance with increasing front displacement was observed. The modulus was zero.

The pull-out resistance-displacement responses of each sand/geotextile test configuration clearly showed that for any given front displacement, the higher the confinement, the greater would be the resistance to pull-out failure. This was expected since the higher the applied normal pressure, the higher the induced contact stresses causing the two surfaces, i.e. sand and geotextile, to adhere and interlock more at the points of contact thereby producing a corresponding increase in resisting shear stresses. However, the practical limit on the increase of pull-out resistance with confinement is imposed by the rupture of the geotextile, as observed at a confinement of 70kPa in Klipheuwel sand (see *Fig 7.13*). In this case, the pull-out resistance was greater than the tensile strength of the geotextile specimen, resulting into rupture failure. None of the other sand/geotextile pull-out tests experienced rupture failure at the applied confinements. This implies that the limiting confinement value varies from sand to sand depending on the respective soil mechanical properties, above all, grain size and grain size distribution.

Further observation also showed that the force-displacement relationship exhibited smooth curves in most sand tests apart from Coarse Cape Flats, Klipheuwel and Munich sands. It is suggested that the jagged response of these sand/geotextile test configurations was caused by interlock-slip phenomena arising from the repeated forming and collapsing of resistance forces between the coarse sand particles and the fabric's surface during pull-out. A similar kind of response by coarse sands was also observed in the direct shear stress-displacement relationship (*Fig 7.1*).

It was noted that for any particular normal pressure, the pull-out resistance of the geotextile specimen was highest in the three mentioned sands of significant coarse components; the Klipheuwel, the Munich and the Coarse Cape Flats sands. Among the three sands, Coarse Cape Flats sand had the lowest resistance. This was a matter of grain size distribution; the well graded sands show higher resistance than the uniformly graded sands.

For a closer assessment, the respective peak results of each sand/geotextile test at an applied normal pressure of 70kPa were read off from the graphs in *Fig 7.9* to *Fig 7.14* and tabulated. In *Table 7.3*, the values are listed.

Sand	Bulk density (kg/m^3)	Peak pull-out resistance (N)	Front displacement (mm)
Cape Flats	1766	2863	20.5
Coarse Cape Flats	1795	2885	24.0
Medium Cape Flats	1643	2454	23.6
Fine Cape Flats	1642	1539	13.2
Klipheuwel	2094	5319	19.7
Munich	2185	3372 (2900)	35.2 (30)

Table 7.3 Summary of pull-out peak results at a confinement of 70kPa

At the normal pressure of 70kPa, Munich sand had the highest front displacement required to mobilise pull-out resistance to a maximum value. This was followed by Coarse Cape Flats sand with 24 mm. Fine Cape Flats sand had the least displacement of 13.2 mm. Klipheuwel sand had a lower displacement to the peak pull-out resistance mobilisation than expected, since the mode of failure was not sliding (like in the other configurations); the geotextile ruptured when the pull-out resistance reached 5319 N.

The results from *Table 7.3* reveal that at the same pressure, Klipheuwel had the highest pull-out resistance followed by Munich sand. Fine Cape Flats sand had the least pull-out resistance. As discussed in *Section 7.2.2*, Klipheuwel sand had the highest internal friction angle, ϕ', followed by Munich sand, and Fine Cape Flats sand had the lowest ϕ' value. The results indicate that the higher the soil's internal friction angle, the higher the pull-out resistance provided the resistance is not higher than the tensile strength of the geotextile. The geotextile ruptures once the pull-out resistance exceeds the geofabric's tensile strength.

7.3.2 Geotextile stretching characteristics

The geotextile stretching behaviour in different test sand materials confined at 70kPa (at 40kPa in Klipheuwel sand), is also shown in *Fig 7.9* to *Fig 7.14*. Stretch is shown on the right-hand axes of the individual plots with the stretch responses in '*dashed*' lines. The three responses are identified with 25 mm, 75 mm and 150 mm; where the numbers represent the respective distances from the front end of the test specimen.

During each pull-out test, the displacements of the three different points along the geotextile specimen (25, 75 and 150 mm from the front end) were monitored by the attached extensometer threads as described in *Section 6.3*. Knowing the local displacements of these three points during testing enabled the study of the geotextile specimen elongation behaviour, termed as '*stretch*'. The confining pressure of 70kPa was chosen as a basis for comparison because it is the approximate value of vertical stress at the average depth of geotextile reinforced soil structures. The average depth usually lies between 3 and 5 metres. In the case of Klipheuwel sand at a normal pressure of 70kPa, the stretching behaviour became irrelevant since the specimen tore apart.

The geotextile specimen was subdivided into three sections based on the location of the three extensometer threads, as shown in *Fig 7.15*. The first section at 25mm was closest to the pull-out (front) end. The second section was 50 mm, while the third one, furthest from the loaded end, was 75mm in length. The details of the positioning of the extensometers and their measuring techniques were dealt with in *Section 6.3*.

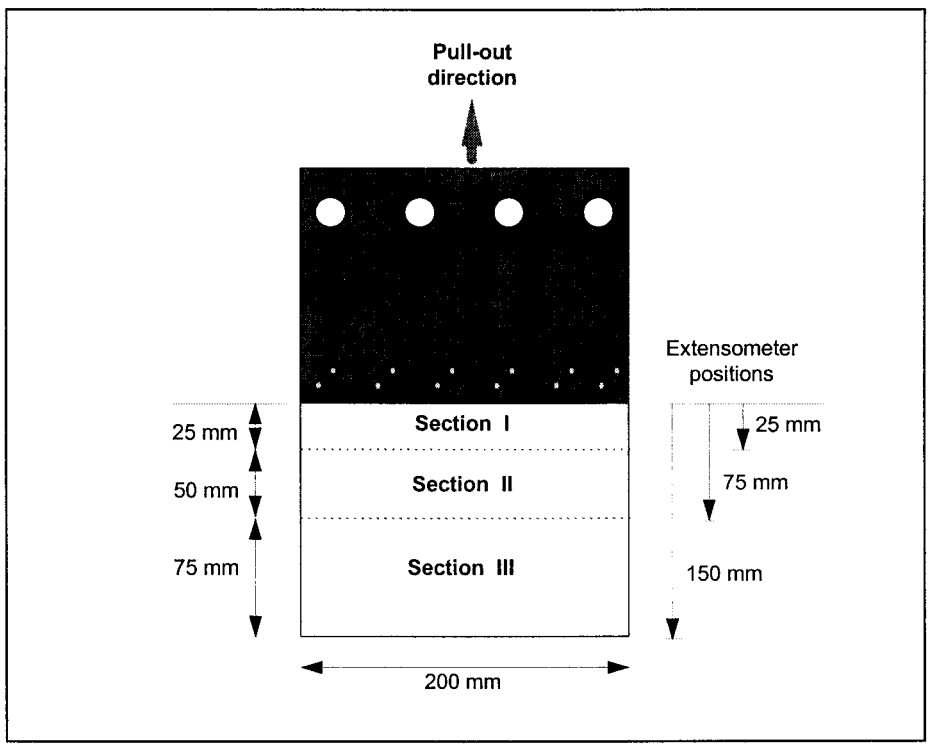

Fig 7.15 Schematic of the geotextile specimen with the three measuring sections

In *Fig 7.9* to *Fig 7.14*, the stretch responses marked by 150mm measured the elongation of the whole geotextile, i.e. from the loaded end to the free end of the specimen. The stretch responses marked 75 and 25 mm, measured the stretch of Section I plus Section II and the stretch of Section I, respectively.

In general, responses showed a *bi-linear* stretch-front displacement relationship. In all investigations, the behaviour could be described by two characteristic slopes, with a smooth transition just prior to the peak pull-out resistance developed by the geotextile. The initial slope is relatively steep in the Cape Flats sand and subgroups, levelling off to a constant measure of stretch, while in the coarser materials stretching continues but at a reduced rate. The steep slope occurs in the region of high *pull-out resistance modulus* on the pull-out resistance-front displacement graph (*Fig 7.9* to *Fig 7.14*). This implies that the geotextile stretching behaviour and the pull-out resistance are interrelated. Any resistance to pull-out is expected to cause extensibility in the non-woven geotextile due to its elastic nature as well as the interface interaction. This observation was exploited later on to assist in the interpretation of the pull-out test results. In addition, it was used to *'back-predict'* (*Section 7.3.3*) the pull-out resistance behaviour of a geotextile specimen so as to investigate in detail the interface interaction characteristics of geotextiles in sands of different sizes and grading, as well as to assess the shear stress distribution along the test specimen during pulling-out.

Of particular interest is the location of the transition points on the two slopes of the stretching behaviour with relation to the front displacement. The stretch response monitored at 25 mm from the pull-out end showed that this point is reached at a relatively small displacement. The transition point of stretch monitored at 75 mm is shortly followed by that at 150 mm from the pull-out end. This indicates a progressive stretch along the length of the confined geotextile fabric. And since the stretch and pull-out resistance are interrelated, it implies that the pull-out resistance is also transferred progressively along the entire length of the test specimen. This, in essence, means that the pull-out resistances are first experienced at the loaded end when the test commences, and then transferred progressively backwards along the geotextile to the free end. Failure in sliding then occurs and is reflected in the reduction of pull-out resistance values beyond the peak point. This mechanism is, in principle, also valid for the test in Klipheuwel sand at a confinement of 70kPa up to the point of rupture.

From *Fig 7.9* to *Fig 7.14*, the incremental stretches within each of the three sections along the geotextile specimen, confined at 70kPa in the various research sand materials (apart from Klipheuwel which was at 40kPa), were computed for every increment of 10 mm front displacement and the results are tabulated below. As mentioned earlier, the last column giving the stretch increments from 30 mm to 40 mm front displacement are not relevant due to the boundary effects.

Sand	Geotextile section	Stretch (in mm) at displacements of: 10mm	20mm	30mm	40mm
Cape Flats	I	3.9	0.4	0.4	0.1
	II	2.2	1.3	0.0	-0.2
	III	1.9	0.8	0.3	0.2
Coarse Cape Flats	I	3.2	1.2	0.7	0.6
	II	3.5	2.2	1.6	-0.2
	III	2.2	1.8	0.5	0.3
Medium Cape Flats	I	3.4	0.9	0.7	0.4
	II	3.4	2.7	0.4	-0.1
	III	1.6	1.4	0.1	0.4
Fine Cape Flats	I	3.1	0.4	0.1	0.3
	II	3.0	1.2	0.2	-0.4
	III	1.6	0.0	0.2	1.6
Klipheuwel	I	4.2	1.8	1.6	2.6
	II	2.9	2.2	1.6	0.6
	III	1.5	1.4	1.4	1.5
Munich	I	3.5	1.5	1.2	2.1
	II	2.2	1.2	1.2	0.3
	III	1.7	0.7	1.2	0.3

Table 7.4 Incremental stretches of the three sections during testing

Although, Section I was the shortest of the three sections, it experienced the highest stretches. In fact, about 50% of the total stretch, (in most sands), occurred in this section of the geotextile. The percentage contribution to the total stretch diminished backwards along the test specimen. It can therefore be concluded that the greatest deformation along the geofabric occurs at the pull-out edge and is transferred progressively towards the free end of the geotextile specimen.

7.3.3 Distribution of pull-out resistance along the test specimen

In order to establish the skin friction distribution characteristics along the geotextile test specimen, it was necessary to first determine the nature of pull-out resistance acting along the particular specimen. To achieve this, there had to be a mechanism of computing the *Young's Modulus* of the geotextile. However, the modulus was constantly changing as the test progressed due to the stretching behaviour of the geofabric. The search for this mechanism led to a '*back-prediction process*', which is discussed in this section.

In order to avoid repetition, only the Cape Flats sand/geotextile test configuration was selected for the in-depth illustration of the process conducted in this attempt. Each of the other sand/geotextile pull-out responses were *back-predicted* in the same manner and only their results are presented. Also, for the purpose of comparing the different sand/geotextile tests, the pull-out tests results conducted at the confinement of 70kPa have been considered here. In Klipheuwel sand, the confining pressure considered was 40kPa, as earlier mentioned.

The incremental stretches after every front displacement increment of 2 mm were determined, for the three geotextile specimen sections, I, II and III (*Fig 7.15*). The selected value of 2 mm was

based on the shear stress-displacement behaviour of the direct shear tests. It appeared to be a representative displacement after which shear stress is *'reasonably'* mobilised. The stretches of each geotextile section were directly computed as the differences of the stretches of the three sections of the test specimen at the distances of 25 mm, 75 mm and 150 mm from the loaded end as monitored with the extensometers. For each sand/geotextile pull-out test configuration, the stretch increments were calculated from the start of the test through to the displacement when the maximum pull-out resistance force occurred. In *Fig 7.16*, the incremental stretch-front displacement relationship is shown for the three sections of the geotextile, confined in Cape Flats sand, at a confinement of 70kPa.

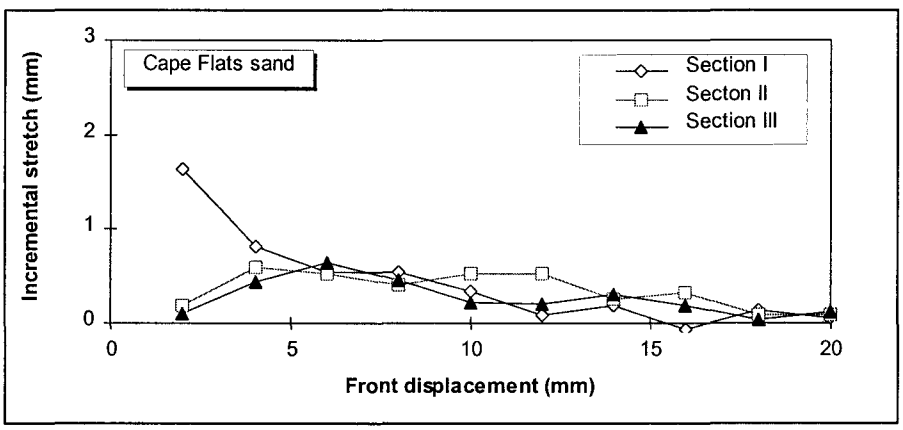

Fig 7.16 Incremental stretch variation with front displacement in Cape Flats sand

The progressive stretching behaviour of the three geotextile sections is clearly evident. As the stretch in Section I drops progressively with the increasing front displacement, Sections II and III are activated in series. The amount of stretch is a measure of the pull-out resistance force (*Section 7.3.2*). It gives an indication of the distribution of the pull-out resistance per section which is changing continuously. The observations can be expressed in terms of the interface shear stresses (or skin friction) which is the pull-out resistance distributed on the surface area of the respective section.

The incremental stretches generally become smaller as the test progresses. At about 20 mm front displacement these stretch increments are almost zero. Interestingly, the incremental stretches in Section I reduced to zero before the ones in Section II and Section III did. This emphasises the fact that incremental stretches are highest at the start of the test but reduce as the failure point is approached. There is no more stretching once the geotextile specimen slides as a whole.

Because of this interrelation between the stretch, Δl, and the pull-out resistance, F, which can be expressed based on the *Equations 6.3* to *6.7* in *Section 6.5.2* as $\Delta l \cong f\left(\frac{F}{E}\right)$, an extrapolation procedure was developed to quantify the *Young's Modulus*, E, (referred to as the *deformation modulus* from here onwards) using the stretch calculations results. The deformation modulus was

envisaged to capture the combined elastic response of the geofabric material as well as the interface interaction.

The *'stretch gradient'* for each of the three sections of the geotextile, defined as the rate of change of stretch, was determined for every 2 mm front displacement. In *Fig 7.17* the stretch gradient of the different sections of the geotextile test specimen is shown as a function of the front displacement.

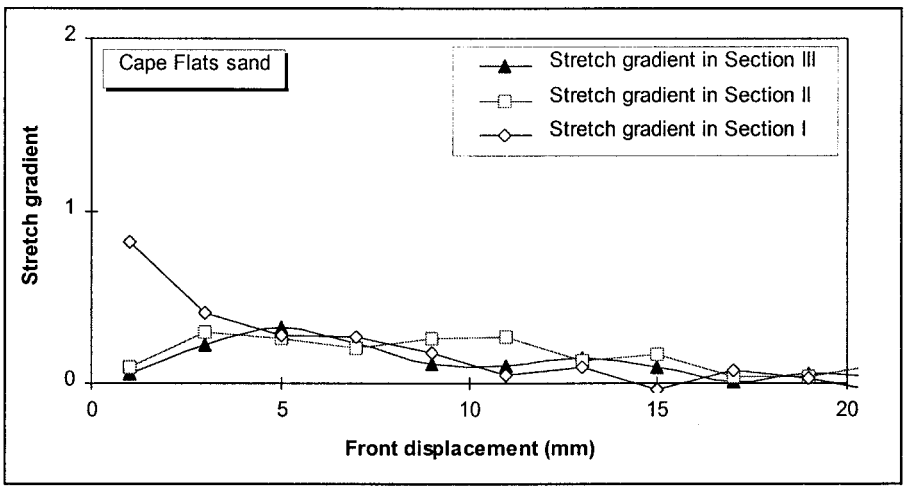

Fig 7.17 Stretch gradient - front displacement relationship

Since the highest measure of stretch occurred in Section I at the very beginning of the pull-out test, it was anticipated that at this stage the deformation modulus was highest. The deformation modulus deteriorated as the pull-out test progressed, to the extent that eventually only the Young's modulus of the geotextile of about 21MPa was taken into account. This Young's modulus was determined in in-isolation tests of the geotextile material (Wise, 1997). This lower limit is considered to be conservative since the material itself deteriorates while being stretched. However, no tests were undertaken to investigate the elastic modulus due to stretching and thinning of the geotextile fibre structure.

With the lower limit value of the deformation modulus fixed (at a stretch gradient of zero), the moduli per section could be extrapolated in relation to the respective stretch gradients in such a manner that the calculated forces per section added up to the measured pull-out force at a specific front displacement. Using this algorithm, the pull-out resistance versus front displacement could thus be recalculated, or *back-predicted*.

As an example of the back-predictions undertaken for all the research materials, the Cape Flats sand test is shown *Fig 7.18*. The figure shows a comparison between the *back-predicted* and laboratory measured values in the Cape Flats sand pull-out test.

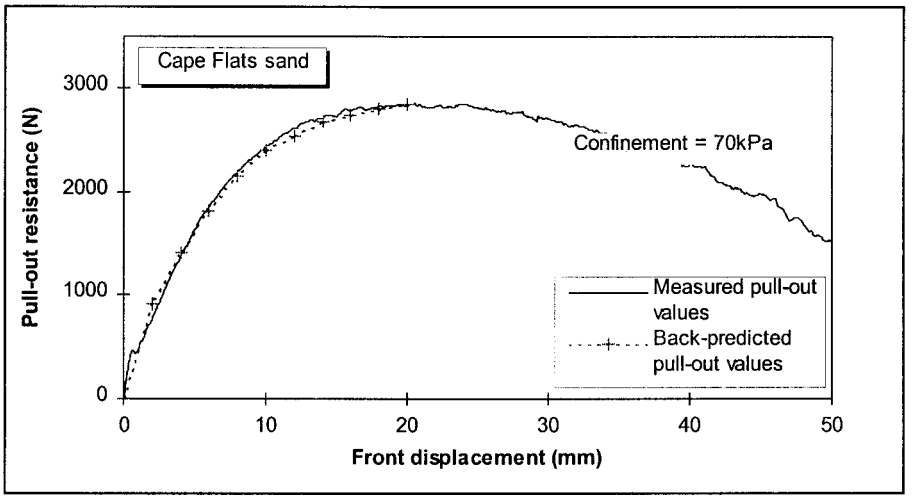

Fig 7.18 Graph showing a relation of measured and back-predicted pull-out values with front displacement

All the other pull-out tests were *back-predicted* in the same manner resulting in the same level of accuracy as demonstrated in *Fig 7.18*.

As a matter of interest, the initial deformation moduli of each of the sand/geotextile pull-out test configurations are listed in *Table 7.5*.

Sand	Initial deformation modulus (MPa)
Cape Flats	37
Coarse Cape Flats	53
Medium Cape Flats	31
Fine Cape Flats	33
Klipheuwel	43
Munich	39

Table 7.5 Initial deformation modulus for the different sands

Coarse Cape Flats sand, unexpectedly, had the highest initial deformation modulus while Medium Cape Flats sand had the lowest. This is an indication that the Coarse sand and the geotextile material complied best in terms of the initial resistance to pull-out.

Fig 7.19 shows the respective *back-predicted* relationships using the described procedure and the appropriate deformation moduli per section.

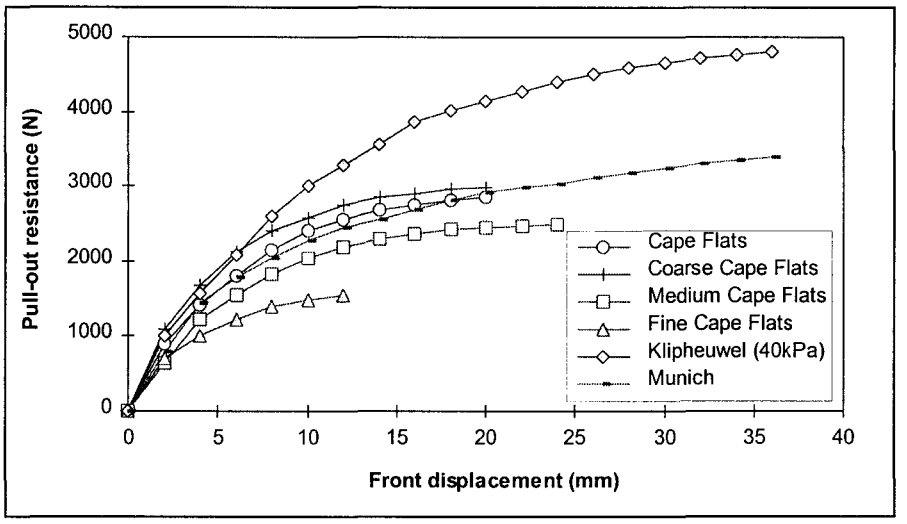

Fig 7.19 Back-predicted pull-out resistance - front displacement relationship at confinement of 70kPa

Having reproduced the pull-out resistance responses (*Fig 7.19*), an attempt was made to study the distribution of pull-out resistance, particularly at failure, along the geotextile specimen confined at 70kPa in the different sands. All the pull-out resistances at failure in each of the three geotextile sections were computed. The corresponding resistance values were plotted at the mid points of the respective geotextile sections along the entire specimen length. The results are shown in *Fig 7.20*.

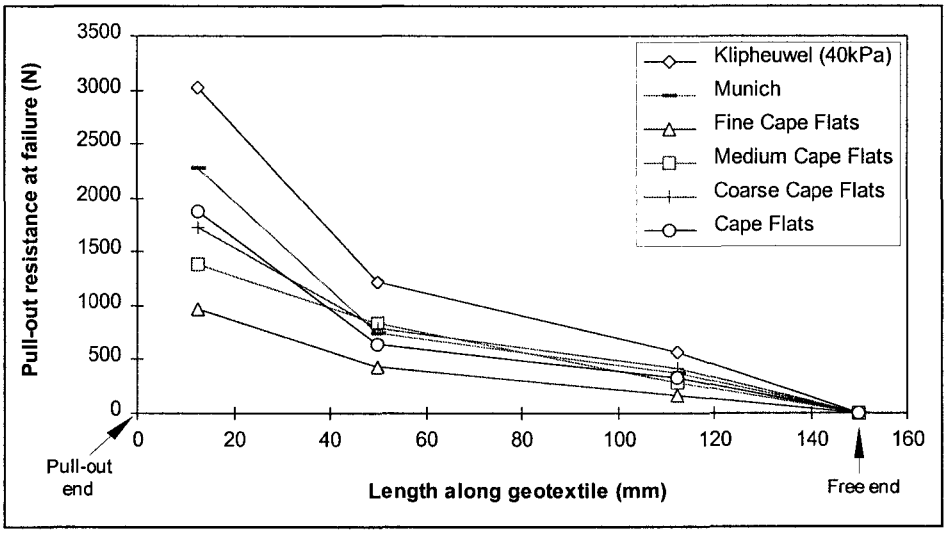

Fig 7.20 Sand/geotextile pull-out resistance distribution along the test specimen length at failure

The results clearly show that during failure (i.e. at peak pull-out resistance), the highest pull-out resistance exists in the section closest to the front end and drops off to zero at the free end of the geotextile specimen in a more or less rapid fashion.

Observations also show that even at a confinement of 40kPa, Klipheuwel sand had the highest pull-out resistance distribution along the geotextile specimen followed by Munich sand. Both sands

were well graded and had the highest angles of internal friction. Fine Cape Flats sand had the lowest pull-out resistance distribution at failure.

7.3.4 Distribution of skin friction along the test specimen

The skin friction values within the three sections of the geotextile specimen, for the different sand/geotextile test configurations at peak pull-out resistance, were obtained by dividing the resisting force values per section by their corresponding section areas. The computed skin friction values were then plotted against the length of the geotextile (at mid section). *Fig 7.21* shows the distribution of interface skin friction at failure along the 150 mm long geotextile specimen confined at 70kPa in the different sand materials (confined at 40kPa in Klipheuwel sand).

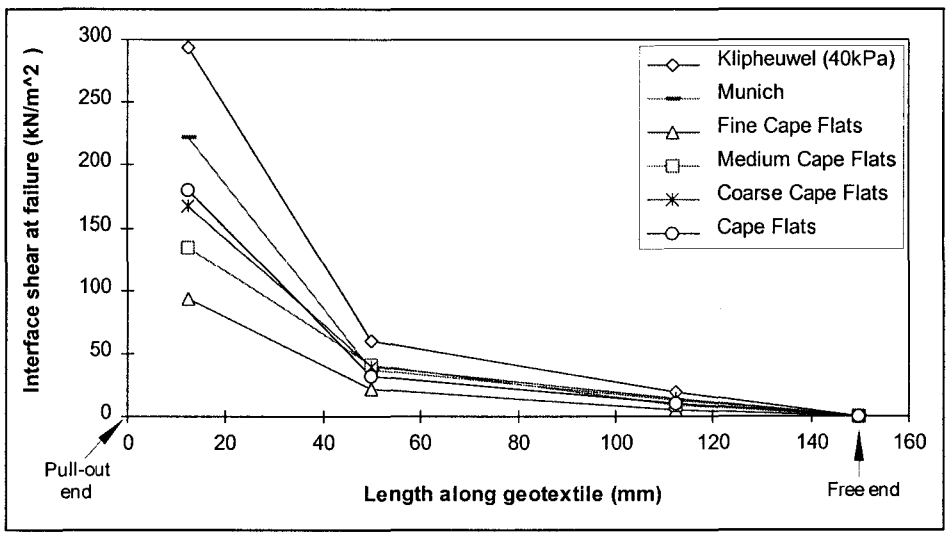

Fig 7.21 Sand/geotextile interface shear distribution along the test specimen length

Once again, experimental observations in these pull-out tests show that at failure, the maximum skin friction along the geotextile specimen occurs at the pull-out end in all the different sand materials, and by no means is the skin friction along the specimen constant. Additionally, at no stage during testing was the skin friction uniformly distributed (not shown here). The maximum was always close to the pull-out end, and decreased to zero towards the free end.

The highest skin friction values were observed in Klipheuwel sand (in the order of 300kPa), followed by Munich sand with about 220kPa. In Fine Cape Flats sand the lowest skin frictions were observed. It can be concluded that the soils with highest internal friction angles generate the highest skin friction distributions along the test specimen.

7.3.5 Maximum average interface shear stress - confining pressure relationship

'*Maximum average interface shear stress*', is used to refer to the shear which occurs at the sand/geotextile interface at failure. The term '*average*' is used because the stress is computed the conventional way, by distributing the total pull-out resistance force uniformly over the entire sand/geotextile contact surface.

Fig 7.22 shows typical failure envelopes generated by the data obtained based on the responses shown in *Fig 7.9* to *Fig 7.14*. The maximum pull-out resistances at particular confinements were read off these curves, after which the maximum average interface shear stresses were calculated using *Equations 6.1* and *6.2* defined in *Section 6.5.1*. The computed stress values were then plotted against the corresponding applied normal pressures.

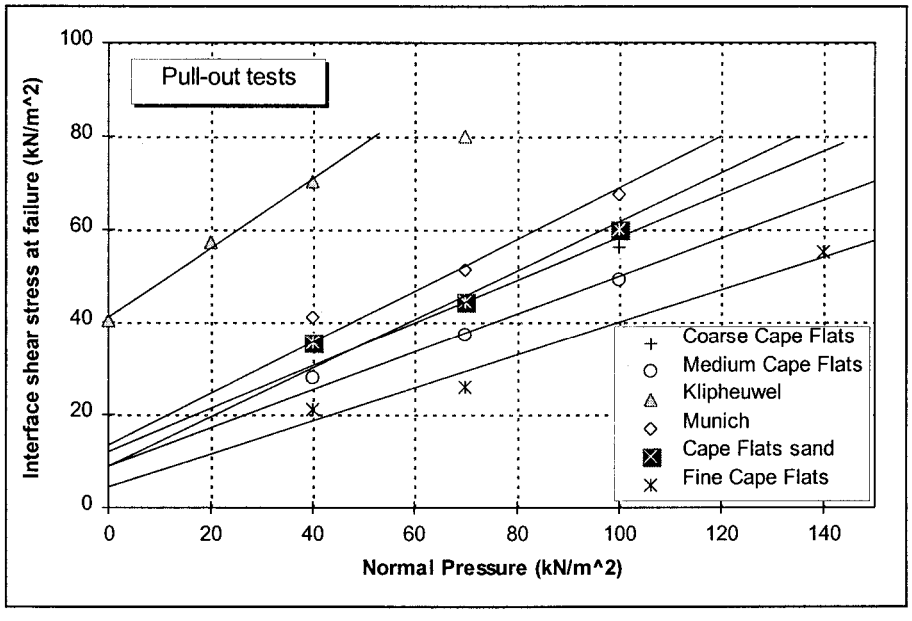

Fig 7.22 Maximum interface shear stress versus normal stress at the sand/geotextile interface

As in *Section 7.2* straight lines were fitted within the tested pressure range, with the inclination to the horizontal axis being equal to the angle of interface resistance, δ_p, and the intercept to the vertical (interface shear stress) axis being the apparent adhesion, denoted by c_p'. The graph clearly shows that the interface shear stress at failure for all the examined sand/geotextile test configurations increased linearly with increasing applied normal pressure. A similar linear interface relationship was observed by other researchers like Venkatappa and Pandey (1990), and Forsman and Slunga (1994).

The interface shear strength parameters were quantitatively summarised in *Table 7.6*. The individual soil shear strength parameters have also been included for comparison.

Sand	Sand direct shear results		Sand/geotextile pull-out results		$\alpha_p = \frac{\tan \delta_p}{\tan \phi'}$
	Cohesion, c_s' (kN/m^2)	Friction, ϕ' (°)	Adhesion, c_p' (kN/m^2)	Friction, δ_p (°)	
Cape Flats	2.8	41.0	9.0	27.5	0.60
Coarse Cape Flats	2.1	40.5	12.0	25.0	0.55
Medium Cape Flats	5.3	38.0	9.0	22.5	0.53
Fine Cape Flats	6.5	36.5	4.5	19.5	0.48
Klipheuwel	5.3	54.0	41.0	37.0	0.55
Munich	8.2	48.5	13.6	29.0	0.49

Table 7.6 Summary of direct shear strength and pull-out interface shear strength parameters

The interface shear strength in Klipheuwel sand, with a bulk density of 2094 kg/m^3, was highest with a δ_p of 37.0° followed by Munich sand with 29.0° at a bulk density of 2185 kg/m^3. Fine Cape Flats sand had the lowest value of interface friction angle of 19.5°. At any particular confinement, Klipheuwel had the highest interface shear stress resistance to pull-out, followed by Munich sand. The high shear strength in Klipheuwel and Munich sands was attributed to their grading and grain structures. As mentioned before, they were both well graded sands. The grading and angularity (refer to *Section 4.4*) of these sands enabled the grains to interlock into the geotextile structure with more intensity increasing the resistance to pull-out during testing. It is apparent that a better distribution of particle sizes produces an increased interlocking effect.

Amongst Cape Flats sand and its subgroupings, Cape Flats sand (ρ = 1766 kg/m^3) had the highest interface friction angle of 27.5°, followed by Coarse Cape Flats sand (ρ = 1795 kg/m^3) and Medium Cape Flats sand (ρ = 1643 kg/m^3) with 25° and 22.5°, respectively. Fine Cape Flats sand had the lowest interface friction angle. Cape Flats sand, with the coefficient of uniformity of 2.26, was relatively well graded compared to its subgroups. The interlocking due to this slightly 'better' grading in Cape Flats sand is likely to have produced the high interface friction angle. The low friction values in Fine Cape Flats sands are due to a thin film of fine uniform particles developing at the surface of the geofabric. Hence at failure, it is believed that the resistance during sliding of the geotextile consists of mere rolling and rearranging of fine particles within this thin shear zone on the geotextile surface.

In *Table 7.6* the friction angle ratios, α_p, of the researched materials are calculated and listed. The sand/geotextile interface friction angle, δ_p, obtained in pull-out tests is generally lower than the

internal friction angle, ϕ', of the respective sand materials. In general, it is safe to say that based on these results, the friction angle ratio is in the order of 0.5.

Comparison of the interface adhesion values to the respective sand cohesion values in *Table 7.6*, shows that adhesion values from pull-out tests are higher throughout. In Klipheuwel sand/geotextile pull-out test configuration, the adhesion values were highest.

7.4 Comparison of direct shear - pull-out test results

A brief comparative study of all research results was undertaken. In essence, it involved comparing the shear strength parameters obtained from the direct shear tests to those from pull-out tests. *Table 7.7* shows a summary of peak results of sand material tests.

Sand	Direct Shear Test				Pull-out Test	
	Sand/Sand		Sand/Geotextile		Sand/Geotextile	
	Cohesion, c_s' (kN/m^2)	Friction, ϕ' (degrees)	Adhesion, c_g (kN/m^2)	Friction, δ_d (degrees)	Adhesion, c_p (kN/m^2)	Friction, δ_p (degrees)
Cape Flats	2.8	41.0	1.6	32.5	9.0	27.5
Coarse Cape Flats	2.1	40.5	3.5	30.0	12.0	25.0
Medium Cape Flats	5.3	38.0	2.7	32.0	9.0	22.5
Fine Cape Flats	6.5	36.5	3.5	31.0	4.5	19.5
Klipheuwel	5.3	54.0	3.6	37.5	41.0	37.0
Munich	8.2	48.5	2.5	37.5	13.6	29.0

Table 7.7 Peak shear strength parameters determined in direct shear and pull-out tests

The results show that for all the sands investigated, with different grading and grain sizes, the values of their respective interface friction angle obtained from both the direct shear tests and the pull-out tests, were lower than the angles of internal friction, ϕ'. All the sand/geotextile configurations further showed that the interface friction angles, δ_p, from pull-out tests were lower than the interface values δ_d from direct shear tests. It was also found that the values of interface adhesion, c_g, obtained from the direct shear tests, were lower than the cohesion values, c_s', of the soil whereas the interface adhesion, c_p, values from pull-out were greater than both the adhesion c_g and the cohesion c_s'.

Basing on these results, it can be concluded that if shear is induced along a given shear plane or interface, the frictional shear parameters of the interface are lower than the angle of internal friction of the sand, 50 to 60% in the case of pull-out tests and 70% to 80% in the case of direct interface testing. However, the adhesion observed in the pull-out test, assuming a constant skin friction

distribution at failure, is significantly higher than the cohesion of the sand and the adhesion observed in the direct shear tests.

It has also been shown from both tests that the inclusion of a geotextile material as a reinforcement in a cohesionless soil reduces the soil's shear strength which is measured in terms of interface friction angle. However, according to pull-out test results the inclusion of geotextile reinforcements increases '*cohesion*' of the reinforced cohesionless soil mass.

CHAPTER 8

PRACTICAL APPLICATIONS

8.1 Introduction

The objective of this chapter is to put the research findings presented in *Chapter 7* into context and apply the developed skin friction concept to a practical design situation.

The chapter initially discusses the design method which is generally employed for the design of geotextile reinforced soil structures. The weakness of the conventional geotextile design strength procedure, in view of the experienced interface strength parameters based on pull-out tests, has been exposed and the use of the pull-out results (in terms of ultimate resistance force versus confinements) explicitly in the design calculations is advised. Further analyses result in the development of a generalised '*skin friction distribution graph*' from which realistic geotextile shear strength values could be obtained. A basic design problem of a geotextile reinforced slope is finally carried out to clarify the design steps.

For the purposes of illustration, as well as to avoid repetition, only the Cape Flats sand was considered as the backfill material of the reinforced soil embankment structure. The design principle, however, applies equally to all the other investigated sand materials.

8.2 Design method

The design of a reinforced soil structure consists of checking for the external and the internal stability. External stability is achieved if the entire reinforced structure, a wall or a slope section, is safe against failure due to sliding, overturning, bearing and slip. The reinforced structure is herein considered to act as a rigid block. The internal stability consists of two analyses: the internal stability of the reinforced structure and the internal stability of the individual reinforcement elements. In this thesis, the applications of the former are primarily addressed and are concerned with the transfer of the load at the interfaces and thus the bonding of the geotextile with the soil. The latter analysis, regarding the reinforcement sheets, is to check if the induced tensile force in the geotextile is within the tensile strength of the geofabric material.

Although both the external and internal stability of reinforced soil structures must be considered in the design procedures, the most critical aspects of design tend towards the internal modes of failure. Therefore, the design procedures discussed in this chapter focus on internal stability

aspects of the reinforced soil structure and particularly on the soil/reinforcement interface interaction.

At present there are a number of limit equilibrium methods available for use in the assessment of the internal stability of reinforced soil (BS 8006:1994). In principle, they are all concerned with the computation of the balance of forces acting on one (or more) free body (bodies) which is (are) limited by an assumed failure surface. This failure surface may be a circular or non-circular arc, a logarithmic spiral or any other irregular surface. Of all the limit equilibrium methods, the two-part wedge analysis and the log-spiral failure analysis are the most suitable for the design of reinforced slopes (Jewell, 1996). A two-part wedge method was chosen in the design of the forthcoming embankment problem because the method provided a reasonable representation of the potential failure surfaces. The approach shown is consistent with the general procedures employed for limit equilibrium methods defined in the British Code of Practice, BS 8006:1994.

The two-part wedge method is based on the assumption of a bi-linear failure surface, as shown in *Fig 8.1*. The analysis involves checking various trial failure surfaces by considering the equilibrium of forces acting on the volume of soil block, ***ABCDE***, above the selected surface. This is done by varying the slopes, θ_1 and θ_2, of the two failure surfaces. Each trial considers a pair of rigid soil wedges (***ABDE*** and ***BCD*** in this case) assumed to be separated from the rest of the soil mass by a failure surface, ***CDE***, passing through the toe, ***E***, of the slope. The critical block is the one which requires a maximum force, F_{req}, to ensure the stability of the slope or, in terms of the vector diagram, the force required to close the force polygon.

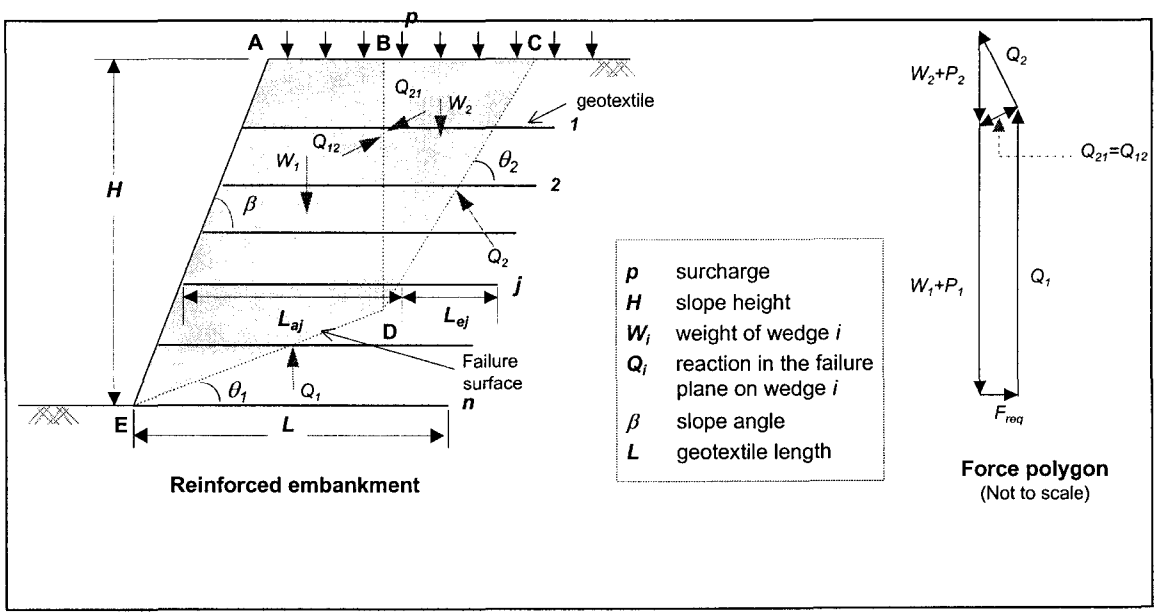

Fig 8.1 Two-part wedge analysis of reinforced embankment slope structure

Once the critical failure surface has been obtained, the '*available*' resisting forces can be calculated. Knowing the reinforcement layout, the reinforcement length and vertical spacing, those resisting forces are represented by the sum of the tensile forces which develop along the reinforcements protruding into the resistant zone (refer to *Fig 2.6*). The stability of the slope is achieved if the '*available*' forces, F_{avail}, exceed the '*required*' value, F_{req}, with an appropriate factor of safety, FS.

The factor of safety, FS, is expressed as the ratio of the *available* forces to the *required* forces for equilibrium or,

$$FS = \frac{F_{avail}}{F_{req}} \tag{8.1}$$

A value of unity represents the state of equilibrium or, in other words, the structure is on the verge of collapse. An appropriate but economical value of FS is therefore necessary.

The analysis considers various trial surfaces. The critical potential failure surface yields the maximum disturbing force that must be resisted to ensure limit states do not occur. This resisting force depends on the slope geometry, the soil properties, the surface loading and the assumed interface conditions between the two parts of the wedges.

In assessing the bond performance for the purposes of the analysis of the *available* forces, the shear stresses between the soil and the reinforcement are assumed to act uniformly over the embedment length. The magnitude of these shear stresses is taken to be the product of the vertical effective stress acting on the reinforcement and the tangent of the interface friction angle, δ.

Thus, the pull-out resistance is calculated to be the product of the surface area of the reinforcement along the bond length, the tangent of the interface friction angle ($tan\delta$), and the vertical stress (overburden stress or confinement) acting on the bond length. The tangent of the interface friction angle is calculated using the respective coefficients of interaction relating the soil/geotextile interface property, α, with the shear strength property of the backfill material, $\tan\phi_p'$. If the backfill is cohesive, the adhesion is obtained in a similar manner; the cohesion c' of the backfill material is multiplied with the interface adhesion ratio α_c.

According to BS 8006:1994 (disregarding the partial factor of safety approach), the maximum reinforcement tensile load, T_j, per metre run at level j in the slope can be expressed as,

$$T_j \leq 2L_{ej}\left[\left(\gamma h_j + p\right)\cdot\alpha\cdot\tan\phi_p' + \alpha_c c'\right] \tag{8.2}$$

where,

L_{ej} minimum required reinforcement anchorage length at level j in the embankment

γ unit weight of the backfill

h_j is the height of backfill above level j in the slope

p external surcharge due to dead load and live load

α ratio relating soil/reinforcement interface friction angle with $\tan \phi_p'$

ϕ_p' peak angle of internal friction of the backfill in effective terms

α_c adhesion coefficient relating soil/reinforcement interface to c'

c' cohesion of the backfill in effective terms

To prevent reinforcement rupture, the reinforcement forces per layer must be compared with the tensile strength, T_y, of the geotextile sheets, which is defined per unit width. This condition can be expressed as ;

$$\boxed{T_j \leq T_y} \qquad (8.3)$$

As shown in this research work (refer to *Section 7.3.5*), the friction angle ratios (or coefficients) obtained in the pull-out tests were even lower than the ratios established in the direct shear interface tests. Therefore, it is recommended to use the more critical ratios in *Equation 8.2* as shown in *Table 7.6* in *Section 7.3*. However, it is advantageous without performing the detailed calculations (*Equation 8.2*), for the backfill investigated in this work, to apply the '*design chart*' shown in *Fig 8.2*, which depicts the relationship between the maximum pull-out resistance force versus the normal pressure.

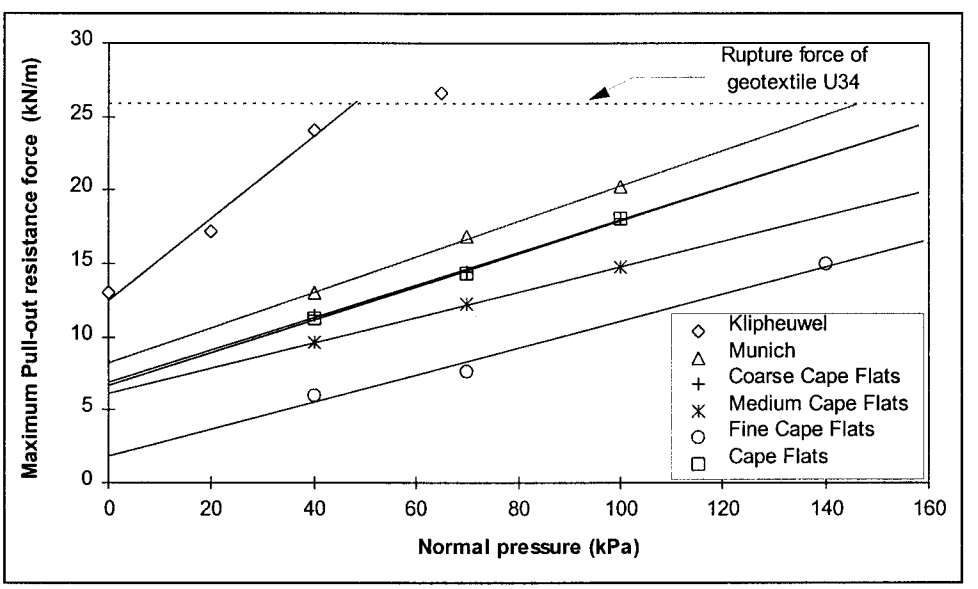

Fig 8.2 Maximum pull-out resistance force-normal pressure relationship

Fig 8.2 is in principle the same as *Fig 7.22*. The difference here is that the pull-out resistance responses from the experimental results were transformed into resistance force per metre width. Thus for a given effective vertical stress (i.e. confinement), the respective maximum pull-out load

per metre run is shown explicitly. Using this chart has the added advantage of showing the rupture load of the specific type of reinforcement confined in a given sand as experienced in the pull-out test, as well as the level of confinement which causes rupture of a U34 geotextile, are indicated. The checking of the reinforcement load against the tensile strength is therefore no longer required.

In the case of a U34 geotextile embedded in Cape Flats sand, the rupture load is in the order of 26kN/m, which is obtained at a confinement of about 160kPa. A geotextile reinforcement confined at a lower normal pressure will fail in sliding.

In addition, the analysis consists of a check on the disturbing force at each layer as a function of the vertical spacing of the reinforcement which must be in accordance with practical reasons of the face stability.

The disturbing force is considered to be related to the lateral earth pressure which increases approximately linearly with depth over the slope height. Thus, the disturbing force or reinforcement force per layer, T_{dj}, is the product of the vertical effective stress and the coefficient of active lateral earth pressure, K_a.

$$T_{dj} \geq S_{vj} \cdot K_a \left(\gamma h_j + p\right) \tag{8.4}$$

with

S_{vj} vertical reinforcement spacing at level j in the embankment

and γ, h_j and p are as defined before.

The wall face is assumed to be smooth and consequently K_a can be defined as the Rankine condition by the familiar expression,

$$K_a = \frac{1 - \sin \phi_p'}{1 + \sin \phi_p'} \tag{8.5}$$

Therefore, in summary, the resisting forces at each layer j must fulfil the condition:

$$T_{dj} \leq T_j \leq T_y \tag{8.6}$$

The *available* resisting force is the sum of all forces accumulated in each layer of reinforcement.

$$F_{avail} = \Sigma T_j \tag{8.7}$$

8.3 Generalised skin friction distribution graph

Using the results of the back-prediction analysis described in *Section 7.3.3*, an attempt was made to develop a standardised skin friction distribution graph which accommodates the variation in the soil/geotextile interface interaction.

The skin friction (interface shear) values per geotextile section at failure, for each sand/geotextile test configuration at the three confining pressures (i.e. 40kPa, 70kPa and 100kPa) as shown in *Fig 7.21* were divided by the respective confinement. It was interesting to note that the new distributions, now in terms of shear stress/confinement ratio responses along the geotextile specimen in each sand/geotextile test configuration, fell in close proximity to each other, thus producing a relatively thin band per test material. In a further step, the averages of the three responses representative of each sand/geotextile configuration, were plotted against their corresponding positions along the geotextile specimen which was expressed in terms of unit length as shown in *Fig 8.3*. With this generalised '*skin friction*' distribution, and both axes being dimensionless, the ultimate skin friction values developing in a wide range of overburden stress or confinements could be evaluated. The mode of failure is, of course, slippage of the reinforcement sheet.

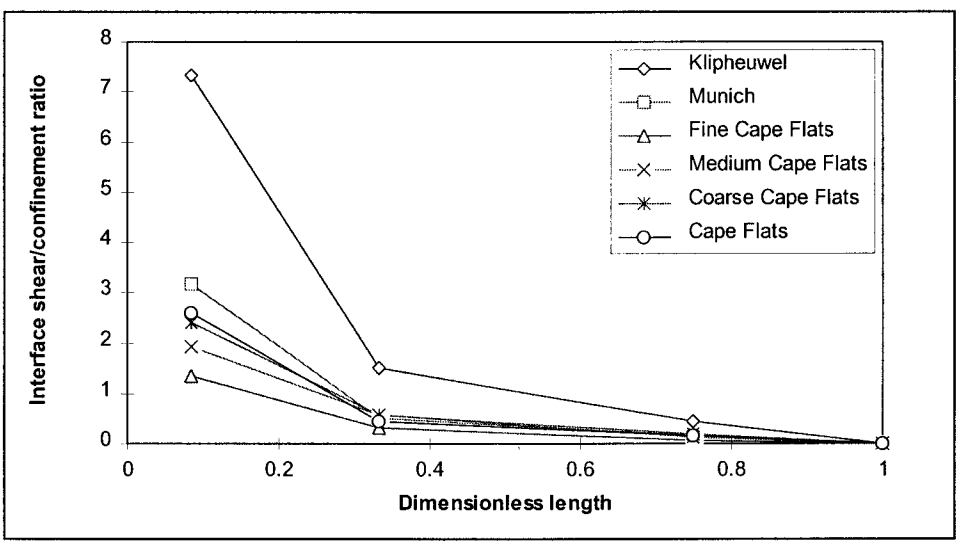

Fig 8.3 Interface shear/confinement ratio characteristic distribution graph

As already shown in *Fig 7.21*, the highest values were again observed in Klipheuwel sand followed by the responses in Munich sand. The characteristic distribution at failure in the various Cape Flats sands and subgroups are slightly lower with the peak always located close to the loaded end.

It is believed that the observed distributions are a quantitative representation for all pull-out tests of the reinforcements of that type even if different in length. Infact, this was the underlying hypothesis

in transforming the geotextile specimen into unit length. However, further testing is required which eventually may support this assumption.

Provided this generalised skin frictin distribution will be validated in other backfill materials, the diagram would allow the evaluation of deformations which could lead to the development of a serviceability criterion for reinforced soil structures.

8.4 Design example

8.4.1 Problem definition

An embankment of a height 4.5 m with a slope face angle, β, equal to 75° and a horizontal crest, is required in order to support a drive-way with an estimated surcharge, p, of 10kPa acting on the crest of the slope. Cape Flats sand, a free-draining granular backfill material, a non-woven geotextile and a wrap-around facing technique will be used. The existing ground conditions provide a strong and competent foundation for the embankment slope.

The expected unit weight, γ, of the backfill compacted in-situ is 18 kN/m^3. Direct shear tests on the fill compacted to the expected field density resulted in a peak angle, ϕ', of 41° and about zero cohesion. The applied normal pressures ranged between 25 kN/m^2 and 100 kN/m^2 (refer to *Chapter 4*).

The embankment is to be designed using a two-part wedge method of analysis. Four 2.7 m long non-woven geotextile reinforcement sheets, each layer approximately 1.0 m in height spacing, are to be considered and analysed for internal stability. The reinforcement will have to form a wrapped slope face angle of about 75°. The manufacturers recommend the strength of the geotextile to be equal to 18 kN per metre width.

The example problem is schematically summarised in *Fig 8.4*.

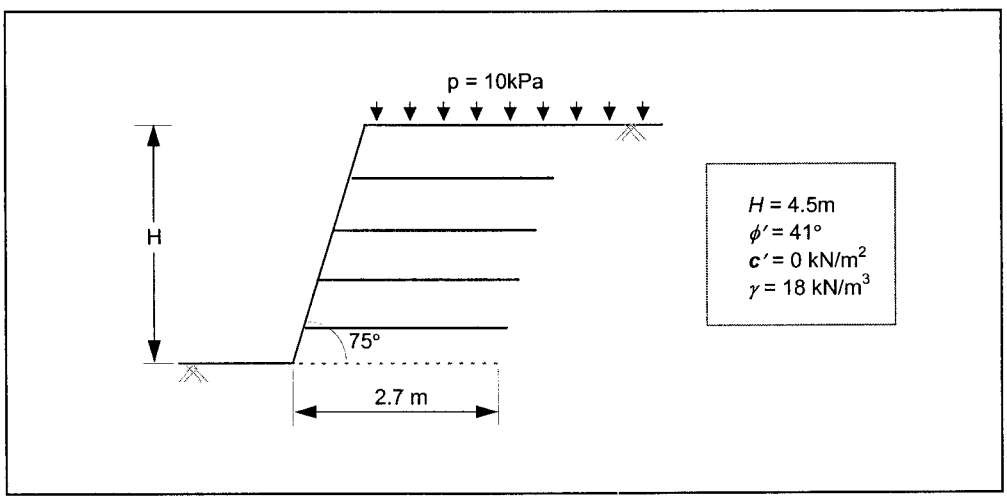

Fig 8.4 Design example for an embankment reinforced with geotextile sheets

8.4.2 Solution

The following design values are selected for the analysis;

- ◊ design height, H = 4.5 m
- ◊ vertical reinforcement spacing, S_v = 1.0 m
- ◊ Geotextile length, L = 2.7 m
- ◊ Geotextile tensile strength = 18 kN per metre width
- ◊ unit weight of backfill material, γ = 18 kN/m^3
- ◊ uniform surcharge, p = 10kPa
- ◊ porewater pressure, u = 0 (the backfill is free-draining)

For the purposes of this exercise, no partial factors of safety were introduced. The design loads and design strengths are applied in unfactored form. Only three trial cases have been considered, and the most critical was selected for further analysis.

Case I

The first trial failure surface is a single failure plane from the toe of the embankment sloped at an angle of 49° and forming a single wedge of soil with the reinforcements crossing the plane of failure.

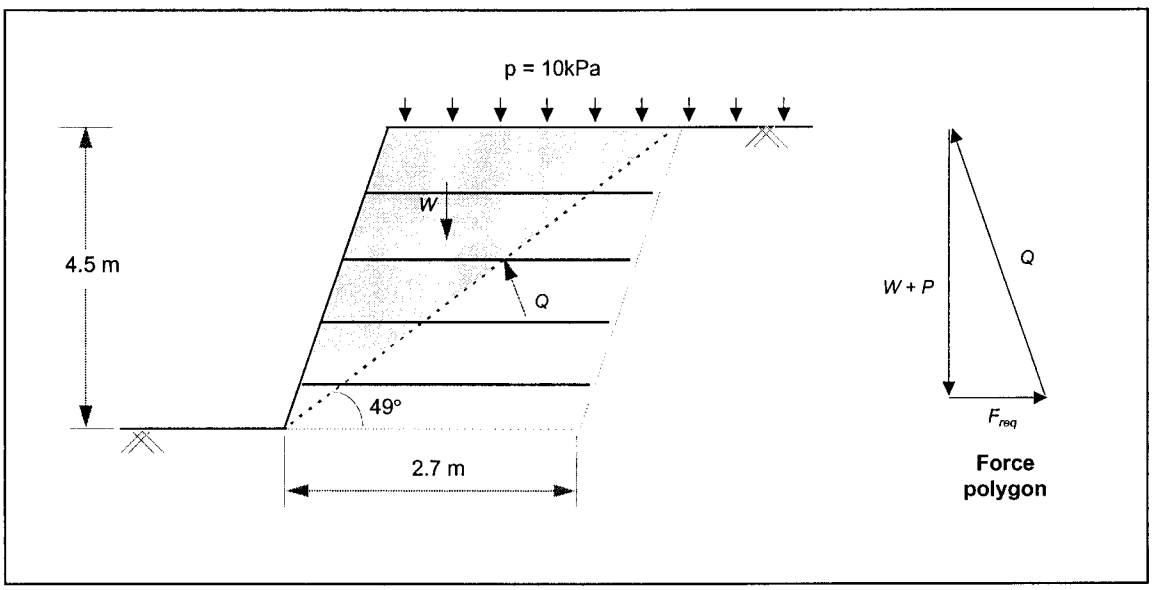

Fig 8.5 First trial wedge consisting of a single failure surface

Analysis of forces acting on the wedge:

Force due to the surcharge, P = 10 x 2.7 = 27 kN/m

Force due to the weight of soil, W = 0.5 x (2.7 x 5.95 sin 49° x 18) = 109.4kN/m

From the force polygon *required* force, F_{req}, = **19.1kN/m**

Case II

Considering a bi-linear trial failure surface cutting a block of soil consisting of a pair of wedges, wedge 1 and wedge 2, as shown in *Fig 8.6*.

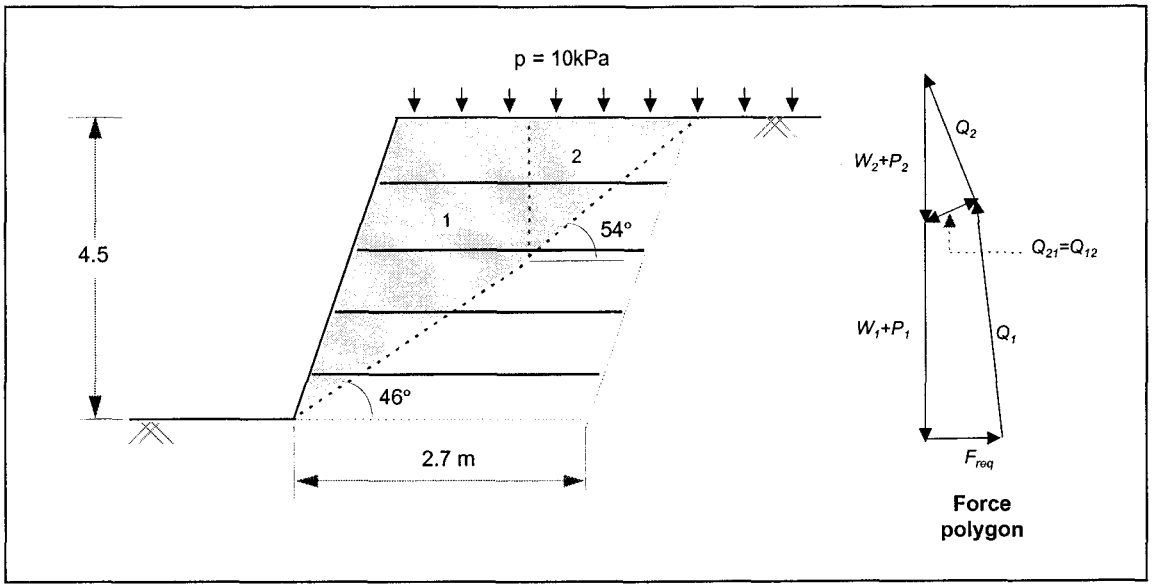

Fig 8.6 Second trial wedge consisting of a bi-linear failure surface

Analysis of forces acting on wedge 1:

Force due to the surcharge on wedge 1, $P_1 = 10 \times 1.45 = 14.5kN/m$

Force due to the weight of soil in wedge 1, $w_1 = [0.5x(4.66 \times 3.84 \sin 29° \times 18)] + [0.5x(1.45 \times 1.72 \times 18)] = 100.52kN/m$

Analysis of forces acting on wedge 2:

Force due to the surcharge on wedge 2, $P_2 = 10 \times 1.25 = 12.5kN/m$

Force due to the weight of soil in wedge 2, $w_2 = 0.5 \times (1.25 \times 1.72 \times 18) = 19.35kN/m$

From the force polygon; '*required*' force, F_{req}, = **19.4kN/m**

Case III

The third trial failure wedge surface is in principle a repetition of Case study II with angles θ_1 and θ_2, of the two failure surfaces of the critical soil block being 47.5° and 50° respectively.

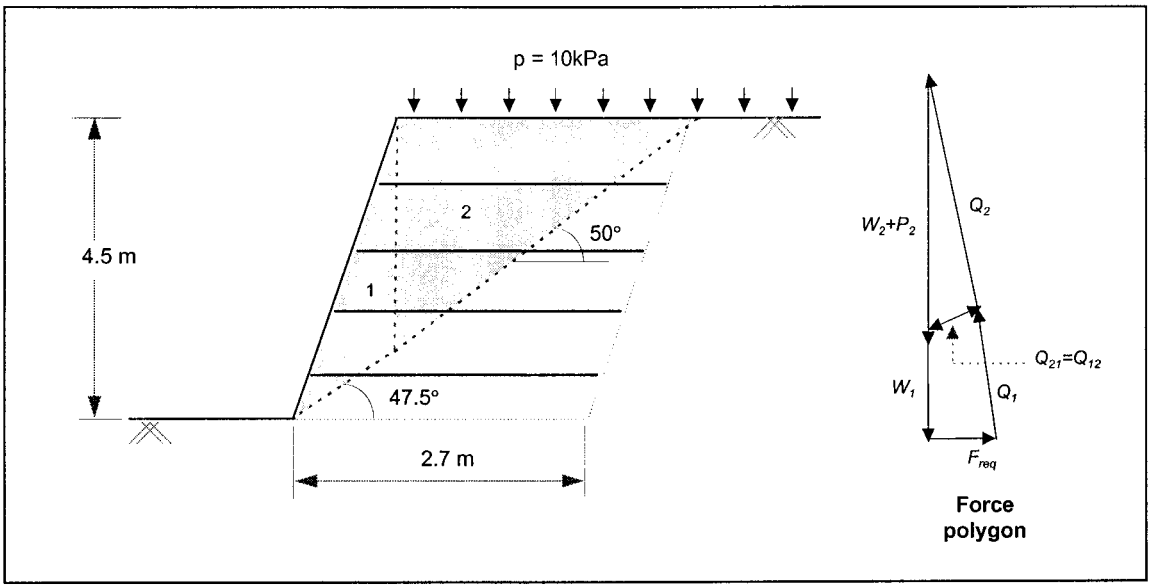

Fig 8.7 Third trial wedge consisting of a bi-linear failure surface

Analysis of forces acting on wedge 1:

Force due to the surcharge on wedge 1, P_1 = 0kN/m

Force due to the weight of soil in wedge 1, w_1 = [0.5x(4.66 x 1.82 sin27.5° x 18)] = 35.25kN/m

Analysis of forces acting on wedge 2:

Force due to the surcharge on wedge 2, P_2 = 10 x 2.7 = 27kN/m

Force due to the weight of soil in wedge 2, w_2 = 0.5 x (2.7 x 3.16 x 18) = 76.79kN/m

From the force polygon; '*required*' force, F_{req}, = **19.8kN/m**

Of the three cases investigated, the critical potential failure surface is the one that gives the maximum '*required*' total force. In this situation the critical potential failure surface is Case III with; θ_1 = 47.5° and θ_2 = 50° and was therefore selected to investigate its stability with the available reinforcements.

Computation of '*available*' resisting forces using the conventional method;

The lengths, L_{ej}, of the reinforcement sheets 1, 2, 3 and 4 (numbered from the top) protruding into the resistant zone are 0.47 m, 1.15 m, 1.75 m and 2.37 m, respectively.

The total bond length of the reinforcement sheets per metre run are,

$$\sum L_{ej} = 0.47 + 1.15 + 1.75 + 2.37 = 5.74 \text{ m}$$

The respective reinforcement force per layer *j* was calculated using Equation 8.2;

- At a depth of 1.0m

$$T_1 = (2 \times 0.47)\left[(18 \times 1 + 10) \cdot 0.73 \cdot \tan 41° + (0.57 \times 2.8)\right] = 18 \text{ kN/m}$$

- At a depth of 2.0m

$$T_2 = (2 \times 1.15)\left[(18 \times 2 + 10) \cdot 0.73 \cdot \tan 41° + (0.57 \times 2.8)\right] = 70.81 \text{ kN/m}$$

- At a depth of 3.0m

$$T_3 = (2 \times 1.75)\left[(18 \times 3 + 10) \cdot 0.73 \cdot \tan 41° + (0.57 \times 2.8)\right] = 147.73 \text{ kN/m}$$

- At a depth of 4.0m

$$T_4 = (2 \times 2.37)\left[(18 \times 4 + 10) \cdot 0.73 \cdot \tan 41° + (0.57 \times 2.8)\right] = 254.21 \text{ kN/m}$$

Checking for the balance of forces due to wall facing (Equation 8.4) at the front of the reinforcement of the forth layer (at a depth of 4.0 m), the overburden stress is highest at this level :

$$T_{d4} \geq (1.0 \text{x} 0.207)(18 \text{x} 4 + 10) = 17.0 \text{ kN/m}$$

However, the geotextile tensile strength per meter width is 18kN/m.

$$T_{d4} < T_4$$

Since T_j is greater than the geotextile tensile strength at the depth of 2.0, 3.0 and 4.0 m the geotextile tensile strength will be taken as the respective forces at those depths.

Using Equation 8.7 to obtain the available forces,

$$F_{avail} = \sum T_j = 18 + 18 + 18 + 18 = 72 \text{ kN per meter run}$$

Thus, the factor of safety is, $FS = \dfrac{F_{avail}}{F_{req}}$

$$FS = (72 \div 19.8) = 3.6$$

Computation of '*available*' forces using the chart in Fig 8.2

- At a depth of 1.0m

Confinement on the geotextile reinforcement σ_{n1} = 10 +(18 x 1) = 28kPa
Maximum mobilised pullout resistance force at a confinement of 28kPa, T_1 = 10kN/m

- At a depth of 2.0m

Confinement on the geotextile reinforcement σ_{n2} = 10 +(18 x 2) = 46kPa
Maximum mobilised pull-out resistance force at a confinement of 46kPa, T_2 = 12kN/m

- At a depth of 3.0m

Confinement on the geotextile reinforcement σ_{n3} = 10 +(18 x 3) = 64kPa
Maximum mobilised pull-out resistance force at a confinement of 64kPa, T_3 = 14kN/m

- At a depth of 4.0m

Confinement on the geotextile reinforcement σ_{n4} = 10 +(18 x 4) = 82kPa
Maximum mobilised pull-out resistance force at a confinement of 82kPa, T_4 = 16kN/m

$$F_{avail} = \Sigma T_j = 10 + 12 + 14 + 16 = 52 \text{ kN per meter run}$$

$$FS = (52 \div 19.4) = 2.7$$

This result appears to be much more realistic since all forces are below the rupture load, and all ***Tj*** are smaller than the disturbing forces developing at the wall facing as assigned by the geotextile manufacturer.

CHAPTER 9

CONCLUSIONS

9.1 Introduction

The summary of findings emerging from this study as well as some recommendations for further research work are presented in the following sections.

9.2 Summary of findings

1. At present, interface shear properties of geotextiles in reinforced soils/fills are mostly investigated using direct shear interface tests in which the respective backfill soil is sheared on geotextile specimen. In analogy to the Mohr-Coulomb evaluation of direct shear tests, the interface friction angle, δ_d and adhesion, c_g were determined. Generally, these parameters are lower than the shear strength parameters of the respective sands. Research results have shown that the interface friction angle ratio is in the order of 0.7 and 0.8 depending on the backfill material.

   It was noted that the interface shear angles obtained from direct shear tests were the same as the sand residual friction values. This implies that it may not be necessary to conduct interface direct shear tests if the soil residual properties, in which the reinforcement is embedded, are known.

2. In this study, pull-out tests of a certain type of geotextile embedded in backfill were developed and undertaken by using a variety of sand materials. The comprehensive investigation of the test data, one of which was the evaluation of the interface shear properties, once again in analogy to Mohr-Coulomb relationship, resulted in even lower shear strength parameters than the ones obtained in the direct shear interface tests.

   The ratio of the angle of interface friction angle to the angle of internal friction of the respective backfill, was in the order of 0.5 to 0.6.

3. Since the pull-out tests were undertaken applying a variety of highly controlled confinements, a significant distinction in the modes of failure could be made. At low confinements the geotextile failed in slippage. After stretching, depending on the magnitude of confinement, the geotextile eventually pulled out as a whole.

Beyond a certain confinement, rupture failure was observed when the geotextile stretched by a critical amount, and thereafter tore part. This type of failure mode was particularly typical in the well graded, angular and sharp-edged granular sand material.

4. By attaching extensometers to various locations along the geotextile, the displacement behaviour of the specimen as the pull-out load was applied could be monitored. These measurements allowed a detailed study of stretching characteristics of the geotextile sample as the test progressed.

   It was observed that the greatest stretch (deformation) along the geotextile occurs at the pull-out end of the specimen and transfers progressively towards the free end of the geofabric as the load is applied.

5. Using an extrapolation procedure to approximate the constantly changing deformation modulus of the geotextile during pull-out testing, and capturing the combined soil/geotextile response of the reinforcement, the resistance force distribution along the geotextile could be established. This, in turn, allowed for the quantification of the limiting force distinguishing between slippage and rupture failure in a specific backfill material. This limit load was in all soil/geotextile configurations higher than the unconfined tensile strength of the geotextile provided by the manufacturer.

6. Furthermore, the force distribution along the geotextile specimen allowed the development of skin friction distribution which was by no means constant as assumed in the design procedures of reinforced soils or fills. The skin friction distribution is highly non-linear with a peak value close to the loaded end dropping off rapidly to the free end of the geotextile. This distribution could be generalised for all the sands and confinements investigated in this study.

7. The pull-out laboratory results allowed the detailed study of the sand/geotextile reinforcement mechanisms as well as the interface properties. Monitoring the stretch characteristics of the geotextile as it pulled out, gave and enhanced understanding of the mechanisms involved. This deemed the pull-out test method *superior* to the direct shear tests where only shear versus displacement graphs and possibly shear versus confinement plots could be analysed.

   It is therefore believed that the pull-out test configuration provides a more adequate interface test simulation of the geotextile reinforcement behaviour in a soil reinforced structure.

8. In all direct interface shear and pull-out laboratory investigations, it was observed that the shear properties are a function of sand grading and grain size. The coarser and better graded a particular soil is, the higher the respective angles of internal friction, interface friction in direct shear as well as in pull-out. Such consistency was, however, not observed with respect to the cohesion and adhesion properties of the sand/geotextile interface tests.

9.3 Recommendations

1. The shear resistance/displacement behaviour of a U34 type of geotextile in a variety of sands on a laboratory scale has been well understood. It is strongly recommended that pull-out tests on a field scale be undertaken not only with varying dimensions of the geotextile sheet, but also on a variety of different geotextile and backfill material types.

2. Since strain measurements at the surface of geotextiles are problematic, the developed *back-prediction* algorithm should be further developed to establish or confirm the generalised skin friction distribution.

3. With the knowledge of the local skin friction distribution along geotextile reinforcements, an improved and more suitable design procedure for reinforced soil may be developed.

REFERENCES

1. Abramento, M., and Whittle, A. J., June 1995, *Experimental Evaluation of Pullout Analyses for Planar Reinforcements*, Journal of Geotechnical Engineering, pp. 486-492.
2. ASTM 04.08, 1993, *Construction; Soil and Rock, Dimension Stone, Geosynthetics*, Annual Book of ASTM Standards, Section 4, Volume 04.08, Philadelphia, PA 19103-1187 USA.
3. ASTM Standard Method D1777-64, 1975, *Standard Method for Measuring Thickness of Textile Materials*, American Society for Testing Materials.
4. ASTM Standard Method D4595-86, 1986, *Standard Method for Tensile Properties of Geotextiles with Wide Width Strip Method*, American Society for Testing Materials.
5. ASTM Standard Method D 5321, *Determining the Coefficient of Soil and Geosynthetic or Geosynthetic and Geosynthetic Friction by Direct Shear Method*, American Society for Testing Materials.
6. Bolton, M. D., 1990, *Reinforced soil: Laboratory testing and modelling*, Proceedings of the International Reinforced Soil Conference organized by the British Geotechnical Society and held in Glasgow, 10 - 12 September 1990, Thomas Telford, London, pp 287-298.
7. Bonczkiewicz, C., Christopher, B. R., and Atmatzidis, D. K., 1988, *Evaluation of Soil-Reinforcement Interaction by Large Scale Pull-out Tests*, Transportation Research Record, No. 1188, pp. 1 - 18.
8. Bourdeau, Y., Gourc J. P., Gotteleland, P., and Perrier, H., 1990, *Pull-out Behaviour-Experimental Study*, Proceedings of the 4th International Conference on Geotextiles, Geomembranes and Related Products, The Hague, Netherlands, pp. 800.
9. BS 1377 : Part 2: 1990, *British Standard Methods of test for Soils for civil engineering purposes, Part 2. Classification tests*, British Standards Institution, 1990.
10. BS 1377 : Part 7: 1990, *British Standard Methods of test for Soils for civil engineering purposes, Part 7. Shear strength tests (total stress)*, British Standards Institution, 1990.
11. BS 8006 : 1994, *Code of Practice for Strengthened/Reinforced Soils and other fills*, (final draft), Document No. 94/104108, British Standards Institution, June 1994.
12. Chandrasekaran, B., 1988, *An Experimental Evaluation of Fabric Strength Properties and Behaviour of Fabric Reinforced Soil,* Master of Engineering Thesis, National University of Singapore, pp. 275.
13. Chang, J. C., Hannon, J. B., and Forsyth, R. a., 1977, *Pull-out Resistance and Interaction with Earth Reinforcement and Soil*, Trans. Res. Rec. No. 640, Washington, D.C.
14. Chen. R. H., et al., 1990, *Investigation of frictional characteristics between sandy soils and non-woven fabrics*, Proceedings of the 4th International Conference on Geotextiles, Geomembranes and Related Products, The Hague, Netherlands, pp. 792.
15. Cowburn, S. J., 1990, *Full Scale Pile Tests using an Electrically controlled Load Actuator*, BSc Thesis, University of Cape Town.

16. Cowburn, S. J., 1993, *An Experimental Investigation of Cyclically Axially Loaded Piles in Sand*, MSc Thesis, University of Cape Town.

17. Dembicki, E., Alenowicz, J., 1987, *Determination of Frictional Properties of Geotextiles*, Geotextiles and Geomembranes, Vol. 6, pp 307-314.

18. Delmas, P., Gourc, J. P., and Giroud, J. P., 1979, *Analyse Experimentale de l'interaction Mechanique sol/geotextile*, Proceedings of International Conference on Soil Reinforcement, Paris, France,1, pp 29-34 (in French).

19. El-Fermaoui, A., Nowatzki, E., 1982, *Effect of Confining Pressure on Performance of Geotextiles in Soils*, Proceedings of the 2nd International Conference on Geotextiles, Las Vegas, USA, pp. 799-805.

20. El Mogahzy, Y. E., Gowayed, Y., Elton, D., 1994, *Theory of Soil/Geotextile Interaction*, Textile Research Journal, Vol. 64, No. 12, pp. 744-755.

21. Forsman, J., Slunga, E., 1994, *The Interface Friction and Anchor Capacity of Synthetic Geo-reinforcements*, Proceedings of the 5th International Conference on Geotextiles, Geomembranes and Related Products, Singapore, pp. 405-410.

22. Fourie, A. B., and Fabian, K. J., 1987, *Laboratory Determination of Clay-Geotextile Interaction*, Geotextiles and Geomembranes, Vol. 6, pp. 275-294.

23. Garbulewski, K., 1990, *Direct Shear and Pull-out Frictional Resistance at the Geotextile-Mud Interface*, Proceedings of the 4th International Conference on Geotextiles, Geomembranes and Related Products, The Hague, Netherlands, May 28 - June 1.

24. Head, K. H., 1980, *Manual of Soil Laboratory Testing* ,Volume 1, Soil Classification and Compaction Tests, Engineering Laboratory Equipment Limited, Pentech Press, London: Plymouth.

25. Holtz, R. D., 1990, *Design and Construction of Geosynthetically Reinforced Embankments on Very Soft Soils*, Proceedings of Performance of Reinforced Soil Structures, British Geotechnical Society.

26. Jewell, R. A., 1996, *Soil reinforcement with geotextiles,* Construction Industry research and Information Association, Special Publication 123.

27. Jones, C. J. F. P., 1990, *Construction influences on the performance of reinforced soil structures*, Proceedings of the International Reinforced Soil Conference organized by the British Geotechnical Society and Held in Glasgow, 10 - 12 September 1990, Thomas Telford, London, pp 97-116.

28. Jones, C. J. F. P., 1995, *The development and use of Polymeric Reinforcements in Reinforced Soil*, Proceedings of the Symposium, The Practice of Soil Reinforcing in Europe, Institution of Civil Engineers, Thomas Telford, London, pp 1-32.

29. Jones, C. J. F. P., 1996, *Earth reinforcement and soil structures*, Thomas Telford, ASCE Press.

30. Juran, I. and Chen, C. L., 1988, *Soil-Geotextile Pull-Out Interaction Properties: Testing and Interpretation*, Transportation Research Record, No. 1188, pp. 37 - 47.

31. Juran, I., and Christopher, B., 1989, *Laboratory Model Study of Geosynthetic Reinforced Soil Retaining Walls*, Journal of Geotechnical Engineering, Vol. 115, No. 7, pp 905-926.

32. Kaytech Geotechnical & Industrial Fabrics, 1995, *Kaymat Geotextiles*; *Manufactured in South Africa*, General Civil Engineering Applications, No. 5.4/93, Proprint.

33. Kharchafi, M., Dysali, M., 1993, *Study of Soil-Geotextile Interation by an X-Ray Method*, Geotextile and Geomebranes, Vol. 12.

34. Lai Sang, L. H., 1995, *Tensile Behaviour of Geotextiles in Soils*, BSc. Thesis, University of Cape Town.

35. Leshchinsky, D., Field, D. A., 1987, *In-Soil Load Elongation, Tensile Strength and Interface Friction of Non-woven Geotextiles*, Proceedings of Geosynthetic '87 Conference, New Orleans, USA, pp. 238-249.

36. Makiuchi, E., Miyamori, T., 1988, *Mobilization of Soil-Geofabric Interface Friction*, Proceedings International Geotechnical Symposium on Theory and Practice of Earth Reinforcement, Fukuoka, Japan, pp 129-134.

37. Miyamori, T., Iwai, S., Makiuchi, K., 1986, *Frictional Characteristics of Non-woven Fabrics*, Proceedings of 3rd International Conference on Geotextiles, pp. 701-705.

38. Myles, B., 1982, *Assessment of Soil Fabric Friction by means of Shear*, 2nd International Conference on Geotextiles, Las Vegas, USA, pp 787-791.

39. Palmeira, E. M., 1987, *The Study of Soil-Reinforcement Interaction by Means of Large Scale Laboratory Tests*, PhD thesis, University of Oxford, United Kingdom.

40. Palmeira, E. M., Milligan, G. W. E., 1990, *Large Scale Pull-out Tests on Geotextiles and Geogrids*. Proceedings of the 4th International Conference on Geotextiles, Geomembranes and Related Products, The Hague, Netherlands, pp. 743-746.

41. Pasley, C. W., 1822, *Experiments on Revetments*, Vol. 2, Murray, London

42. Recalcati, P., Rimoldi, P., 1995, *Steep Reinforced Slopes*, The practice of soil reinforcing in Europe, The Practice of Soil Reinforcing in Europe, Institution of Civil Engineers, Thomas Telford, London, pp 153-166.

43. Rowe, R. K., Ho, S. K., Fisher, D. G., 1985, *Determination of Soil-Geotextile Interface Strength Properties*, Proceedings of 2nd Canadian Symposium on Geotextiles and Geomembranes, Edmonton, Canada, pp. 25-34.

44. Saran, S., et al., 1979, *Earth pressure distribution on Retaining Wall with Reinforced Earth Backfill*, Proceedings of International Conference on Soil Reinforcement, Paris, France, 1.

45. Saxena, S. K., Budiman, J. S., 1985, *Interface Response of Geotextiles*, Proceedings of the 11th International Conference on Soil Mechanics and Foundation Engineering, Vol. 5, pp. 1801-1804.

46. Scheele, F., 1981, *Load Carrying Capacity of Pressure Grouted Anchors in Cohesionless Soils*, PhD thesis, Technical University of Munich, Germany.

47. Schlosser, F., Elias, V., 1978, *Friction in Reinforced Earth*, Proceedings ASCE Symposium on Earth Reinforcement, Pittsburg, pp. 735-762.

48. Shen, C. K., Mitchell, J. K., deNatale, J. S., Romstad, K. M., 1979, *Laboratory Testing and Model Studies of Friction in Reinforced Earth*, Proceedings of International Conference on Soil Reinforcement, Paris, France, 1, pp. 169-174.

49. Smith, G. N., 1990, *Elements of Soil Mechanics,* Sixth Edition BSP Professional Books, London.

50. Smith, R. J. H., 1990, *The Development of Terratrel for the Construction of Steep Slopes*, Proceedings of the International Reinforced Soil Conference on Performance of reinforced soil structures, organised by the British Geotechnical Society and held in Glasgow, Thomas Telford, London.

51. Solomone W. G., Boutrup, E., Holtz, R. D., Kovacs, W. D., and Sulton, C. D., 1980, *Fabric Reinforcement Designed Against Pull-Out*, The use of Geotextiles for Soil Improvement, ASCE, Portland, USA, pp. 80-117.

52. South African Code of Practice, 1989, *Lateral support in surface excavations*, The South African Institution of Civil Engineers, Geotechnical Division, Sigma Press Limited.

53. Steward, J. R., Williamson and Mohney, J., 1977, *Guidelines for Use of Fabrics in Construction and Maintenance of Low-Volume Roads*, USDA Forest Service, Portland, USA.

54. Tzong, W. H., and Cheng-Kuang, S., 1987, *Soil-Geotextile Interaction Mechanism in Pullout Test*, Proceedings of the Geosynthetics '87 Conference, New Orleans, USA, pp. 250-259.

55. Venkatappa, R., Kate, J. M., 1990, *Interface Friction Evaluation of Some Indian Geotextiles*, Proceedings of the 4th International Conference on Geotextiles, Geomembranes and Related Products, The Hague, Netherlands, May 28 - June 1.

56. Vidal, H., 1966, *La terre armee* , Armales de l'Institut Technique du Batiment et des Travaux Publics,19, pp 223-224, France.

57. Wise, C.C., 1997, *Experimental and Numerical Investigation into the sand/geotextile shear interaction behaviour*, MSc(Eng.) Thesis, University of Cape Town.

58. Yazdani, George, August 1996, *Interface Friction for Geosynthetics*, Poly-Flex Newsletter, Issue 4, http://www.poly-flex.com/news4.htm

APPENDICES

Appendix A. Equipment and test procedures

The following tests are presented in Appendix A:

Appendix B. Test data and work sheets

The following test sheets were used and are given in Appendix B:

Appendix C. Pull-out data acquisition

The following hp-BASIC programs were used in the pull-out tests and are given in Appendix C:

Appendix A. Equipment and test procedures

A.1 DETERMINATION OF LIMITING DENSITIES

Aim : To determine the dry densities in the two extreme states of packing sand material

A.1.1 DETERMINATION OF MAXIMUM DENSITY OF SAND

Apparatus : a) Drying oven (105°C - 110°C)
b) Compaction mould - Diameter 101.56 mm
- Height 116.40 mm
c) Drop hammer (2.5 kg)
d) Straight steel edge

Method : 1. Sufficient oven dried sand to fill at least three moulds
2. Cool oven dried sand sample in desiccator
3. Weigh empty mould
4. Place sand in mould to one third of its height
5. Compact sand layer using 55 blows of hammer falling through a height of 300mm
6. Repeat steps 4 and 5 until end of 3rd layer
7. Remove collar from mould and trim excess sand using straight edge
8. Weigh mould with the sand
9. Repeat the test at least three times

Results :

Sand Type	Test No.	Mass of Mould + Sample (g)	Mass of Mould (g)	Mass of Sand (g)	Density of Sand (Mg/m^3)	Average Density (Mg/m^3)
Fine Cape Flats	1	4397.1	2851.2	1545.9	1.634	1.632
	2	4400.9	2851.2	1549.7	1.638	
	3	4388.0	2851.2	1536.8	1.624	
Medium Cape Flats	1	4437.7	2851.2	1586.5	1.677	1.679
	2	4440.5	2851.2	1589.3	1.680	
	3	4439.9	2851.2	1588.7	1.679	
Coarse Cape Flats	1	4518.0	2851.2	1666.8	1.762	1.758
	2	4512.5	2851.2	1661.3	1.756	
	3	4513.1	2851.2	1661.9	1.757	

Note :

Maximum densities of Cape Flats and Munich sands were determined in previous research studies (Cowburn, 1990 and Scheele, 1981).

A.1.2 DETERMINATION OF MINIMUM DENSITY OF SAND

Apparatus :

a) Drying oven (105°C - 110°C)
b) Funnel
c) Drop hammer (2.5 kg)
d) Straight steel edge

Method :

1. Sufficient oven dried sand to fill at least three moulds
2. Cool oven-dried sand sample in a desiccator
3. Weigh empty mould
4. Insert funnel inside mould
5. Pour sand in funnel
6. Carefully retract funnel, causing sand to slowly empty into mould. Care should be taken to ensure that sand does not '*fall*' into the mould
7. Continue steps 5 and 6 until entire mould is full
8. Using straight edge, carefully trim excess sand above the mould
9. Weigh mould with the sand
10. Repeat the test at least three times

Results :

Sand Type	Test No.	Mass of Mould + Sample (g)	Mass of Mould (g)	Mass of Sand (g)	Density of Sand (Mg/m^3)	Average Density (Mg/m^3)
Fine Cape Flats	1	4196.6	2851.4	1345.2	1.422	1.428
	2	4202.9	2851.4	1351.5	1.428	
	3	4208.9	2851.5	1357.4	1.435	
Medium Cape Flats	1	4243.8	2851.5	1392.3	1.472	1.477
	2	4256.9	2851.5	1405.4	1.485	
	3	4246.6	2851.5	1395.1	1.475	
Coarse Cape Flats	1	4308.0	2851.2	1456.8	1.540	1.547
	2	4314.9	2851.2	1463.7	1.547	
	3	4321.7	2851.2	1470.5	1.554	

Note :

Minimum densities of Cape Flats and Munich sands were determined in previous research studies (Cowburn, 1990 and Scheele, 1981).

A.2 DETERMINATION OF SPECIFIC GRAVITY OF SAND

Aim : To determine the specific gravity (G_s) of sand material

Apparatus :

a) Vacuum pump
b) 50 ml glass flask
c) Vacuum flask with stopper
d) Weighing scale (accuracy 0.001g)
e) Plastic squeeze water bottle
f) Thermometer
g) Distilled water
h) Drying oven (105°C - 110°C)

Method :

1. Half-fill the vacuum flask with distilled water and de-air for about 10 minutes to obtain distilled, de-aired water
2. Fill water bottle with distilled de-aired water
3. Record mass of 50 ml flask, (M_1)
4. Put oven-dried sand sample in flask (about 10 g)
5. Record mass of 50 ml flask with sand sample, (M_2)
6. Fill 50ml flask with de-aired water until water just covers sand sample
7. Place flask inside vacuum flask and insert stopper
8. Apply a vacuum to remove air for about two and a half minutes
9. Remove 50 ml flask and add more de-aired water until flask is half full
10. De-air for a further two and a half minutes
11. Fill flask up to scribed level so that the bottom of the meniscus coincides with marking
12. Record mass of flask + sample + water, (M_3)
13. Finally empty the flask and fill it up with distilled de-aired water
14. Record mass of flask + water, (M_4)
15. Repeat the test at least three times

$$G_s = \frac{M_2 - M_1}{M_4 - (M_3 - M_2)} \qquad \text{(A.1)}$$

Results :

Sand	Flask No.	Flask mass (M_1) (g)	Flask mass + Sample (M_2) (g)	Flask mass + Sample + Water (M_3) (g)	G_s
Klipheuwel	1				2.71
	2				2.68
	3				2.70

Note :

Specific gravities of Cape Flats and Munich sands were determined in previous research studies.

A.3 DETERMINATION OF MOISTURE CONTENT

(According to BS 1377 : Part 2 : 1990)

Aim : To determine the moisture content (w) of sand material

Apparatus :

a) Drying oven (105°C - 110°C)

b) Drying container

c) Weighing scale (accuracy of 0.1g)

d) Desiccator

Method :

1. Determine the mass of dry container, (W_1)
2. Place chosen sample in container
3. Determine the mass of sample + container, (W_2)
4. Place container in oven to dry for about 24 hours
5. Remove container from oven and allow to cool in the desiccator
6. Determine mass of container and sample, (W_3)

Calculations:

$$w(\%) = \left(\frac{W_2 - W_3}{W_3 - W_1}\right) \times 100 \qquad \textbf{(A.2)}$$

A.4 STANDARD COMPACTION TEST

(According to BS 1377 : 1975, Test 12)

A.4.1 Aim

To determine the maximum dry density and optimum moisture content of sand material

A.4.2 Apparatus

a) Compaction mould (proctor), internal dimensions 101.8 mm diameter and 116.3 mm high
b) Detachable base-plate
c) Removable extension collar
d) Metal rammer with 50 mm diameter face, weighing 2.5 kg, sliding freely in a tube which controls the height of drop to 300 mm
e) Measuring cylinder
f) Metal tray 600 × 500 × 80 mm deep
g) Weighing scale
h) Tins for moisture content determinations
i) Drying oven, 105 - 110°C

A.4.3 Test Procedure

A.4.3.1 Apparatus Preparation

The mould body and the base-plate were weighed to the nearest 1g (m_1). Diameter (D, mm) and height (L, mm) were measured in several places to 0.1 mm using a vernier calliper and the mean dimensions obtained. The internal volume (V, cm^3) was then calculated with the equation;

$$V = \frac{\pi \cdot D^2 \cdot L}{4 \cdot 1000} \qquad \text{(A.3)}$$

The mould body and the base were weighed.

A.4.3.2 Sample collection

The bulk sample of sand was air dried and mass required weighed. Because the sample contained granular material, and was likely to be broken by the action of the rammer, separate batches were prepared for compaction at each moisture content.

A.4.3.3 Batches Preparation

From the sieved sand sample, about seven representative batch samples each of about 2 kg were taken. Each batch was mixed with a different amount of water to give a suitable range of moisture contents. Samples were then thoroughly mixed with water.

A.4.3.4 Compaction

The mould assembly was placed on a solid base. Loose wet sand was added to the mould so that it was about half filled. A rigid circular steel plate, 100 mm in diameter and 13 mm thick, was then carefully placed on top of the filled sand. This was to prevent the sand '*jumping*' out of the mould during compaction. The sand was compacted by applying 25 blows of the rammer dropping from the controlled height of 300mm on to this plate. Care was also taken to make sure that the rammer was properly in place before it was released.

After compaction of the first layer of sand, an approximately equal amount of the second layer of sand was placed in the mould and compacted with 25 blows as before.

The procedure was repeated with the third layer, which brought the compacted surface in the extension collar to about 5 mm above the level of the mould body.

A.4.3.5 Trimming of sample

The extension collar was carefully removed. Excess sand was cut away and levelled off to the top of the mould checked with a straight-edge.

A.4.3.6 Weighing of sample

Because the sample was granular and would not hold together well, the base-plate was left on. The sample, the mould and the base-plate were then weighed to the nearest 1g (m_2).

A.4.3.7 Removal of Soil

The sample was removed from the mould by hand.

A.4.3.8 Measurement of Moisture Content

Moisture content samples were taken, one from each layer, as the sand was being placed in the mould for compaction. Moisture content, *w (%)*, was then measured using standard procedures (*Appendix A.3*).

The above stages were repeated for each batch in turn.

A.4.3.9 Evaluations

The bulk density of each compacted specimen was calculated using;

$$\rho = \frac{m_2 - m_1}{V} \text{ Mg/m}^3 \qquad \textbf{(A.4)}$$

The moisture content, *w (%)*, for each compacted specimen was also calculated.
The corresponding dry density was then obtained using the equation;

$$\rho_D = \left(\frac{100}{100 + w}\right) \cdot \rho \quad \text{Mg/m}^3 \qquad \textbf{(A.5)}$$

Each dry density was plotted against the corresponding moisture content. A smooth curve was drawn through the points. The maximum dry density values and the corresponding moisture content were then read off.

A.4.4 Results

Table of the Maximum Dry Densities with the corresponding Optimum Moisture Content.

Sand	Maximum Dry Density (Mg/m^3)	Optimum Moisture Content (%)
Fine Cape Flats	1.542	8
	1.562	16
Medium Cape Flats	1.572	6
	1.581	12
Coarse Cape Flats	1.665	1.4
	1.670	8.8
Cape Flats *	1.660	7
	1.690	13.4
Klipheuwel	1.915	10.8
Munich #	2.040	8.7

** Cowburn, 1993*

 # Scheele, 1981

Note :

Two peaks were observed in Fine Cape Flats, Medium Cape Flats, Coarse Cape Flats and Cape Flats sands.

A.5 DIRECT SHEAR TEST

(According to BS 1377 : Part 7 : 1990)

A.5.1 Aim

To determine the angle of internal friction, (ϕ') and cohesion, (c') in effective terms, and the residual shear strength parameters ϕ'_r and c'_r of the sand materials, respectively.

A.5.2 Apparatus

a) Water-tight shearbox carriage on ball bearings

b) Shearbox assembly, comprising

- shearbox body, in two halves, the upper fitted with a '*swan-neck*' yoke with the point of application of the shear force on the yoke in line with the plane of separation of the two halves of the box,
- Lower pressure plate (base plate)
- Upper pressure plate (load pad)
- Upper and lower porous plates (filter stones)
- Upper and lower grid plates, both plain and perforated ones

c) Loading yoke and weight hanger

d) Lever-arm loading

e) Loading ring

f) Electric motor and multi-speed drive unit

g) Loading jack

h) Tailstock unit

i) Stop clock

j) Balance and measuring instruments

k) Apparatus for determining moisture content

A.5.3 Test Procedure

A.5.3.1 Preparation of Test Specimen

For each sand category under investigation, test samples were mixed with the correct mass of water to obtain the optimum moisture content (*refer to Tables 4.2 to 4.4*). A known mass of sand was placed in the shearbox in three layers. Each layer was then subjected to 10 tampings with a hand tamper. The hand tamper consisted of a steel rod attached to a solid rectangular plate with a drop weight of 2.325 kg. Each layer received 10 blows of the weight, dropped through a height of 100 mm. The exact amount of compaction had previously been determined by trial. The compaction of the test sand samples was aimed at achieving 96% of the maximum dry density from the Proctor test. Placement ensured that the mid-height of the middle layer was about level with the plane of shear.

Because of the large mass of the shearbox itself, the mass of the sand used (m in grams) was obtained by weighing the amount left over after compaction, and calculating the difference.

The density, ρ, of the specimen in the box is;

$$\boxed{\rho = \frac{1000 \cdot m}{L^2 \cdot H}} \text{ Mg/m}^3 \qquad \textbf{(A.6)}$$

where,

H height of the specimen in the shear box (mm)

L length of side of the square shearbox (mm)

m mass of the sand used (g)

A.5.3.2 Assembly of Apparatus

The shearbox was then placed in the carriage taking care not to jolt the box. The top grid plate was checked to make sure it was correctly positioned and that there was a small clearance all around the edge. The filter plate was placed on top of the grid plate. The load pad was then placed on top, again ensuring that there was a small all-round clearance.

The worm drive unit and the tail stock were adjusted by hand, so that the contact was just made at all the necessary contact points. The worm drive was positioned so that it could give at least 12 mm of forward movement.

The ball-bearing was placed in the spherical seating on the load pad. The load hanger was then lifted and placed gently until the recess under the yoke registered the ball-bearing.

The load ring was then adjusted to the zero load position and the dial gauge set to zero.

A.5.3.3 Application of normal stress

The amount of weight required on the hanger was calculated to give the desired normal stress on the specimen.

a) *Loading yoke only* : was used for the normal stress of 25 kN/m^2 since it was within the capacity of the loading yoke.

b) *Lever arm loading* : The use of the lever arm was necessary for the normal stresses of 50 and 100 kN/m^2. Since these stresses were greater than those which could be sustained with the hanger weights alone.

A.5.3.4 Lifting top half of box

The clamping screws which lock the two halves of the shearbox together were removed. Separation screws were screwed down until contact with the lower half of the box could just be felt. Both of them were then rotated together a further half turn, so as to separate the two halves of the box by about 0.3 mm. The whole of the horizontal shear could then be transmitted through the specimen itself. The screws were then removed.

A.5.3.5 Final checks

Before proceeding to the shearing stage, the following items were checked :-

- Contact made at all contact points,
- Clamping screws and lifting screws removed,
- Dial gauges set correctly,
- Load pad not tilted or jammed,
- Machine speed and reversing switch correctly set,
- Dial gauge reading recorded in the initial '*zero*' position, and
- Timer wound up, set at zero.

A.5.3.6 Shearing

The motor was switched on and the timer started simultaneously. At regular time, the load dial readings were recorded. Shearing continued until it was well past the maximum stress or '*peak*' point (i.e. horizontal strain at about 12%).

A.5.3.7 Examination of the sheared surfaces

The weights were taken off the load hanger (the hanger and beam were also removed in the cases when the lever arm hanger was used). The hanger yoke was lifted off and placed in the resting place. The load pad and the upper porous plate were taken off.

The shearbox was lifted out using the lifting lugs and placed on the bench.
To examine the surface of shearing, the two halves of the box were separated before pushing the sand specimen out by sliding them horizontally in the same relative direction as in the shear test.

A.5.3.8 Repeat tests

To obtain a set of three points on the Mohr-Coulomb envelope, the procedure was repeated from stage *A.5.3.1* using two additional identical specimens under different normal pressure.

A.5.3.9 Calculations of shear stress

The shear stress, τ, of the material was computed using the equation;

$$\tau = \frac{C_R \cdot R}{L^2} \times 1000 \text{ kN/m}^2 \qquad \textbf{(A.7)}$$

where;

C_R load ring calibration, in Newtons per division (N/div)
R load dial gauge reading, in divisions
L length of side of the square shearbox (mm)

A.5.3.10 Results

Results and their discussion are presented in Chapter 7.

Appendix B. Test data and work sheets

Sheet 1: Determination of maximum and minimum densities

Tested by: ..... Date: .....

1. SOIL TYPE .....

Test No.	Compacted (Maximum Density)		Not Compacted (Minimum Density)	
	1	2	1	2
Mass + Tare (g)				
Tare (g)				
Mass of sample (g)				
Volume of sample (cm^3)				
Density of sample (Mg/m^3)				

Average Max. Density = ... Mg/m^3 Average Min. Density = ... Mg/m^3

Remarks: .....

2. SOIL TYPE .....

Test No.	Compacted (Maximum Density)		Not Compacted (Minimum Density)	
	1	2	1	2
Mass + Tare (g)				
Tare (g)				
Mass of sample (g)				
Volume of sample (cm^3)				
Density of sample (Mg/m^3)				

Average Max. Density = ... Mg/m^3 Average Min. Density = ... Mg/m^3

Remarks: .....

3. SOIL TYPE .....

Test No.	Compacted (Maximum Density)		Not Compacted (Minimum Density)	
	1	2	1	2
Mass + Tare (g)				
Tare (g)				
Mass of sample (g)				
Volume of sample (cm^3)				
Density of sample (Mg/m^3)				

Average Max. Density = ... Mg/m^3 Average Min. Density = ... Mg/m^3

Remarks: .....

Sheet 2 : Proctor test

BS 1377:1990	Test	Location :		Loc. no. :
No. of layers :	Rammer :	Soil description :		Sample no.
Blows per layer :	Drop :	Sample preparation :		Date:
Compacted by :		Sample type :	Operator : .	
Proctor cylinder no.:		No. of separate batches :	Special techniques :	

DENSITY

	Volume of Cylinder (cm^3) :				
Measurement no.	*1*	*2*	*3*	*4*	*5*
Mould & soil (*A*) (g)					
Mould (*B*) (g)					
Wet soil (*A-B*) (g)					
Wet density (Mg/m^3)					

MOISTURE CONTENT

Container no.										
Wet soil & container (g)										
Dry soil & container (g)										
Container (g)										
Dry soil (g)										
Moisture loss (g)										
Moisture content (%)										
AVERAGE MOISTURE (%)										
DRY DENSITY (Mg/m^3)										

Sheet 3: Direct shear test

Location :			Sample No. :	
Operator :			Date :	
Type of Test :			Nominal Size :	mm
Soil description :				
Type of specimen : *UNDISTURBED / REMOULDED / COMPACTED*				
Specimen preparation :				
INITIAL MEASUREMENTS	Length L : mm	Area A : mm^2		Specific gravity, G_s *MEASURED* *ASSUMED*
	Breadth B : mm	Volume V_o : cm^3		
	Height H_o :	Bulky density ρ : Mg/m^3		
	Mass m :	Dry density ρ_D: Mg/m^3		
	Moisture w : %	Voids ratio e_o:		
SHEARING		AFTER CONSOLIDATION		
Machine No. : Load ring No. :		Settlement : mm	Height H_1 :	mm
Mean calibration C_R : N/mm		Dry density ρ_D : Mg/m^3		
Stress factor C_T : kN/m^2 per div.		Voids ratio e_1 :		
Rate of displacement : mm/min		Normal stress σ_n : kN/m^2		

Date	Time	Horizontal displacement (mm)	Load dial reading (divisions)	Horizontal load (N)	Shear stress τ (KN/m^2)	Vertical movement		Remarks
						dial reading (μm)	expansion - settlement + (mm)	

Sheet 4: Geotextile Pull-out test

Test number

Preparation

Date: ..../...../.....

Time of preparation: .....

Layer 1	Layer 2
Mixing tin weight : ..... g	Mixing tin weight : ..... g
Total dry mixing weight : ..... g	Total dry mixing weight : ..... g
Dry soil weight : ..... g	Dry soil weight : ..... g
Desired moisture content (w) : ..... %	Desired moisture content (w): ..... %
Water added : ..... g/ml	Water added : ..... g/ml

from $M_w = \frac{(w \times M_s)}{(1 - w)}$

Compaction details : ..... Layers @ ..... Blows / layer Drop weight ..... Drop height .....

Desired Dry Density : .....g / m^3 Volume to fill: ..... m^3

Mass of dry soil needed in sample : ..... g *from* M_s = *Dry Density x Volume*

Total wet weight needed : ..... g *from* $M_t = \frac{M_s}{(1 - w)}$

Total wet weight needed per layer: ..... g

Frame & press. cell mass : ..... g

Geotextile mass : ..... g Geotextile volume : ..... m^3 Volume of soil: ..... m^3

Moisture content control

Layer	Tin No.	Tin W.	Wet Weight	Wet Soil Weight	Dry Weight	Dry Soil Weight	Water Lost	Water Content	Dry Density

Sand Density

Soil + Frame + Geot. Mass	Frame + Geot. Mass	Wet Soil Mass	Bulk Density	Aver. Moisture content	Dry Soil Mass	Average Dry Density

Pull-out Test

Geotextile type : .....

Width : ..... mm

Exposed length of geotextile : ..... mm

Total embedment depth : ..... mm

Total brass length : ..... mm

Initial length of embedded brass : ..... mm

Time of test : .....

Pressure applied : ..... kPa

Pressure at interface : ..... kPa

Pull-out strain rate : ..... mm/min

NOTES:

Saved as data on disk @ : .....

Saved as data on network @ : .....

Saved as spreadsheet @ : .....

Ch 4 ..... Ch 5 .....

Zero (HP #) .....

Zero (mV) .....

Req. Press. (mV) .....

Req. Press. (HP #) .....

Start: .....

Finish: .....

(Failure pattern and other sketches overleaf)

Appendix C. Pull-out data acquisition

Program 1: Voltage reading of a specific channel and storing of data on a diskette

```
10      CLEAR
20      DIM AV(5,300)
30      DIM SD(5,300)
40      DIM T(5,300)
50      K = 300
55      ! B = 50
56      DISP "Do you want to store the data on this disk? (Y/N)" @ INPUT STQ$
57      IF STQ$ = "N" THEN GOTO 91
60      DISP "**** INSERT STORAGE DISK ****"
70      DISP "Enter test name : " @ INPUT T$
80          CREATE T$, K
90          ASSIGN# 1 TO T$
91      DISP "INPUT # OF VALUES / READING" @ INPUT B
95      DISP "CHANNELS : "@ INPUT C1, C2
100     SETTIME 0,0
110     DISP "CH", "TIME", "READING", "SD"
120     FOR N = 1  TO  K
130     FOR CH = C1 TO C2
140     RESET 6
150     P1 = 7
160     S1 = CH
170     TOT = 0
180     TOT2 = 0
185     T1 = TIME
190     FOR I = 1  TO B
200     SEND 6 ; TALK 7 SCG  S1  MLA
210     ENTER 6 USING "#,w" ; X
220     TOT = TOT + X
230     TOT2 = TOT2 +X*X
240     NEXT I
245     T2 = TIME
250     SEND 6; UNT
255     T(CH,N) = (T1 + T2)/2
260     AV(CH,N) = TOT/B
270     SD (CH,N) = ((TOT2-TOT^2/B)/(B-1))^.5
280     DISP CH, T(CH,N), AV(CH,N), SD(CH,N)
285     IF STQ$ = "N" THEN GOTO 300
290         PRINT # 1; T(CH,N), AV(CH,N), SD (CH,N)
300     NEXT CH
310     NEXT N
320     ASSIGN # 1 TO *
340     NEXT I
```

Program 2: Reading and printing data from diskette

```
1       CLEAR
2       DIM AV(5,300)
3       DIM SD(5,300)
4       DIM T(5,300)
7       PRINTER IS 601
10      DISP "ENTER FILE NAME TO BE READ: " @ INPUT F$
20      ASSIGN# 1 TO F$
25      PRINT "TEST NUMBER : "; F$
26      PRINT " "
27      PRINT "1", "2", "3",, "4", "5"
30      DISP "ENTER THE NUMBER OF RECORDS ON FILE:" @ INPUT K
40      FOR I = 1 TO K
45      FO J = 1 TO 5
50      READ# 1 ; T(J,I)
60      READ# 1 ; AV(J,I)
65      READ# 1 ; SD(J,I)
70      DISP "CHANNEL #" ; J ; ":" ; AV(J,I); "SD" ; SD(J,I); "T" ; T(J,I)
75      ! PRINT J; ":" ; AV(J,I) ; "SD:" ; SD(J,I) ; "T" ; T(J,I)
80      NEXT J
85      PRINT "|" ; T(1,I) ; AV(1,I) ; "|" ; T(2,I) ; AV(2,I) ; "|" ; T(3,I) ; AV(3,I) ; "|"
86        PRINT "  [" ; T(4,I) ; AV(4,I); "|" ; T(5,I) ; AV(5,I) ; "]"
87      PRINT "  "
90      NEXT I
100     ASSIGN# 1 TO *
110     STOP
120     END
```